UNIVERSITY OF CALIFORNIA, SAN DIEGO

Experimental Study of Proppant Settling in a Narrow Fracture Analyzed with Particle Image Velocimetry

A Thesis submitted in partial satisfaction of the requirements
for the degree Master of Science

in

Structural Engineering

by

Lan Luo

Committee in charge:

Ingrid Tomac, Chair
Qiang Zhu, Co-Chair
Daniel M. Tartakovsky

2016

The Thesis of Lan Luo is approved and it is acceptable in quality and form for publication on microfilm and electronically:

_____

_____

Co- Chair

_____

Chair

University of California, San Diego

2016

TABLE OF CONTENTS

LIST OF FIGURES

LIST OF TABLES

ACKNOWLEDGEMENTS

I would like to express my sincere gratitude to my advisor Dr. Ingrid Tomac for her ongoing guidance, support and patience throughout the research. I am very grateful for her supervision during the research of my thesis.

Besides, I would also thank Dr. John McCartney for his great help on preparing the experiments.

And, finally, I would like to thank my family and friends for their motivation and support.

ABSTRACT OF THE THESIS

Experimental Study of Proppant Settling
in a Narrow Fracture Analyzed with Particle Image Velocimetry

by

Lan Luo

Master of Science in Structural Engineering

University of California, San Diego, 2016

Ingrid Tomac, Chair
Qiang Zhu, Co-Chair

This study presents results of an experimental study of the micromechanical proppant behavior during settling in both narrow smooth and rough fractures. This fundamental analysis seeks to better understand dynamics of particle interactions in a dense phase slurry on a small particle size scale, representing proppant settling in narrow hydraulic fractures. Particle Image Velocimetry (PIV) is used for analysis of velocities of individual particle and group particles and their relative paths, collisions and agglomerating in viscous Newtonian fluid. The displacement vectors show the movements of group of particles and global velocity trends of the observed area. The results from this experimental study indicate dependency of settling velocity on particle size and shape, as well as the dependency of different size of particle or agglomerate particles. The measured results, including vertical velocities and displacement vectors of singular particle and

agglomerated particles, were compared with previously published theoretical and empirical relationships. It can be seen that forming of proppant agglomerates during settling, caused by frequent particle-particle and particle-wall collisions and interactions, changes the overall settling velocities predicted by the previous experiments in larger slots. The slurry settling velocity depends on the relationship between settlement, proppant concentration and occurrence of proppant agglomeration. This study also compares the different agglomerations in different fluid. This study presents the influence of proppant concentration and proppant agglomeration. The effect of wall can also been found when the concentration and agglomeration is high. In order to better understanding proppant settling in hydraulic fracture where mostly rough, the proppant settling in narrow slot with adding rough surface is also analyzed. By comparing experimental results of proppant settling in narrow slot with both smooth surface and rough surface, it can be found that the rough surface can diminish average settling velocity. The decreasing of proppant concentration and agglomeration is also found in this study.

CHAPTER 1: INTRODUCTION

1.1. Proppant flow and transport in georeservoirs background

Hydraulic fracturing is a process of creating new fractures in underground rock deposits by using pressurized fluid for breaking rock mass. Hydraulic fracturing is used in igneous rock for creation of geothermal reservoirs, or in sedimentary formations including shales for oil and gas extraction. Viscous fluid is used in conjunction with placing small granular material called proppant into hydraulic fractures for maintaining the created artificial permeability. In geothermal reservoirs, water is continuously cycled through propped fractures, while in oil and gas reservoirs permeable fractures permit production. Selection of proppants and fracturing fluid affects the process of hydraulic fracturing and weather the new fractures can maintain open after hydraulic fracturing operation. Therefore, proppant flow and transport plays a significant role in hydraulic fracturing of georeservoirs. Previously, experimental, numerical and theoretical research has been conducted for developing predicting equations for proppant placement in hydraulic fractures. However, the particle-particle and particle-fracture interaction effects on flow and transport of proppant have not yet been fully addressed.

1.2. Literature review

1.2.1. Role of proppants in georeservoirs

A proppant is a solid material, typically sand, treated sand or man-made ceramic materials. The size and shape of proppants plays a critical role in keeping fractures open and at the desired conductivity. The hierarchy of conductivity according to different types of proppants is shown in Figure 1.1. The more regular shape of proppants lead higher

conductivity. When the proppants hold uniform size and have spherical shape, the conductivity is the highest.

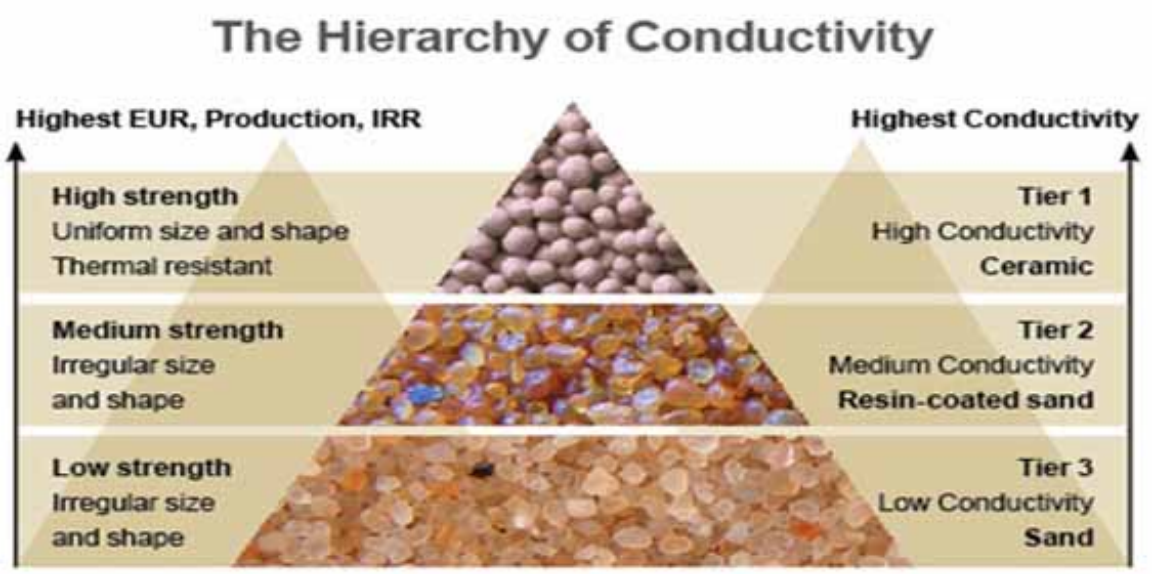

Figure 1.1 Hierarchy of conductivity (CARBO Ceramics)

When the fracture formed in georeservoirs, the proppant can be packed in fracture. Figure 1.2 shows proppant packing with different types of proppants in georeservoirs with gas and oil. Figure 1.2 (a) shows well rounded ceramic proppant which can form well flow in fracture. However, when in proppant sand is poorly sorted and angular, the proppant can be clogged in fracture.

In addition to proppant shape, size is also a major factor in conductivity. Size is generally measured by the mesh size that could be used to sieve the particular particles. The larger the sieve size, the larger the gaps in the sieve, and hence the larger the grain. When the grain size is smaller, the conductivity of fracture is higher. However, when the grain size increases, the fracture is easily to be clogged. Thus, choosing the appropriate grain size is also an important factor in proppant transport.

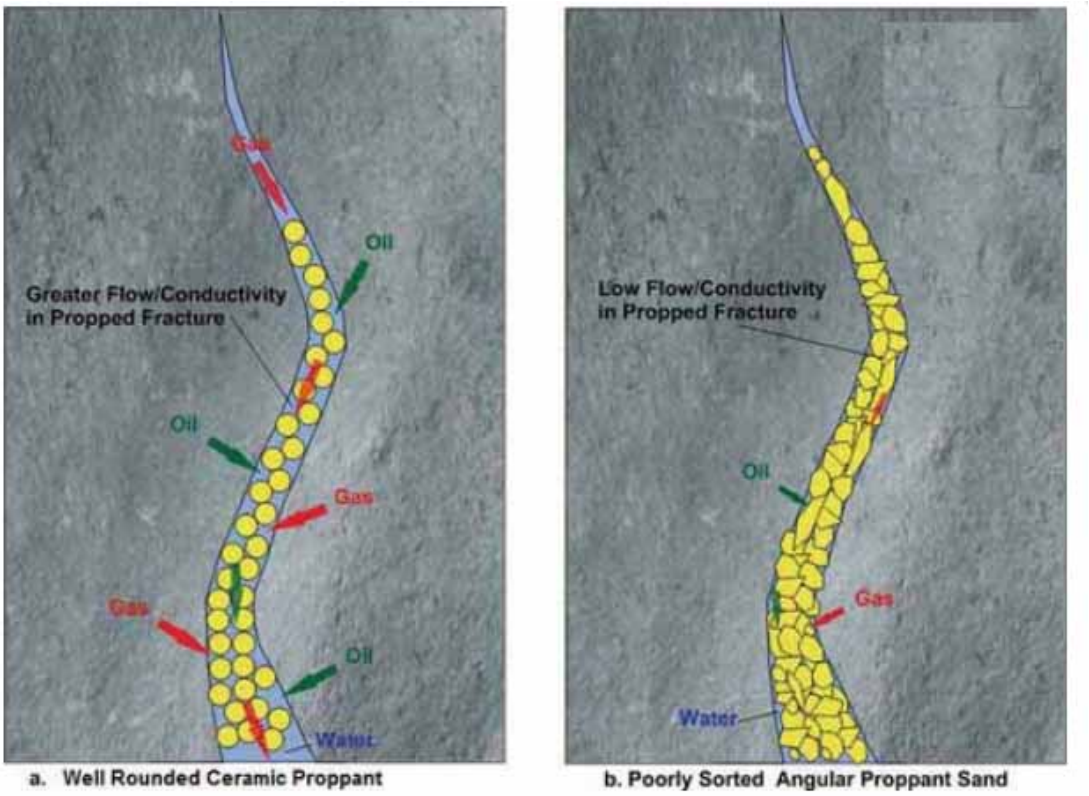

Figure 1.2 Proppant packing in fracture (Wan, 2014)

1.2.2. Proppant flow and transport in rock fractures

Proppant transport within a hydraulic fracture is influenced by a number of factors including: fracture width, fluid leak-off, fluid viscosity, density difference between the fluid and the proppant, and proppant size (Palisch et al., 2008, and King, 2010). Proppant transport in hydraulic facture has been studied both in numerical and experimental. Deng et al. (2014) uses the DEM code to investigate the shale-proppant interactions. The influence on the opening of fracture with different stress levels, different shale's Young's modulus and varying of proppant's size is evaluated. By comparing numerical result with calibrated parameter with experimental stress-strain curve of oil shale, Deng et al. (2014) concluded the softer the shale particle is, the higher the pressure and larger the proppant

size implying a smaller crack aperture and larger plastic zone for other given conditions. Trykozko (2016) uses pore-scale simulations to study non-Darcy effects of high flow rate and migration of fine particles on proppant conductivity and reduction. According to the computational approach on proppant pack, Trykozko (2016) stated that the reduction in the fracture conductivity and subsequent reduction in the productivity of a hydraulically fractured reservoir due to the high flow rates. It is also being concluded that the migration ends up with pore throat bridging. Hammond (1995) did numerical analysis on the gravity-driven vertical motion of proppant in a hydraulic fracture. Two major gravity-driven movements were analyzed: settling and slumping. It was being concluded that concentration of proppants can significantly change the rearrangement rates during settling and slumping. During proppant transport in a hydraulic fracture, the rates of settling and slumping are similar (Hammond, 1995). Shiozawa and McClure (2015) discussed proppant transport in natural and hydraulic fractures by using a two-dimensional discrete fracture networks model. The model contains a proppant bed at the bottom of the fracture and a slurry (mixture of fluid and proppant) above the proppant bed. The model takes into account fracture closure around the proppant and the effect of closure on fracture properties. This simulation was verified to describe proppant transport, proppant settling, proppant erosion, and fracture closure. To further analyze the proppants transport by using three-dimensional simulation, Shiozawa and McClure (2016) applied a pseudo-three-dimensional simulation of proppant transport on gravitational settling, formation of proppants banks, tip-screen out and fracture closure. This pseudo-3D code improved by Shoizawa and McClure (2016) aimed at gain computational efficiency. The result came from this pseudo-3D simulation were verified with fully-3D simulation. Donstov and

Peirce (2015) also did three-dimensional simulation on proppant transport. Dontsov and Peirce (2015) extended to observe the tip screen-out effects for proppant transport in hydraulic fractures while the ratio of facture width to diameter of sand particle is small, the effect of the wall cannot be neglected. McClure et al. (2015, 2016) also contributed to the implementing proppant flow and transport in the numerical model to describe propagation of hydraulic fractures and opening and shear stimulation of natural fractures. They used nonlinear empirical equations are used to relate normal stress, fracture opening, and fracture sliding to fracture aperture and transmissivity. Eskin and Miller (2008) presented governing equations which are composed of boundary conditions and constitutive relations for the proppant flow and transport model which takes the micro-level particle dynamics into account. Eskin and Miller (2008) concluded that the slurry dynamics is governed by particle fluctuation in a high-shear-rate flow and that slurry flow in a fracture is characterized by non-uniform solids concentration across the fracture width. Tomac and Gutierrez (2014) studied numerically proppant agglomeration in viscous fluid and the aggregation was related to fracture width and fluid viscosity. It has also been found that particle concentration affects the particle settling velocity. Both numerical and experimental studies were conducted (Shokir and Quraishi, 2009). In this study, proppant transport and placement efficiency of four non-Newtonian fluids with different densities was investigated. It has been observed that convection was significant flow mechanism even with small density contrast. Convection settling decreased and proppant placement efficiency increased when increasing slurry injection rate or decreasing proppant concentration. Couples of tests by changing slot complexity, pump rate, proppant concentration, and proppant size were conducted in laboratory to investigate proppant

transport in complex fracture networks (Sahai et al., 2014). Sahai et al. (2014) concluded that proppant flew around the corner at higher pump rate and the gravitationally motion would pull proppants settling down. Roy et al. (2015) also conducted both experimental study and numerical simulation on proppant transport in fractures. By using the same shale surface, the author concluded that the proppants pack appeared dispersion movement in proppant transport. Goel and Shah (2001) conducted a laboratory test by using a field-scale test facility. The minimum elastic modulus criterion for a satisfactory proppant transport in a fracturing treatment was obtained based on the experimental results (Goel and Shah, 2001; Goel et al., 2002). Patankar et al. (2002) conducted both numerical and experimental studies on the sediment flow and transport in pressure driven channel and obtained the power law correlations, which can be used as a basis for sediment transport models. Furthermore, to enhance the design process of hydraulic fracturing, the migration process and the volumetric concentration of proppant were also investigated by Zhao et al. (2008) by using numerical simulation.

1.2.3. Experimental investigation of proppant settling

During proppant transport, proppant settling is being investigated by previous researchers in laboratory in different scale of experiments. Different parameters were studied with proppant settling. Sievert et al. (1981) conducted a large-scale vertical-slot experimental study by varying fluid type, fluid viscosity, proppant concentration and flow. The influence of proppant concentration, fluid viscosity is significant with non-Newtonian fluid (Sievert et al., 1981). Brule and Gheissary (1993) develop an experimental investigation of the effects of fluid elasticity on the settling velocity of spherical particles

in viscoelastic fluids. It was found that the effects of elasticity and shear thinning are opposite and can be comparable in size in viscoelastic fluid (Brule and Gheissary, 1993). The interaction between particles and elastic effects were shown to be important by experimental study on proppants settling (Gheissary and Brule, 1996). Clark et al. (1977) used a larger vertical fracture model to investigate the proppants settling. The measured settling velocity of proppants was compared with single particle fall rate and the agglomeration was observed to be an important factor in proppant transport. Malhotra and Sharma (2012) performed an experimental study on the settling velocity of spherical particles in both unbounded and confined walls in shear thinning viscoelastic fluids. The authors found that the walls affected particle settling in viscoelastic fluid, with increasing significance as the ratio of particle diameter to spacing between the walls increases.

Additionally, some particle agglomerations were observed during proppant settling between parallel walls. Joseph (1994) studied particle-particle interactions and observed correlations between viscoelastic fluid normal stress and particle agglomeration. Liu and Sharma (2005) developed an experimental correlation between proppant settling velocity and dimensionless fracture width. The empirical relationship proposed by Liu and Sharma (2005) divided the proppants into two groups according to particle diameter: one is the ratio of particle diameter to fracture aperture is smaller than 0.9 and the other is larger than 0.9. The relationship introduced by Liu and Sharma (2005) is shown below:

$$\begin{aligned}
&\frac{v_{\mathrm{w}}}{v_0} = 1 - f(\mu)\frac{d}{B}; \left(\frac{d}{B} < 0.9\right) \\
&\frac{v_{\mathrm{w}}}{v_0} = g(u)\left(1 - \frac{d}{B}\right); \left(\frac{d}{B} \geq 0.9\right) \\
&f(\mu) = 0.16\mu^{0.28} \\
&g(u) = 8.26\mathrm{e}^{-0.0061\mu}
\end{aligned} \tag{1.1}$$

Where,

v_w = proppant settling velocity between parallel walls (m/s),

v_0 = single particle settling velocity in unbounded fluid (m/s),

d = particle diameter (m),

B = fracture aperture (m),

μ = fluid dynamic viscosity (Pa·s).

1.2.4. Numerical models for proppant flow and transport

Besides experimental study, numerical models were developed to analyze proppant transport. Different numerical models were introduced based on different objectives.

A prediction of the settling velocity of spherical particle in unbounded cell was provided by Stokes' law. The expression of Stokes' law is shown as Equation 1.2:

$$v_t = \frac{\mathrm{g}d^2(\rho_p - \rho_f)}{18\mu} \tag{1.2}$$

Where,

v_t = flow settling velocity (m/s),

g = gravitational acceleration (m/s^2),

d = particle diameter (m),

ρ_p = particle mass density (kg/m^3),

ρ_f = fluid mass density (kg/m^3),

μ = fluid dynamic viscosity (Pa·s).

Stokes' Law shows the relationship between settling velocity with particle diameter, particle mass density, fluid mass density and fluid dynamic viscosity.

However, during proppant settling, the proppant concentration usually occurs which can influence the settling velocity. A numerical method was developed by Daneshy (1978) to investigate the influence of proppant concentration on settling. The expression of the relationship proposed by Daneshy (1978) is shown below:

$$v_s = v_0[\frac{1 - c_v}{10^{1.82c_v}}] \tag{1.3}$$

Where,

v_s = slurry settling velocity,

v_0 = single particle settling velocity,

c_v = volumetric particle concentration in the slurry.

When concentration of proppants during settling is very low, Clark et al. (1981) proposed a relationship for settling velocity with concentration. The expression is shown as Equation 1.4:

$$v_s = \frac{1}{1 + 6.88c_v} v_0 \tag{1.4}$$

Gadde et al. (2004) also established models for proppant settling in hydraulic fractures and found an empirical correlation which takes particle concentration into account based on Stokes' law. The relationship proposed by Gadde et al. (2004) is:

$$v_s = v_0(2.37c_v^2 - 3.08c_v + 1) \tag{1.5}$$

Joseph (1994) focused on the different effects of particle-wall interaction and particle-particle interaction both in Newtonian and viscoelastic fluids. He concluded that while particles are close to a vertical wall, the wall will attract particles in a viscoelastic fluid and will dissociate particles in Newtonian fluid. Feng et al. (1994) also investigated the effects of channel wall. The author focused on sedimentation of a single particle with

wall effects and concluded that the particles were separated from the wall in a constant distance in Newtonian fluid and the drag reduction can be found on the particles. Dontsov and Peirce (2014) analyzed the gravitational settling of spherical particles in steady flow. They introduced an approximate solution to reduce the complexity of problem of boundary conditions. As for low proppant concentrations in flow through horizontal or near horizontal pipes, Stevenson et al. (2001) obtained a correlation for sand velocity while there is no sand movement by the intermittent flow. Tomac and Gutierrez (2014) studied numerically proppant agglomeration in viscous fluid and the aggregation was related to fracture width and fluid viscosity. It has also been found that particle concentration affects the particle settling velocity. Eskin and Miller (2008) observed that the slurry flow in a fracture is characterized by non-uniform solids concentration across the fracture width. Roy et al. (2015) conducted both experimental and numerical analysis on proppant transport and concluded that the lowest concentration experiment ultimately had the lowest settling velocity.

In spite of the previous efforts which identified particle agglomerations in proppant slurries, the mechanisms which govern slurry erratic behavior have not yet been fully understood. This research hypothesize that fluid viscosity promotes particle agglomerations during settling in a narrow slot. Particle agglomerations occur as a consequence of particle-particle collisions and particle-wall collisions. A thin layer of viscous fluid dissipates the kinetic energy of approaching particles (Barnocky and Davis, 1988, Davis et al., 1986). Depending on particles pre-collision relative velocities and fluid velocity and properties, agglomerates form and fall apart (Tomac and Gutierrez, 2013, Tomac and Gutierrez, 2014, Tomac and Gutierrez, 2015).

1.3 Motivation

The proppant settling were already studied both in experimental and numerical analysis. There are some factors which will influence settling velocity during proppant transport. The influence of proppant size, proppant concentration, wall effect and fluid viscosity (Daneshy, 1978; Clark et al., 1981; Gadde et al., 2004 and Liu and Sharma, 2005) were analyzed. However, it can be found that the proppant agglomerates occurred during settling. The influence of agglomeration on proppant settling are lack of investigate. The relationship between agglomeration with proppant concentration still needs to be studied. During proppant settling in narrow slot, both of the concentration and wall effect need to be considered at the same time. When proppant settling in narrow slot, the relationship between proppant agglomeration with wall effect is also needing investigation. Moreover, proppants can be agglomerated and then felled apart during proppant settling. The particle-particle interaction is still important for proppant transport.

The proppant settling is investigated to obtain the influence of proppant transport in hydraulic fracture. The interface of slurry with fracture is not as smooth as ideality. Thus, the proppant transport with rough surface can also be investigated. The influence of roughness on wall effect, proppant agglomeration and proppant concentration is also valuable to be studied.

1.4 Research objectives

The objective of this work is to study proppant settling in narrow slot. Proppant transport experiments in narrow slot with smooth surface and rough surface are conducted. This fundamental analysis seeks to better understand dynamics of particle interactions in a

dense phase slurry on a small particle size scale, representing proppant settling in narrow hydraulic fractures. The micromechanics of proppant behavior is investigated in this study. The specific research objectives are:

1. Evaluating the settling velocities of individual particle and group of particles in a 2 mm narrow slot with smooth surface in viscous fluid.
2. Investigating whether the Stokes' law predicts and what are the expected deviations from the Stokes' law of the experimental results of single particle and group particles with different diameters falling through a narrow fracture.
3. Better understand the effects of proppant concentration on the slurry settling in a narrow fracture, by comparing the experimental results with previously published relationships (Daneshy, 1978; Clark et al., 1981 and Gadde et al., 2004).
4. Better understand the wall effect on slurry settling in a narrow fracture through comparing the experimental results with predictions for proppant settling velocity in a general fracture (Liu and Sharma, 2005), by evaluating both the diameter of mean particle diameter and the diameter of agglomerated particle.
5. Better understand the effect of rough narrow fracture surface, and adding the investigation of the influence of rough surface on proppant settling velocity according to concentration, wall effect and agglomeration is investigated.

1.5 Thesis organization

Chapter 1 introduces the previous research on proppants transport and hydraulic fracture. The motivation and objectives are also propposed in Chapter 1. Chapter 2 includes the description of experiments for the study and also the methodology that is using for

analysis. Chapter 3 provides a detailed analysis for slurry settling in 2 mm narrow slot with smooth surface in three different fluids: 50 % glycerol-water fluid, 75 % glycerol-water fluid and 85 % glycerol-water fluid. Chapter 4 describes the analysis for slurry settling in narrow slot with rough surface in the same three fluids as Chapter 3. Chapter 5 involves comparison between the results of slurry settling in narrow slot with smooth surface and with rough surface. Chapter 6 briefly descries the observations and recommendations for future work based on this analysis. Referenced used in this thesis are listed in the end of this report

CHAPTER 2: METHODOLOGY

2.1. Setup and organization of experiments

In this experimental study, there are two different sets of tests. The first set of tests consists of proppant and viscous fluid slurry settling in a 2 mm narrow slot with smooth surface. The second set of tests was conducted by adding rough surface in narrow slot to investigate proppant and viscous fluid slurry settling in narrow fracture. During this experimental study, proppants are getting from well-rounded sands as shown in Figure 2.1.

Figure 2.1 Well rounded sands used in laboratory

The proppants are sized by using U.S. traditional testing sieve as shown in Figure 2.2. These sieves are mostly and easily used in laboratory. For different sieve that is chosen for grouping proppants, different size of proppant is chosen for particular use. Proppant size is generally measured by the mesh size in the sieve. The larger the sieve size, the larger

the gaps in the mesh, and the larger the sand. Typically, proppant sizes range from 8 to 140 mesh which represents 0.106 mm to 2.35mm. There are many shorter sieve intervals such as 16/30 mesh and 20/40 mesh.

Figure 2.2 U.S. standard testing sieve

Figure 2.3 U.S. standard testing sieve of 20/40 mesh

In this laboratory study, the sieve interval of 20/40 mesh is chosen to get particular proppant size as shown in Figure 2.3. The diameter of sand getting from this sieve ranges from 0.42 mm to 0.84 mm. The mean diameter of proppant that is chosen is 0.6 mm. Three different fluids are used in this experimental study: 50 % glycerol-water mixture, 75 % glycerol-water mixture and 85 % glycerol-water mixture. The percentages of 50 %, 75 % and 85 % are representing the volumetric percentages of glycerol. For the first set of tests with smooth surface, the experiment has four components: acrylic plate, fluid, proppant and wooden seat. Between the front and back acrylic plates, a 2 mm thick acrylic spacing is placed to obtain a narrow slot. A wooden seat was manufactured to hold the experiment in order to keep the frame steady during the test as shown in Figure 2.4. A piece of paper with blue color is stacked on the back of one acrylic plate in order to have different brightness comparing to the color of proppants.

To record the settling of proppants in narrow slot, a camera (Nikon D610) is placed in front of the experiments as shown in Figure 2.5. The camera zoomed to focus on the investigated scope to record proppant settling.

Another series tests were conducted for slurry settling in narrow slot with rough surface. The data of rough surface came from laboratory hydraulic fracturing test in rock (Brenne, 2014). A three-dimensional scan was conducted to get through the induced rock surface (Brenne, 2014). For rock surface, joint roughness coefficient is an important parameter to determine the roughness of rock. The *JRC* of the rock is evaluated as 0.7-0.8 (Brenne, 2014). The profile of rock surface with different range of JRC is shown in Figure 2.6 (Barton and Choubey, 1977).

Figure 2.4 Experiments of narrow slot with smooth surface

Figure 2.5 Recording process of experimental study

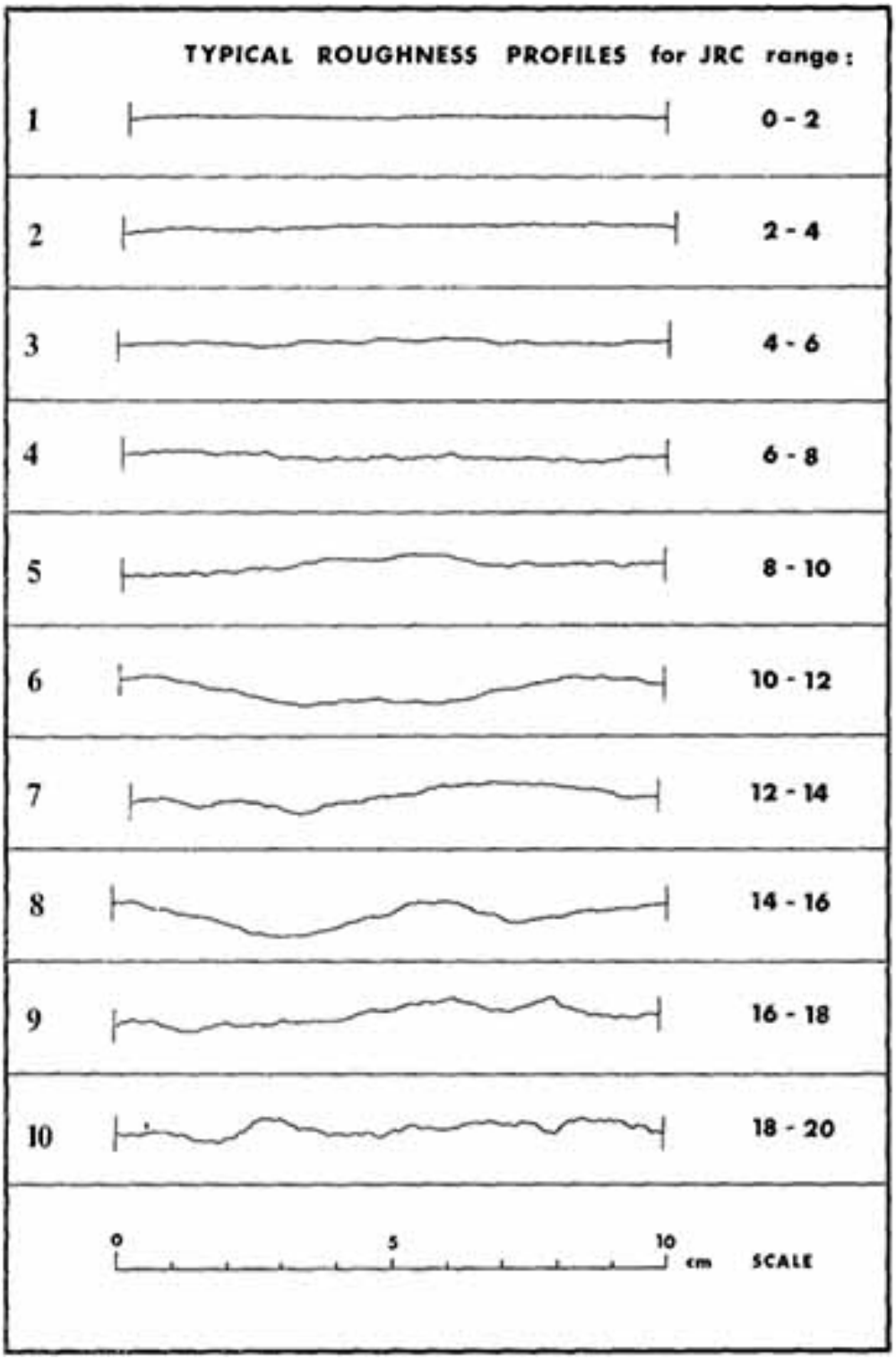

Figure 2.6 Roughness profiles showing the typical range of *JRC* value (Barton and Choubey, 1977)

By using the data from scanner, a three-dimensional printed surface was obtained as shown in Figure 2.7. The surface of rock fracture reached average heights of around 4 mm and the highest is 5.5 mm for this rock fracture (Brenne, 2004). The thickness of spacing acrylic plate using for this set of test is 9 mm, thus the slot width is 3.5 mm.

For these series test with rough surface, the components contain acrylic plate, three-dimensional printed rock surface, fluid and wooden seat as shown in Figure 2.8. The surface of rock fracture reached average heights of around 4 mm and the highest is 5.5 mm for this rock fracture (Brenne, 2004). The thickness of spacing acrylic plate using for this set of test is 9 mm, thus the slot width is 3.5 mm.

Figure 2.7 Three-dimensional printed rock surface

Figure 2.8 Experiments of narrow slot with rough surface

2.2. GeoPIV method

To record the movements of proppants, a camera was placed in front of the transparent side of the frame. Afterwards, the GeoPIV analysis technique was used to transfer the digital figures to manageable data for obtaining proppant velocities and displacement vectors. GeoPIV software uses the principles of the Particle Image Velocimetry (PIV) method for obtaining the particle displacement data from couple of digital images. Images between small time intervals can be extracted from camera directly, or as frames from the video recorded with a high speed camera. Adrian (1991) first introduced the particle-imaging technique for measuring the motion of small, marked regions of a fluid by observing the locations of the images of the markers at two or more

times. Willert and Gharib (1991) developed PIV method to make it easier and faster to handle series of operations. White (2001) came up with the idea of using digital photography and PIV image processing for measuring displacements of partially obscured soils in area of high strain gradient. White (2002) presented a new system for deformation measuring in geotechnical tests based on PIV method with improved the accuracy and precision, adding the displacement array.

In this study, the digital image was first divided into number of meshes as shown in Figure 2.9. Second, the GeoPIV method finds the same or similar mesh within the next digital image. Particle position comparisons between two subsequent frames permit obtaining displacements and particle velocities.

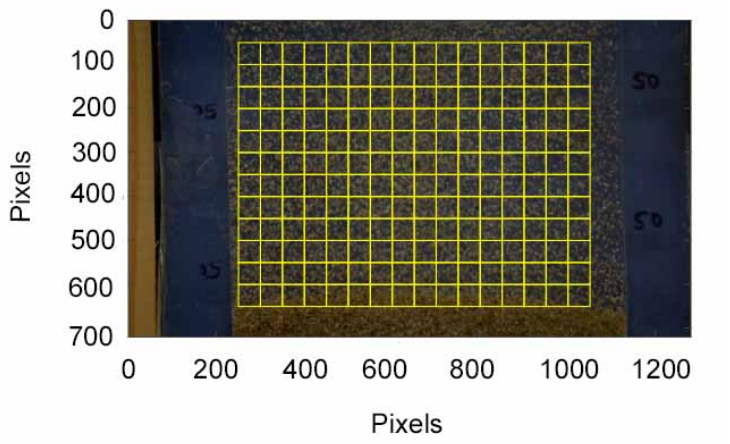

Figure 2.9. Meshes of digital images

Figure 2.10 shows displacement arrays of tracked particles in a predefined mesh in Figure 2.9. The GeoPIV method is chosen because it obtains the particle movement arrays and clearly shows the movement directions. The displacement data can be converted to velocity. In this study, the velocities of particles are the main parameter to be discussed.

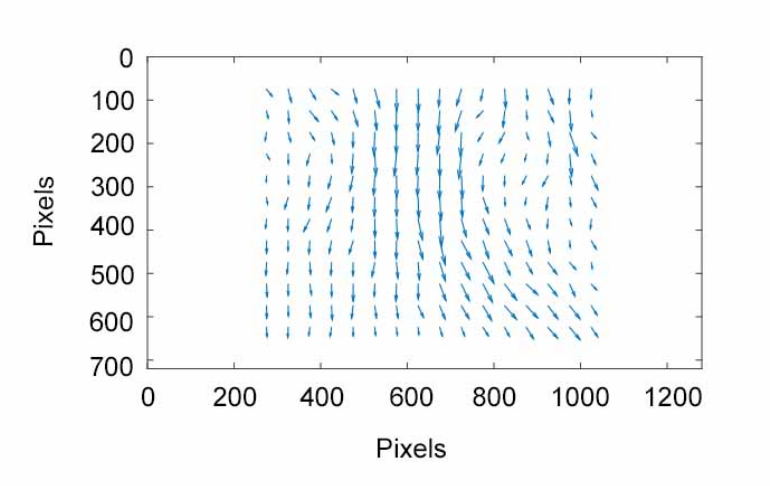

Figure 2.10. Displacement arrays of tracked meshes

2.3. Accuracy and error handling in analysis

Precision is the random difference between multiple measurements of the same quantity which will be influenced by test patch size, soil type and movement distance. Accuracy is he systematic difference between a measured quantity and the true value. In order to see the influence of test patch size on average settling velocity, three different test patch sizes are chosen as shown in Figure 2.11.

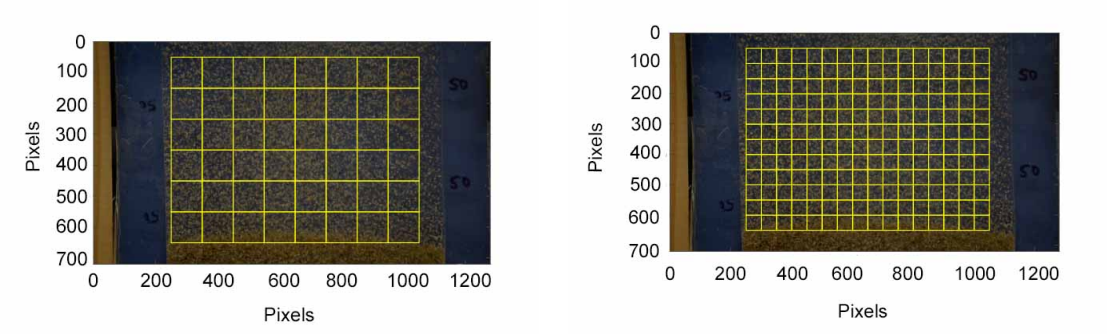

(a) (b)

Figure 2.11 Selected test patches with different sizes (a) patch size of 100×100 pixels, (b) patch size of 50×50 pixels

By using GeoPIV, the displacement vectors of selected patches can be extracted as shown in Figure 2.12.

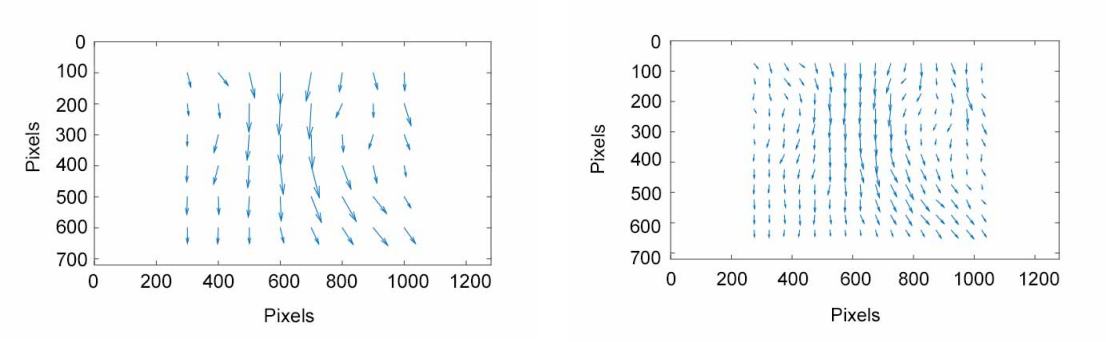

(a) (b)

Figure 2.12 Displacement vector of selected patches (a) patch size of 100×100 pixels, (b) patch size of 50×50 pixels

The errors are a function of the PIV patch size (White et al., 2003). The PIV patch size can influence the number of measurement points. White et al. (2003) concluded that by using smaller PIV patches, the measurement array size can be increased, at a cost of reduced precision. As shown in Figure 2.12, the array size of patches with 50 ×50 pixels size is larger than that of 100 ×100 pixels patch size.

CHAPTER 3: PROPPANTS SETTLING IN A SMOOTH SURFACE SLOT

3.1 Overview

This chapter presents results of experimental study of proppant slurry settling in a 2 mm narrow slot using fluids with different viscosity. Three different fluids are composed of 50 %, 75 % and 85 % glycerol-water volumetric ratios, which represent a wide span of proppant carrying fluid dynamic viscosities used in the field. The 2 mm wide slot represent a relatively narrow part of the hydraulic fracture. One of the goals of this study is to identify pattern and nature of proppant settling in a narrow fracture and make a comparison with existing relationships used in oil, gas and geothermal industry. Therefore, the GeoPIV method is used as a tool for mapping and identifying proppant settling rates on the levels of a single particle, particle agglomerate and multi-particle slurry areas. Results are grouped around relationships between proppant settling velocity, proppant local concentrations, individual particle and agglomerate size, fluid dynamic viscosity, and particle diameter to fracture size ratio. Additionally, the average settling velocities are also compared with previous relationships proposed by Gadde et al. (2004), Clark et al. (1981), Daneshy (1978) and Liu and Sharma (2005).

3.2. Proppant settling in 50 % glycerol-water solution

3.2.1. General slurry behavior

The GeoPIV method is used for analysis of the slurry behavior after turning the experimental setup into vertical position. The general trend of particle velocity directions is investigated in order to isolate patches with a predominant vertical settling motion. Total time of the video recording analysis permits identifying behavior of slurry as a general

motion. In order to analyze the overall slurry settling in 2 mm narrow slot for early and later times, meshes are chosen as shown in Figures 3.1 and 3.2.

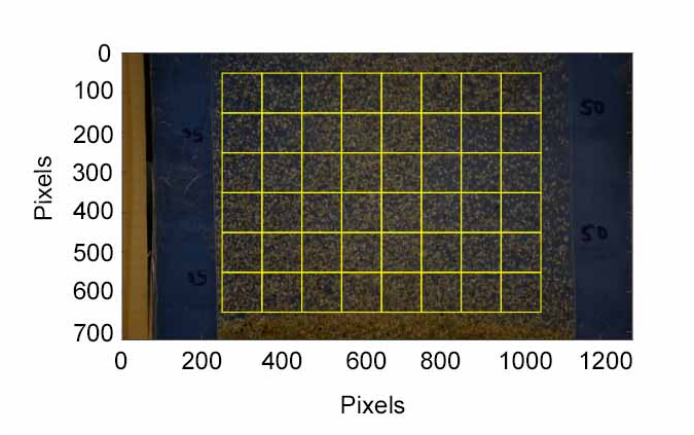

Figure 3.1. Selected patches when t=0.05 s

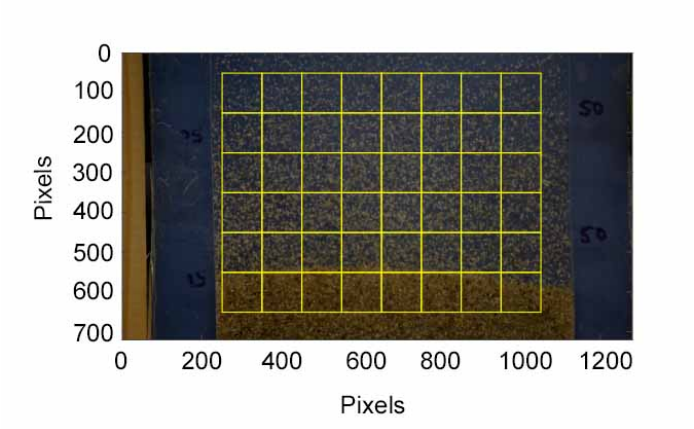

Figure 3.2. Selected patches when t=5.0 s

Figures 3.3a to 3.3f show particle displacement vector arrays extracted from the earlier times at the beginning of settling of the test at times t_1=0.00 s, t_2=0.05 s, t_3=0.10 s, t_4=0.15 s, t_5=0.20 s and t_6=0.25 s. Each vector represents the direction and relative magnitude accumulative of particles displacement for a given patch. At the beginning of the test, horizontal and vertical displacements have approximately the same magnitude, resulting in circular particle motion or swirls. It is reasonable that at the early time of the

test, the horizontal movement cannot be ignored and slurry motion is not treated as the settlement.

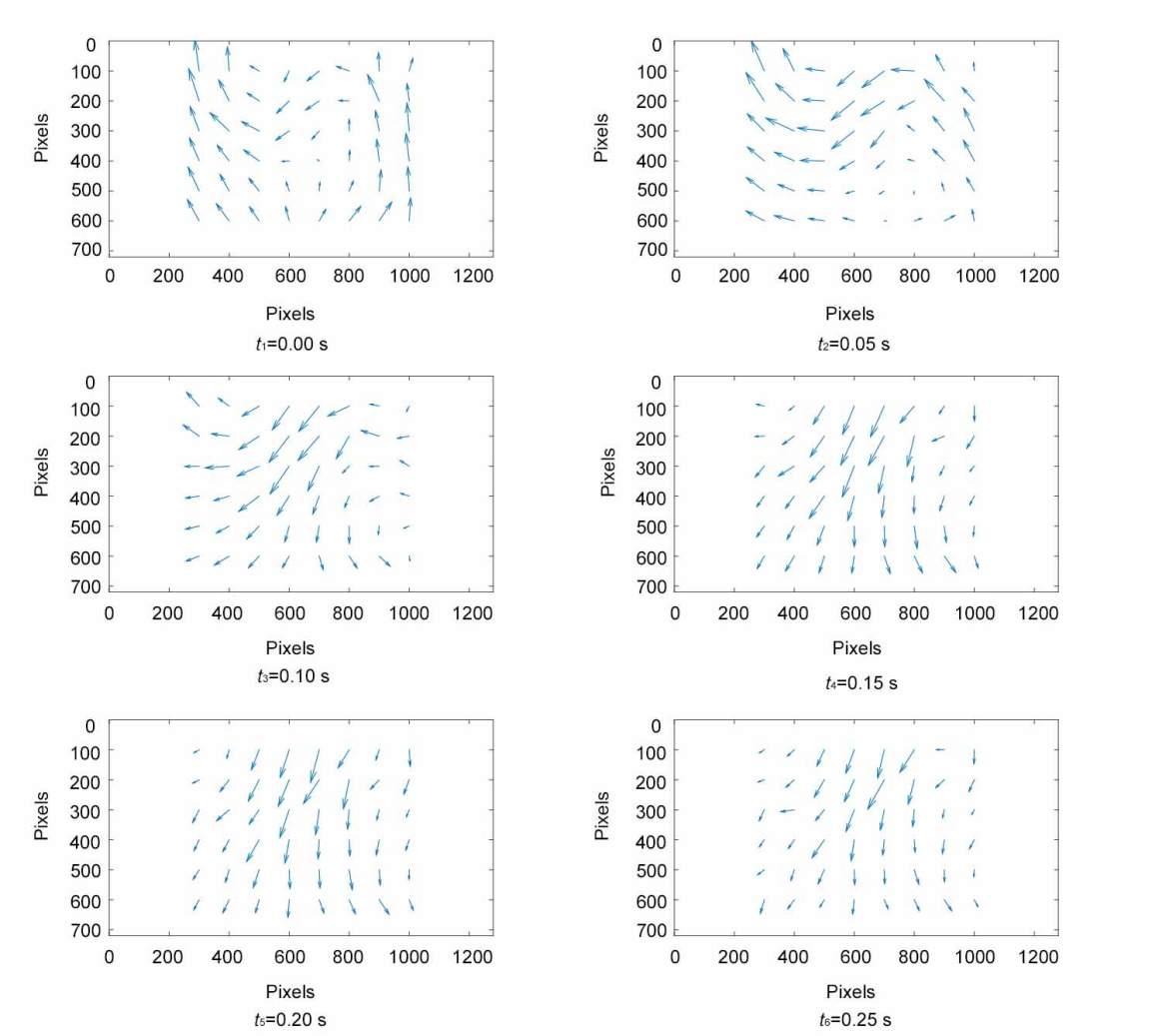

Figure 3.3. Displacement vectors of particles

Particles move in erratic paths dominated by swirling and rotational motion as shown in Figure 3.3. However, the swirling motion gradually calms and vertical settling starts to dominate at later times. Figures 3.4 shows the displacement vectors at the end part of the test, at times t_1=5.00 s, t_2=5.05 s, t_3=5.10 s, t_4=5.15 s, t_5=5.20 s and t_6=5.25 s. The displacement vectors are approximately vertical. Thus after approximately 5 seconds, the overall movement of sand slurry can be treated as settlement.

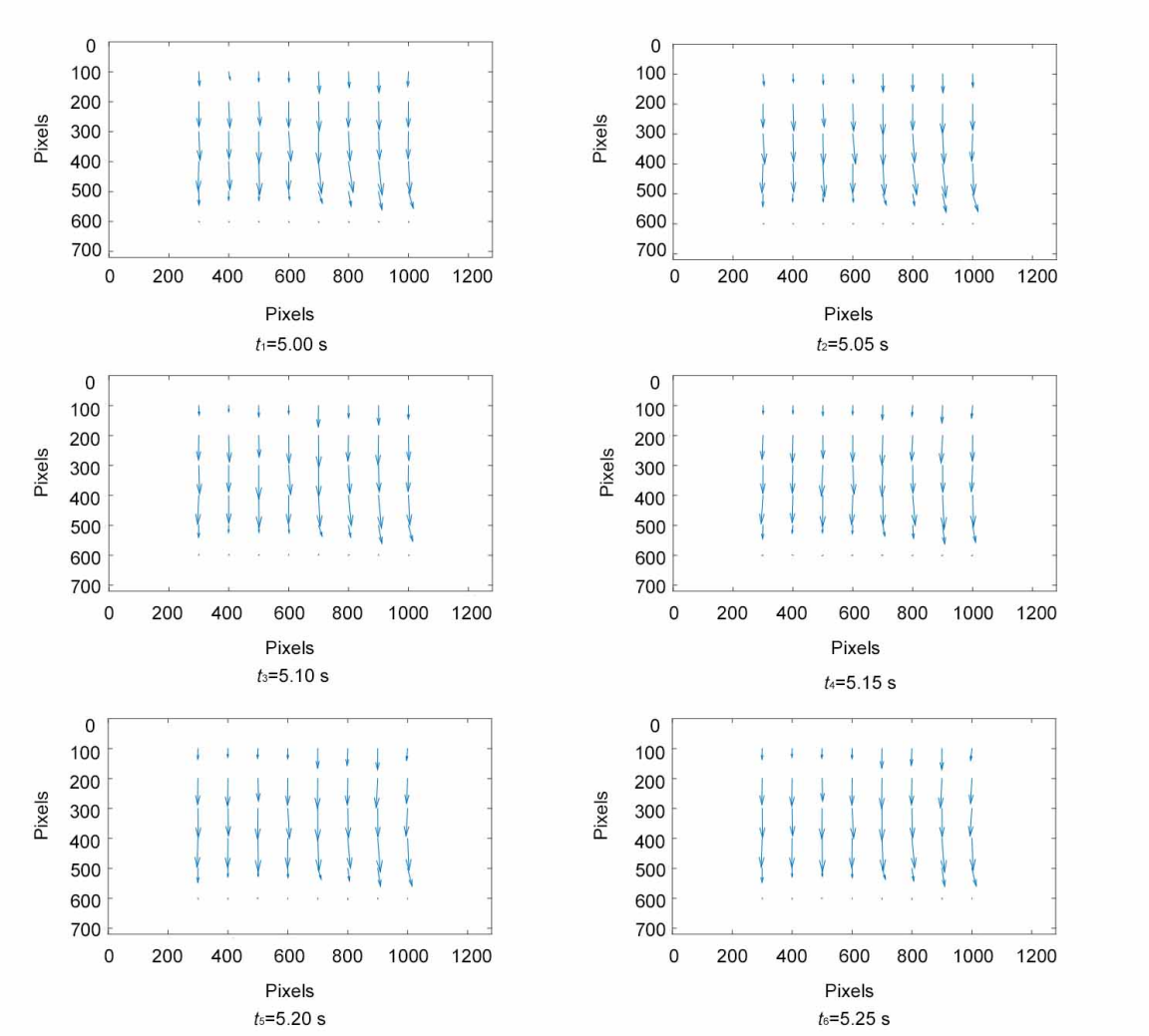

Figure 3.4. Displacement vectors of particles

3.2.2 Analysis of individual particle and agglomerate settling rates

Settling of individual particles is analyzed using the GeoPIV method, where individual particles of several different sizes corresponding to the sieve sizes used are identified and their motion is analyzed in settling regime. Figure 3.5 shows pictures for analyzed single particles with different estimated diameters. Since sand particles are not ideally spherical, the diameter is approximated as shown in Figure 3.5. Particle settling is

related to the Stokes' law sphere settling in unbounded fluid, in order to see if there are any significant wall or slurry concentration effects.

Figure 3.5. Single sand particle diameters

The expression of Stokes' law for the terminal velocity of sphere falling in quiescent fluid is:

$$v_t = \frac{gd^2(\rho_p - \rho_f)}{18\mu} \tag{3.1}$$

where v_t is the flow settling velocity (m/s), g is the gravitational acceleration (m/s^2), ρ_p is the particle mass density (kg/m^3), ρ_f is the fluid mass density (kg/m^3) and μ is the fluid dynamic viscosity (Pa·s). The density of proppant sand used in the tests here is 2650 kg/m^3. When the volumetric percentage of glycerol in water is 50 %, the density of fluid is 1126.3 kg/m^3 and the dynamic viscosity is 0.006 Pa·s (six times larger than water).

Table 3.1. shows calculated prediction of Stokes' settling velocity for approximate different particle sizes which were identified in the experiment. The comparison is made in order to investigate if the individual particle settling can be predicted with Stokes' law for the case when slurry settles between two narrow walls.

Table 3.1. Prediction by Stokes' law for single particle

Particle diameter, d (mm)	Stokes' terminal velocity, v_t (mm/s)
0.29	11.63
0.34	15.98
0.46	29.26
0.69	65.83
0.8	88.49

Figure 3.6 shows the velocity of different particle sizes in *x* direction and Figure 3.7 shows the velocity of different particle sizes in *y* direction. It can be seen that the velocities in *y* direction are much larger than those in *x* direction. Thus the movements can be treated as settling while the movements in *x* direction can be ignored. Comparing the experimental results with predictions made by Stokes' law, it can be found that when the particle size is as small as 0.3 mm or even smaller, the Stokes' law gives acceptable particle settling prediction. However, with increasing of particle size, the predicted particle settling velocity from Stokes' law is larger than test data. The measured settling velocities of single particles of different sizes are similar, with a very small increase as the particle size increases. It can be concluded from these tests that the Stokes' law prediction only works when the particle size is approximately 4-5 times smaller than the fracture width in 50 % glycerol-water solution.

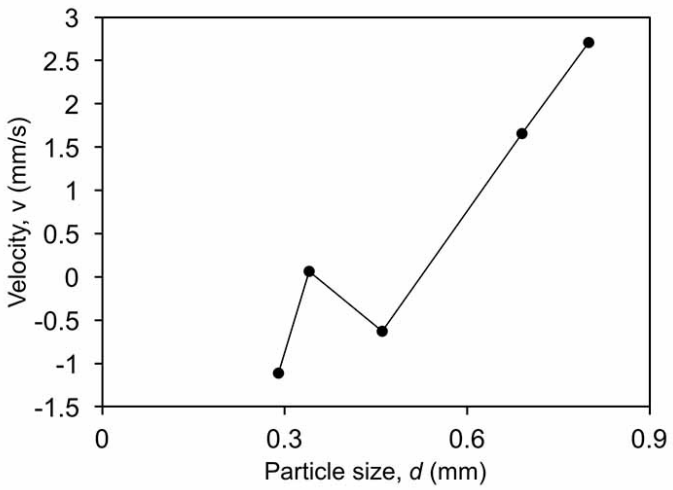

Figure 3.6. Velocities of one single particle in *x* direction vs. particle size

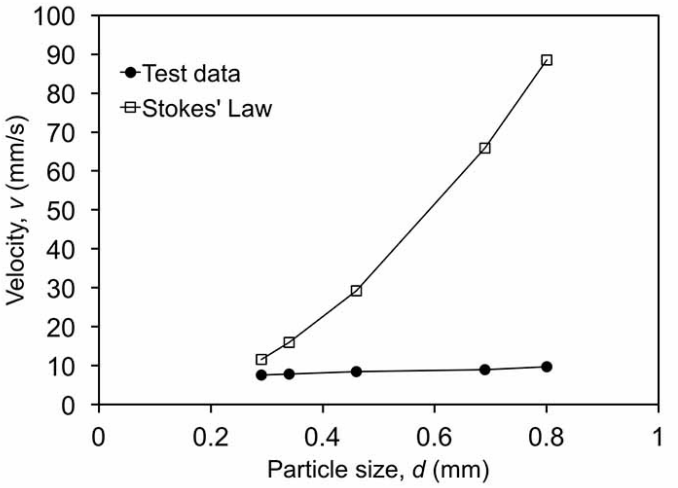

Figure 3.7. Velocities of one single particle in *y* direction vs. particle size and comparison with the Stokes' law prediction

Agglomerates of small and large number of particles can be seen during the settling process. One of the objectives of this study is to investigate how agglomerates affect proppant settling and to detect nature and occurrence of agglomerates in different carrying fluids. Although many of the agglomerated particles shapes are irregular, there are still recognizable regular shapes such as rectangle, triangle and round. First, two brands of agglomerate' shapes are analyzed, "rectangle" and "triangle". Figure 3.8 shows two chosen "rectangular" shaped agglomerates with different lengths and same widths. Comparing Figure 3.9 with Figure 3.10, the average velocities in *y* direction are more than ten times of those in *x* direction, so it is reasonable to neglect the movements in *x* direction. As shown in Figure 3.10, the "rectangular" shaped agglomerates with larger size have faster settling velocity which is consistent with the general effect of size in Stokes' law.

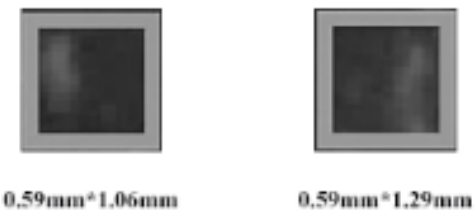

Figure 3.8. Different sizes of the "rectangular" shaped agglomerate

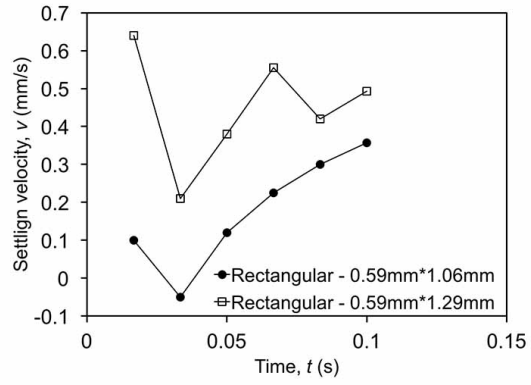

Figure 3.9. Average velocities in *x* direction of "rectangular" shaped agglomerate

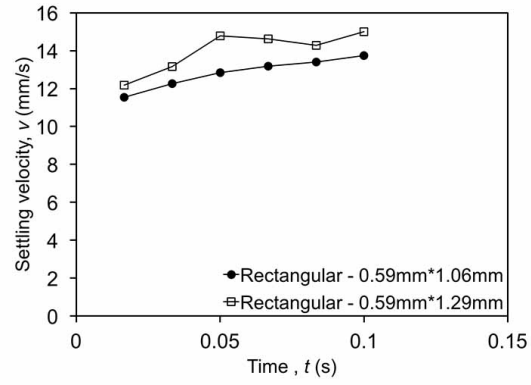

Figure 3.10. Average velocities in *y* direction of "rectangular" shaped agglomerate

Figure 3.11 shows two different "triangle" agglomerates which are analyzed. For the "triangle" shaped agglomerate, the larger size has faster settling during the test as shown in Figure 3.12. Comparing Figure 3.10 with Figure 3.13, it is evident that the average velocities of "rectangular" shaped agglomerates, in spite of their smaller width dimension, are larger than the "triangle" shaped agglomerate during settling. The area of "triangle" shaped agglomerate is larger than "rectangular" shaped agglomerate, thus the average settling velocity of "triangle" shaped agglomerate is faster than rectangular shaped agglomerate.

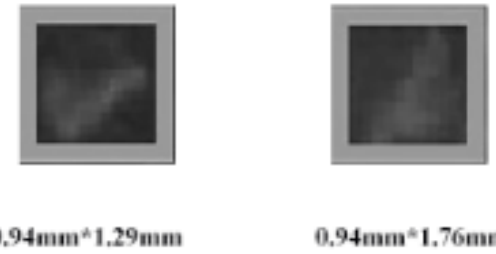

Figure 3.11. Different sizes of the "triangle" shaped agglomerate

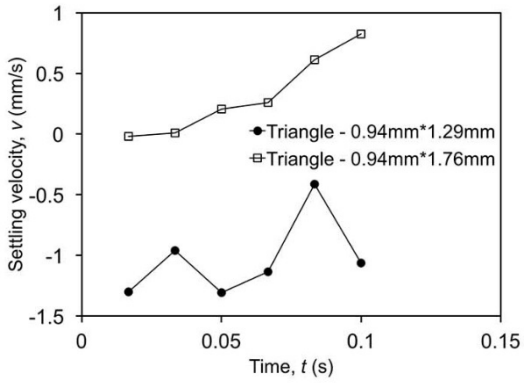

Figure 3.12. Average velocities in *x* direction of "triangle" shaped agglomerate

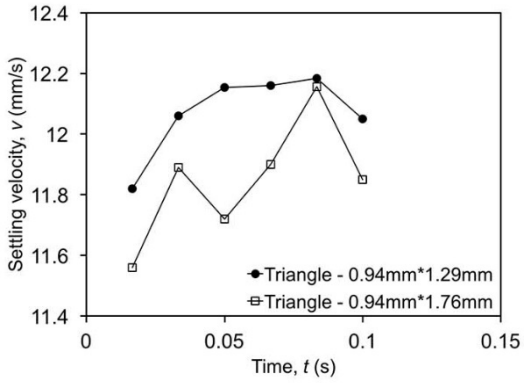

Figure 3.13. Average velocities in *y* direction of "triangle" shaped agglomerate

Figure 3.14 and Figure 3.15 show the ratio of settling velocity with prediction made by Stokes' law.

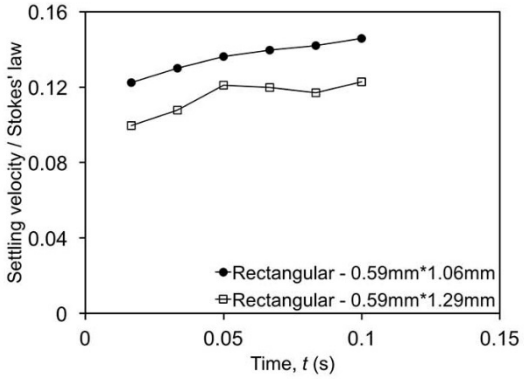

Figure 3.14 Comparison of the average experimental settling velocity of agglomerated particles of rectangular shape for 50 % glycerol-water fluid, where the settling velocities are normalized with the Stokes' law settling velocity

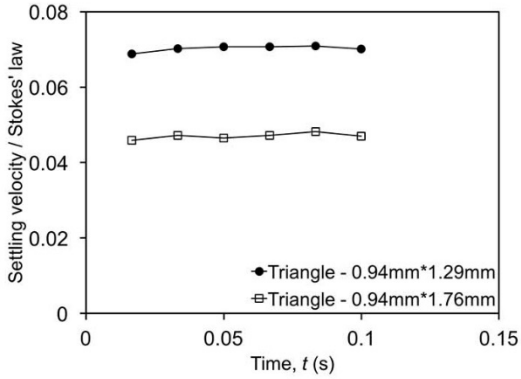

Figure 3.15 Comparison of the average experimental settling velocity of agglomerated particles of triangle shape for 50 % glycerol-water fluid, where the settling velocities are normalized with the Stokes' law settling velocity

As shown in these two figures, the ratio of settling velocity with prediction made by Stokes' law which is using the circumcircle of different shapes of agglomerated particles is smaller when the size is larger. This is consistent with the conclusion for a single particle size, when the particle diameter approaches the slot width. Thus for agglomerated particles

with rectangular shape and triangle shape, the difference between experimental results and predictions made by Stokes' law will increase while the size increasing.

Second, agglomerates that can be approximated as spherical or round are studied. Figure 3.16 shows three selected agglomerates of particles in fluid. The diameter of the agglomerates was estimated and shown in Figure 3.16, in order to obtain the Stokes' law settling velocity prediction. Table 3.2 shows the predicted settling velocity of different agglomerated particle size according to Stokes' law.

Figure 3.16. Different sizes of agglomerated particles

Table 3.2. Prediction by Stokes' law for agglomerates

Agglomerate diameter, d (mm)	Stokes' terminal velocity, v_t (mm/s)
0.94	122.17
1.00	138.26
1.12	171.89
1.20	199.10
1.24	212.59

As shown in Figure 3.17, the differences between test data and the prediction made by Stokes' law are increasing as the agglomerate size increases. The previous Figure 3.7 that refers to a single particle in fluid also shows the comparison between test data with the prediction of Stokes' law, where the same trend can be found as in Figure 3.17.

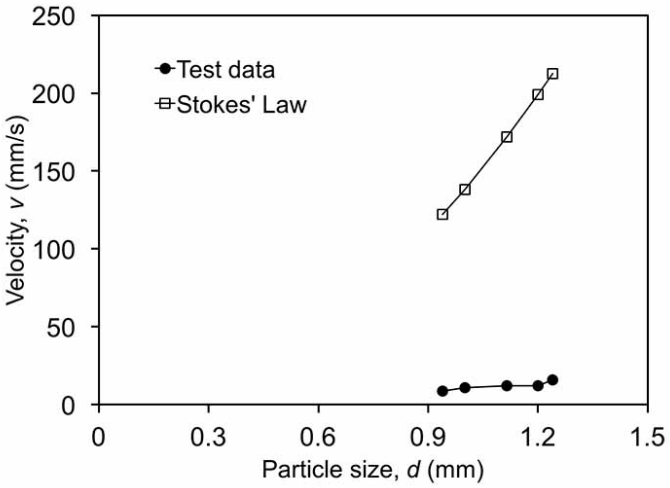

Figure 3.17. Velocities of one agglomerated particles in *y* direction vs. particle size

Figure 3.18 shows settling velocities of both the individual analyzed particles and the agglomerates of particles versus their approximate size.

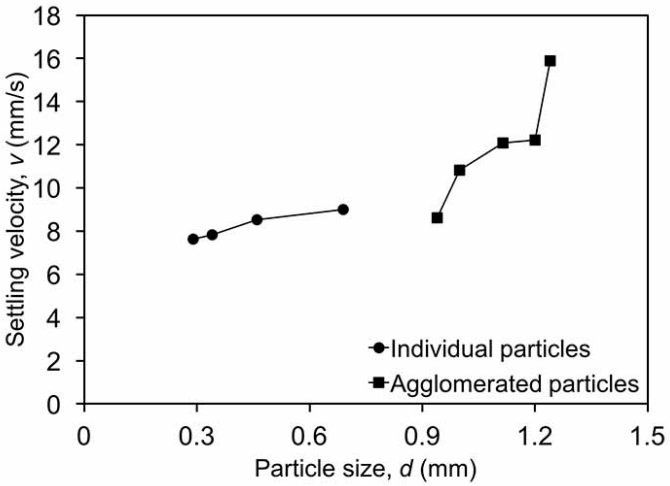

Figure 3.18. Settling velocity of individual particles and particle agglomerates in 50 % glycerol-water fluid

The consistency is visible showing how the settling velocity increases with size. It can be seen that with the increasing of particle size, the settling velocity increases.

It can also be found that the average velocity of the slurry in the observed patch corresponds to the velocity of a single or an agglomerated particle with the diameter of 0.4 - 0.9 mm as shown in Figure 3.19. Since the average particle diameter of the used sand is

0.66 mm, the slurry settles at the similar rate as the used sand. To conclude, the effect of larger agglomerates is almost negligible in 50 % glycerol-water solution, meaning that the agglomerates do not form at an extent that would be sufficient and significant for increasing the general settling rates.

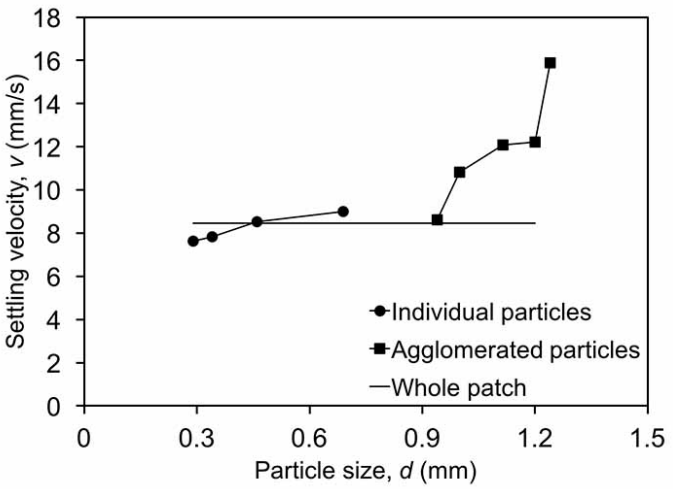

Figure 3.19. Settling velocity of individual particles and particle agglomerates with average settling velocity in 50 % glycerol-water fluid

Figure 3.20 shows a comparison of all observed agglomerates settling rates, normalized with the Stokes' law.

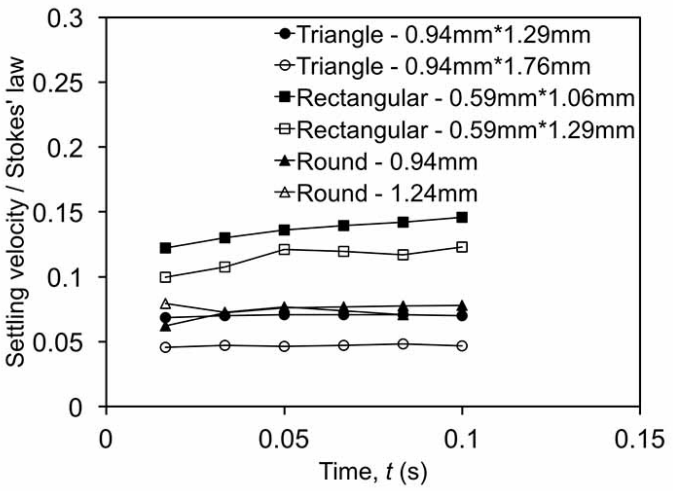

Figure 3.20 Comparison of the average experimental settling velocity of agglomerated particles of different shapes for 50 % glycerol-water fluid, where the settling velocities are normalized with the Stokes' law settling velocity

Comparing the experimental settling velocity of particles of different agglomerated size in Figure 3.20, it can be found that the Stokes' law cannot predict the settling velocity well when the particle size is large. However, among the larger agglomerated particles with different shapes, the differences between Stokes' terminal velocities with experimental results are smaller when the shape is rectangular.

3.2.3. Effects of particle volumetric concentrations on slurry settling

The effects of particle volumetric concentration on slurry settling is analyzed by investigating patches of particles during the settling phase with high and low concentrations using the GeoPIV method. At the same time stage, the particle volumetric concentrations of chosen patches are different for different locations. The objective is to investigate how the proppant concentration affect the settling velocity of the slurry in a narrow fracture. The volumetric concentration is defined by the ratio of whole particles volumes with the volume of chosen patches. The particle volumetric (3D) and superficial (2D) concentrations of analyzed patches with different concentrations are shown in Figure 3.21.

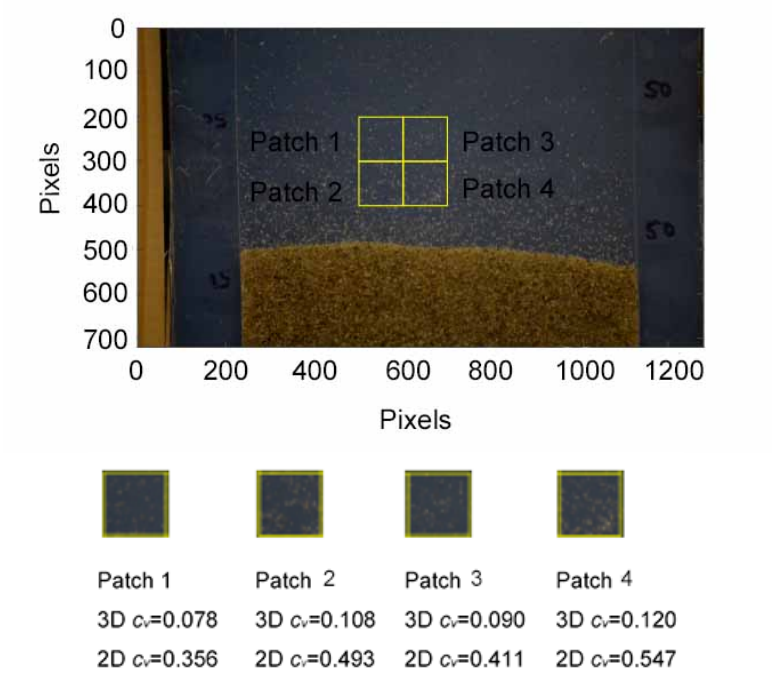

(a)

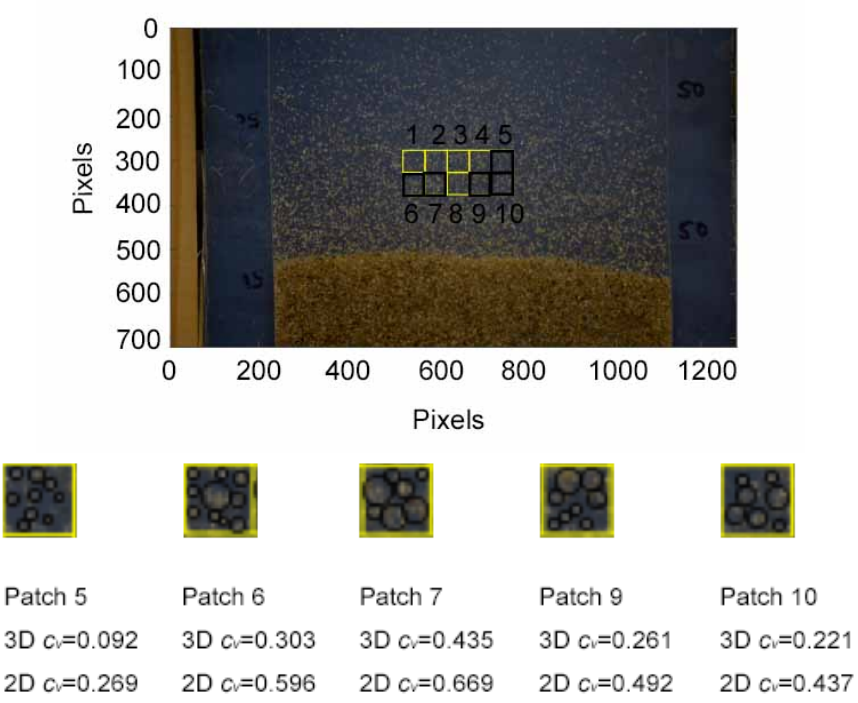

(b)

Figure 3.21. The analyzed patch of settling particles in the 50 % glycerol-water fluid with (a) low concentration c_v=0.099, (b) medium concentration c_v=0.262

Figure 3.22 (a) shows the settling velocity of chosen patches shown in Figure 3.21 (a), where the particle concentrations are relatively low. It can be found that the settling

velocity profile slightly oscillates around average value of 8.5 mm/s. The settling velocity of two upper patches 1 and 3 is slightly larger than of the patches 2 and 4, but the average of the whole area is. Patches 1 and 3 are with the 2D concentrations of c_v=0.356 and 0.411, while the concentrations of patches 2 and 4 are c_v= 0.493 and 0.547. Thus, the average settling velocity of patches with higher concentration (2 and 4) have lower settling velocity. In order to investigate the difference between previous relationships with test data while the concentration is higher, another five patches with c_v=0.092, 0.221, 0.261, 0.303 and 0.435 are analyzed as shown in Figure 3.21 (b). Figure 3.22 (b) shows the settling velocity of five chosen patches and also the average settling velocity of the whole patch. Generally, the average settling velocity of the observed part of the slurry is slightly lower in the case of higher average particle concentrations taken from Figure 3.21 (b). However, local oscillations about the average measured value are observed through looking at individual patches which form the general area.

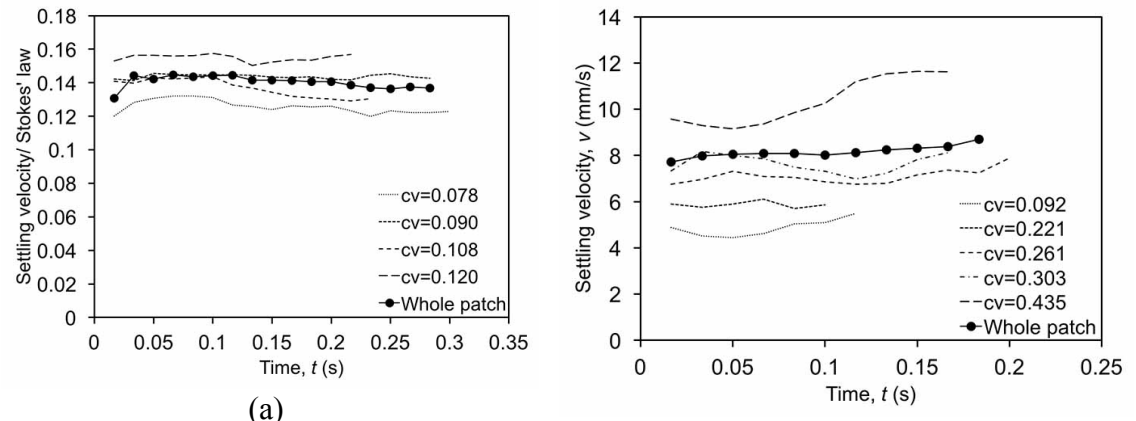

(a) (b)

Figure 3.22. Average settling velocity of proppant in the areas of chosen patches and the whole analyzed area for in 50 % glycerol-water fluid of (a) low concentration, (b) medium concentration

The relationship between particle settling velocity and particle local concentration is derived, as shown in Figure 3.23. Figure 3.23 (b) shows a trend of settling velocity

decrease with particle concentrations increase. It can be found that the average settling velocity would increase with increasing the concentration of selected as shown in Figure 3.23.

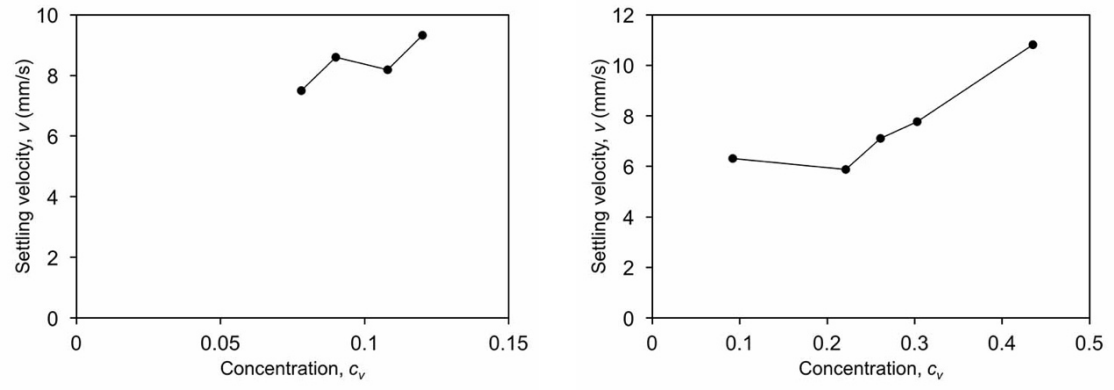

(a) (b)

Figure 3.23 Settling velocity with different concentration in 50% glycerol-water fluid of (a) low concentration, (b) medium concentration

Previous relationships between concentration with settling velocity of proppants which are proposed by other researchers, as given in the literature review chapter. In order to verify the validity of the previously published relationships for the proppant settling in a very narrow slots, comparisons are made with experimental results. Gadde et al. (2004) obtained empirical relationships of proppant settling velocity and proppant concentration:

$$v_s = v_0(2.37c_v^2 - 3.08c_v + 1) \qquad (3.2)$$

where v_0 is the particle settling velocity in unbounded fluid and c_v is particle volumetric concentration. The average concentration of these four patches in Figure 3.21 (a) is c_v=0.099, for 50% glycerol-water fluid, v_0 is equal to 60.23 mm/s when d=0.66 mm predicted by Stokes' law. Thus:

$$v_s = 60.23\times(2.37\times0.099^2 - 3.08\times0.099 + 1 = 43.26 \text{ mm/s}$$

The average concentration of the five patches in Figure 3.21 (b) is c_v=0.262, thus the terminal settling velocity predicted by Stokes' law is:

$$v_s = 60.23\times(2.37\times0.262^2 - 3.08\times0.262 + 1) = 23.16 \text{ mm/s}$$

Figure 3.24 shows settling velocity of particles at low concentrations and medium concentrations in a narrow slot, where the concentration dependent prediction is also plotted. It can be seen that according to Gadde et al. (2004) such low concentrations would not be significantly different from the Stokes' law prediction of a single particle settling velocity. In other words, little effect of concentration is predicted by Gadde et al. (2004) when the particle volumetric concentrations are low.

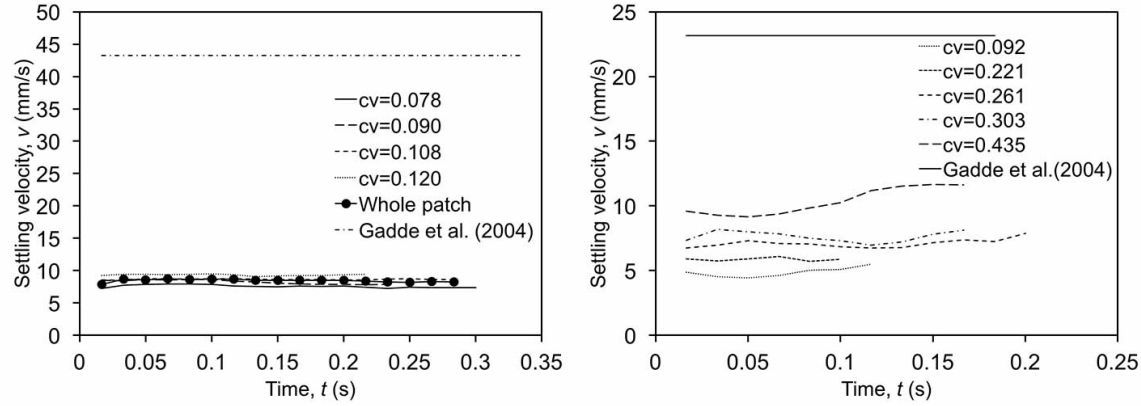

(a) (b)

Figure 3.24 Settling of particles at low concentrations in narrow slot with promoted agglomeration, compared to the relationship given by Gadde et al. (2004) in 50 % glycerol-water fluid of (a) low concentration c_v=0.099, (b) medium concentration c_v=0.262

Daneshy (1978) proposed the correlative equation for settling velocity:

$$v_s = v_0[\frac{1 - c_v}{10^{1.82c_v}}] \tag{3.3}$$

where v_s is the slurry settling velocity, v_0 is the single particle settling velocity and c_v is the volumetric particle concentration in the slurry. For 50 % glycerol-water fluid,

v_0=60.23 mm/s when d=0.66 mm predicted by Stokes' law, c_v=0.099 and c_v=0.262 for the two whole patches, thus:

$$v_s = v_0\left[\frac{1-c_v}{10^{1.82c_v}}\right] = 60.23\times\frac{1-0.099}{10^{1.82\times0.099}} = 35.84 \text{ mm/s}$$
$$v_s = v_0\left[\frac{1-c_v}{10^{1.82c_v}}\right] = 60.23\times\frac{1-0.262}{10^{1.82\times0.262}} = 17.59 \text{ mm/s}$$

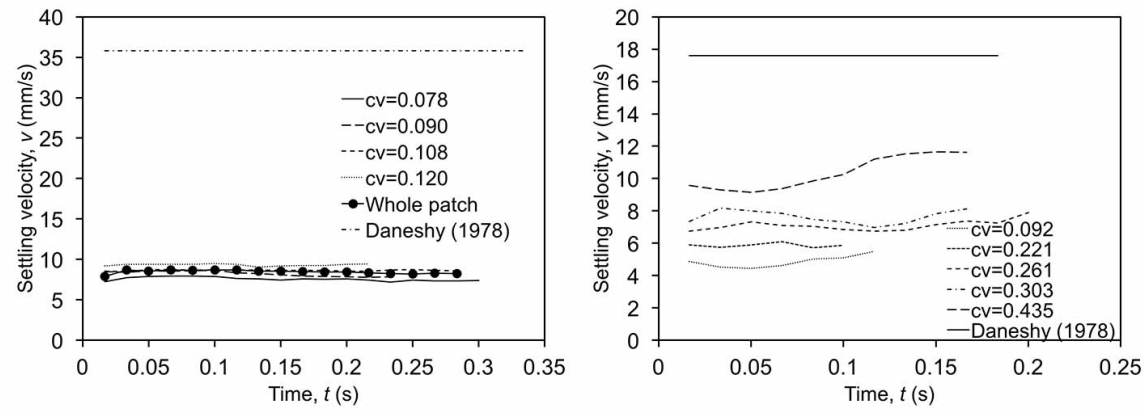

(a) (b)

Figure 3.25. Comparison of the average experimental settling velocities with the relationship proposed by Daneshy (1978) for a narrow slot and low particle concentration in 50 % glycerol-water fluid of (a) low concentration c_v=0.099, (b) medium concentration c_v=0.262

The relationship proposed by Daneshy (1978) also predicts settling velocities close to the Stokes' law prediction at low particle concentration. At higher particle concentrations, the prediction made by Daneshy (1978) is closer to experimental results. Comparing Figure 3.25 with Figure 3.24, when the concentration is low, the prediction made by Daneshy (1978) is more close to test data compared with Gadde et al. (2004). Clark et al. (1981) also proposed the relationship between settling velocity with concentration:

$$v_s = \frac{1}{1+6.88c_v}v_0 \tag{3.4}$$

where v_s is the slurry settling velocity, v_0 is the single particle velocity and c_v is the volumetric particle concentration in the slurry. For 50 % glycerol-water fluid, v_0=60.23 mm/s when d=0.66 mm predicted by Stokes' law, c_v=0.099 and c_v=0.262 for the two whole patch, thus:

$$v_s = \frac{1}{1+6.88c_v} v_0 = \frac{1}{1+6.88\times0.099} \times 60.23 = 35.83\text{mm/s},$$
$$v_s = \frac{1}{1+6.88c_v} v_0 = \frac{1}{1+6.88\times0.262} \times 60.23 = 23.39\text{mm/s}.$$

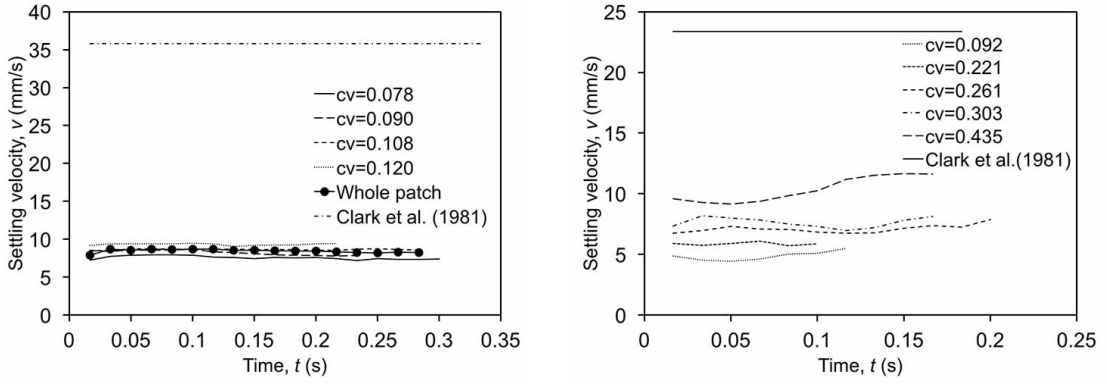

(a) (b)

Figure 3.26. Comparison of the average experimental settling velocities with the relationship proposed by Clark et al. (1981) for a narrow slot and low particle concentration in 50 % glycerol-water fluid of (a) low concentration c_v=0.099, (b) medium concentration c_v=0.262

The relationship proposed by Clark et al. (1981) predicts higher settling velocity at low concentrations as shown in Figure 3.26(a). For the medium concentration, Clark's prediction is closer to experimental results compared with low concentration. Additionally, when the concentration is really low, the prediction made by Clark et al. (1981) seems fits better with experimental results than other two. Compared the relationships made by Gadde et al. (2004), Daneshy (1978) and Clark et al. (1981), it is obviously that at low concentration, the predicted settling velocities at very low particle concentrations are larger than experimental data as shown in Figure 3.27(a). However, among these three predictions,

the Daneshy (1978) and Clark et al. (1981) predict similar values, which are closer to test data. For medium concentrations which are plotted in Figure 3.27(b), comparing the experimental results with relationships proposed by Gadde et al. (2004), Clark et al. (1981) and Daneshy (1978), it can be seen that the predictions are closer to test data when concentrations are approximately larger than 0.35. While increasing concentrations of particles, the difference between predictions with test data become smaller. However, while the concentration is larger than 0.4, Gadde et al. (2004) and Daneshy (1978) predict slower than experimental settling while the prediction made by Clark et al. (1981) is faster.

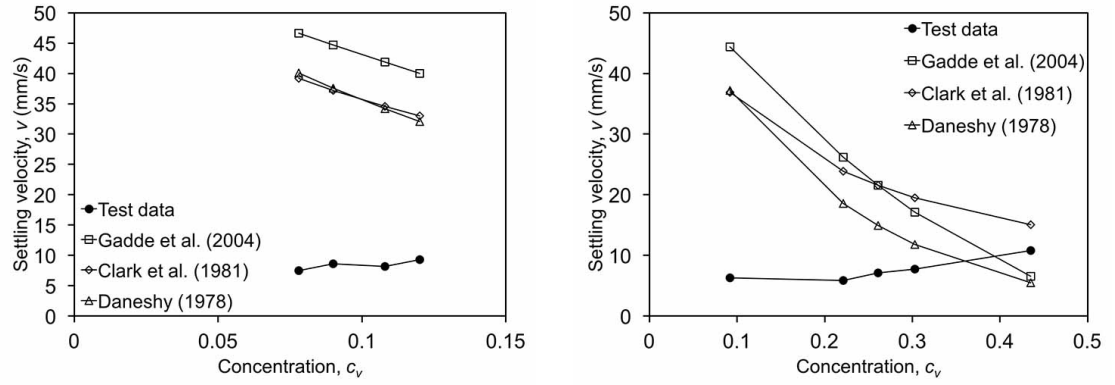

Figure 3.27. Comparison of the average experimental settling velocities with previous relationships for a narrow slot and low particle concentration in 50 % glycerol-water of (a) low average volumetric concentration c_v=0.099, (b) medium average volumetric concentration c_v=0.262

It can be found that by using volumetric calculation, the obtained particle concentrations seem obviously lower than what appears in figures taken with camera. Therefore, an alternative approach is taken to calculate superficial or two dimensional particle concentrations. Figures 3.21 (a) and (b) show both two dimensional and three dimensional estimate of particle concentration in each different patch. Settling velocity predictions by previously published relationships are re-calculated using the superficial

particle concentrations. Figure 3.28 shows the comparison between previous relationships and experimental results. At superficial particle concentrations of approximate c=0.4, Gadde et al. (2004) and Daneshy (1978) accurately predict the slurry settling velocity. At lower concentrations, the experimentally obtained settling velocities are lower than predictions, while being higher at higher concentrations. Clark et al. (1981) over predicts the settling velocities until the superficial concentration reaches c=0.7. Because of the difficulties while obtaining accurate particle volumetric concentrations from the recorded videos, two dimensional and three dimensional estimates are given. It can be argued that the accurate value lies somewhere in-between

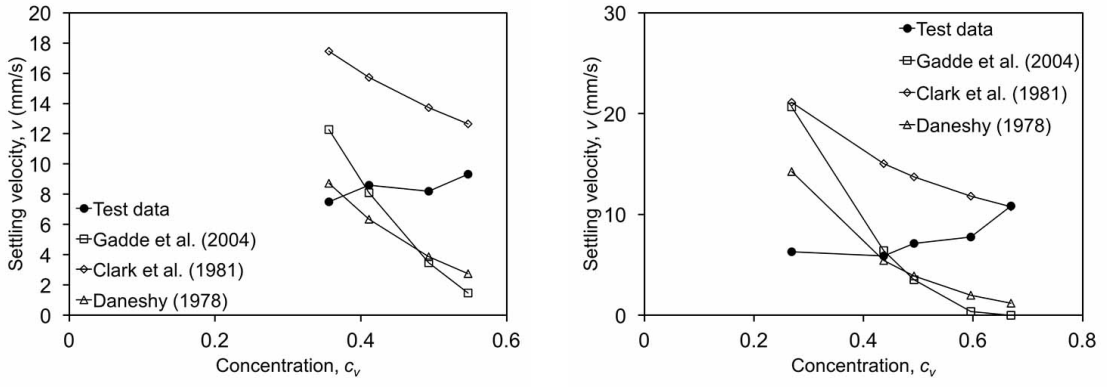

Figure 3.28. Comparison of the average experimental settling velocities with previous relationships for a narrow slot and low particle concentration in 50 % glycerol-water of (a) low average superficial concentration c_v=0.452, (b) medium average superficial concentration c_v=0.493

3.2.4. Effects of narrow slot on slurry settling

In order to better understand the effects of relationship between the fracture walls distance and particle diameters, the obtained experimental results are compared with another previously published relationship. Therefore, another comparison is made with the relationship proposed by Liu and Sharma (2005):

$$\frac{v_w}{v_0} = 1 - f(\mu)\frac{d}{B}; \left(\frac{d}{B} < 0.9\right)$$
$$\frac{v_w}{v_0} = g(u)\left(1 - \frac{d}{B}\right); \left(\frac{d}{B} \geq 0.9\right) \quad (3.5)$$
$$f(\mu) = 0.16\mu^{0.28}$$
$$g(u) = 8.26e^{-0.0061\mu}$$

where v_w is the proppant settling velocity between parallel walls, d is the particle diameter, B is the fracture aperture, v_0 is the single particle settling velocity in unbounded fluid and μ is the fluid dynamic viscosity. For 50 % glycerol-water fluid:

$$f(\mu) = 0.16\mu^{0.28} = 0.16\times 0.006^{0.28} = 0.038$$
$$\frac{d}{B} = \frac{0.66}{2} = 0.33 < 0.9$$
$$\frac{v_w}{v_0} = 1 - f(\mu)\frac{d}{B} = 1 - 0.038\times\frac{0.66}{2} = 0.987$$
$$v_w = 0.987\times 60.23 = 59.47 \text{mm}/s$$

As shown in Figure 3.29, the Liu and Sharma (2005) predict higher settling velocity than experimental data when the average particle diameter is assumed to be d=0.66 mm.

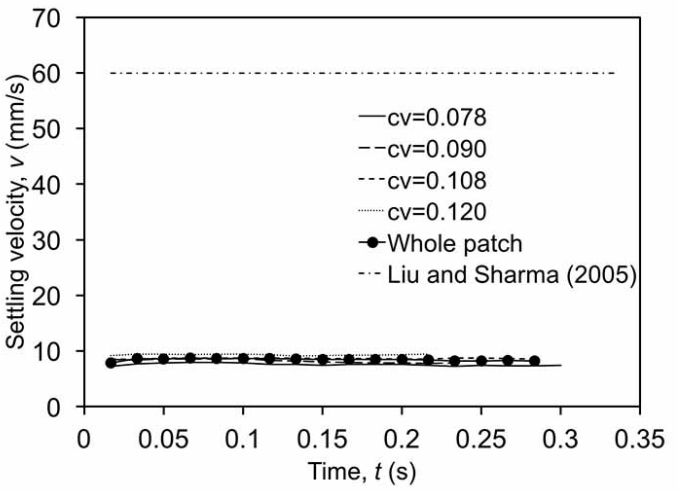

Figure 3.29. Comparison of the average experimental settling velocities with the relationship proposed by Liu and Sharma (2005) for a narrow slot and low particle concentration in 50 % glycerol-water fluid

However, during settling the agglomerates are present in the slurry, which can be easily seen from recorded video. Estimates of several agglomerate sizes are given in the

Chapter 3.2.2. It can be argued that the presence of larger agglomerates decreases the average ratio between slurry "particle" diameter and slot width. Thus the wall effect cannot be estimated using the original average diameter of a single sand particle. Table 3.3 shows calculation of the settling velocities from Liu and Sharma (2005) by using agglomerated particles sizes. Figure 3.30 shows the comparison of relationship proposed by Liu and Sharma (2005) with experimental results. The predicted settling velocity is still much larger than experimental results. Thus the wall effect here is not a dominated parameter for this test.

Table 3.3. Prediction of slurry settling between parallel walls for agglomerated particles

Agglomerate diameter, d (mm)	Liu and Sharma, v_w (mm/s)
0.94	59.15
1.00	59.08
1.12	58.94
1.20	58.85
1.24	58.80

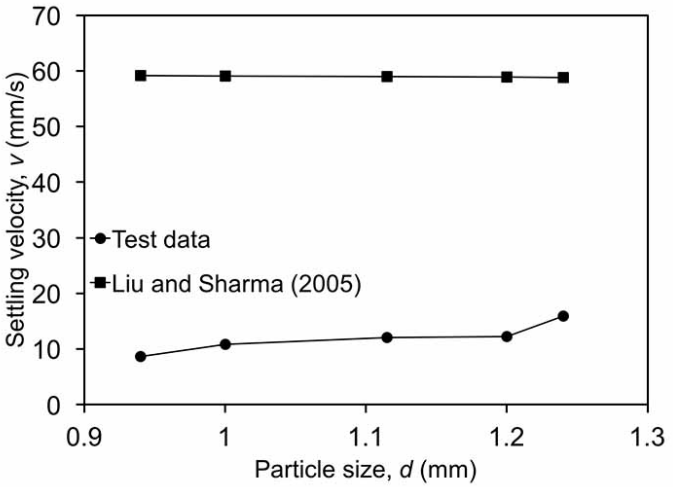

Figure 3.30 Comparison of the average experimental settling velocities with relationship proposed by Liu and Sharma (2005) for a narrow slot of different particle size in 50 % glycerol-water

Considering the wall effect of agglomerated particles, it's not well predicted by relationship proposed by Liu and Sharma (2005). In spite of the agglomeration, Liu and Sharma (2005) consider significant wall effect at d/B=0.9. The experimental results indicate that wall effects at lower particle diameter to wall distance already significantly slow down the slurry settling rates.

3.3 Proppant settling in 75 % glycerol-water solution

3.3.1. General slurry behavior

First, the total trend of particle velocity directions is investigated in order to isolate patches with a predominant vertical settling motion. Total time of the video recording analysis is performed for identifying different general behaviors of the slurry. The selected patches at the beginning and later of proppant settling in 75 % glycerol-water fluid are shown in Figure. 3.31 and Figure 3.32.

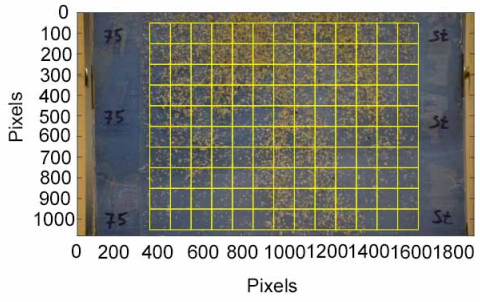

Figure 3.31. Selected patches at beginning period of settling

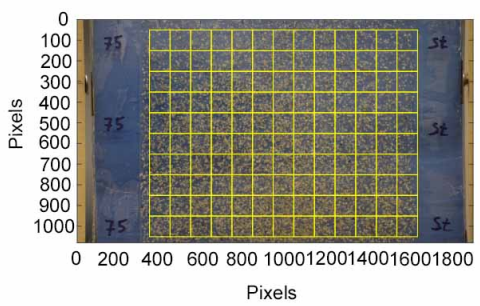

Figure 3.32. Selected patches at stable period of settling

It can be seen from Figure. 3.33 and Figure. 3.34 that at the beginning part of the flow movement, the interruption of adding soils is significant. The velocities in the x direction are large and cannot be ignored. Thus, at the beginning, the soil's behavior is not

settling but circling. After the flow becomes stable as shown in Figure 3.34, the movement of soils can be treated as settlement.

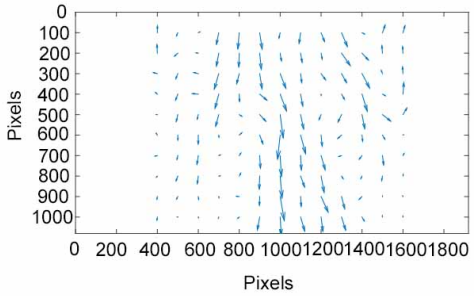

Figure 3.33. Displacement vector of selected patches at beginning period of settling

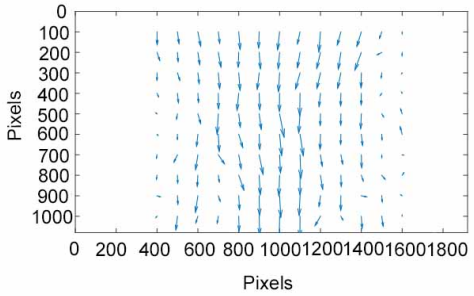

Figure 3.34. Displacement vector of selected patches at stable period of settling

3.3.2. Analysis of individual particle and agglomerate settling rates

Settling of individual particles is analyzed using the GeoPIV method, where individual particles of several different sizes are identified and their motion is analyzed in settling regime. Figure 3.35 shows the analyzed particle sizes.

Figure 3.35 Different sizes of one single particle in 75% glycerol-water mixture

Using the Stokes' law, a comparison is made between the settling of individual particle and ideal particle in unbounded fluid without wall constraints, as shown in Table 3.4. The density of proppants sand particle is 2650 kg/m^3. When the percentage of glycerol is 75 %, the density of fluid is 1198.45 kg/m^3 and the dynamic viscosity is 0.0355 Pa·s. By using the Stokes' law, the settling velocity of an ideal spherical particle with respect of particle sizes was presented in Table 3.4.

Table 3.4 Prediction by Stokes' law for single particle

Particle diameter, d (mm)	Stokes' terminal velocity, v_s (mm/s)
0.38	3.22
0.56	7.00
0.60	8.03
0.75	12.55
0.80	14.28
0.84	15.75
0.94	19.72
1.00	22.32
1.13	28.50

Figure 3.36 shows the comparison between the experimental data and the prediction made by Stokes' law for the individual particle settling. It can be seen that when the particle size increases, the difference between prediction made by Stokes' law with test data also increases. The measured settling velocities of single particles of different sizes are similar, with a very small increase as the particle size increases. It can be concluded that the Stokes' law prediction only works when the particle size is approximately 5-6 times or less small than the fracture width.

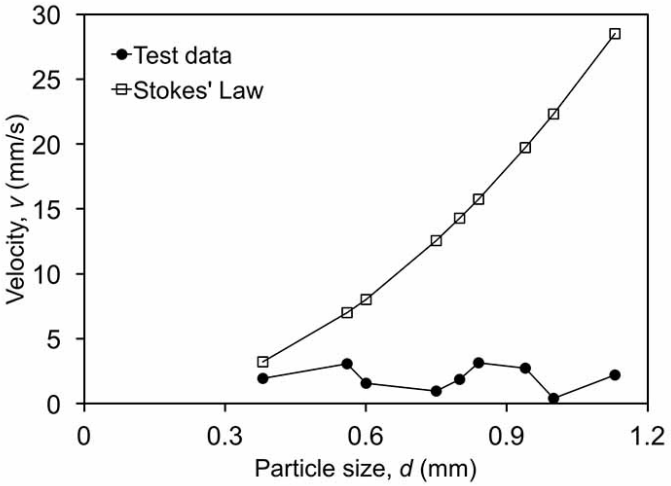

Figure 3.36. Velocities of one single particle in y direction vs. particle size

The single particles are agglomerated with each other and form different sizes of group particles. Figure 3.37 shows the estimated agglomerate sizes in 75% glycerol-water mixture fluid.

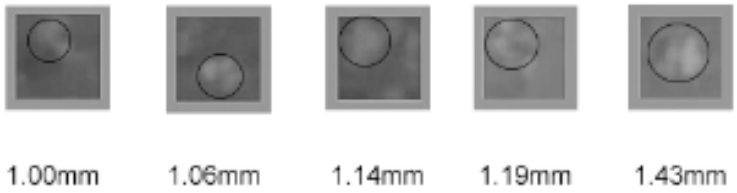

Figure 3.37. Different sizes of agglomerated particles

As shown in Figure 3.37, different sizes of agglomerated particles have different average settling velocities. As the diameter of an agglomerated particle increases, the settling velocity becomes higher. The comparison between the experimental data and the Stokes' law prediction in Figure 3.38 shows that the difference between the two average velocities becomes more significant as the particle size increases.

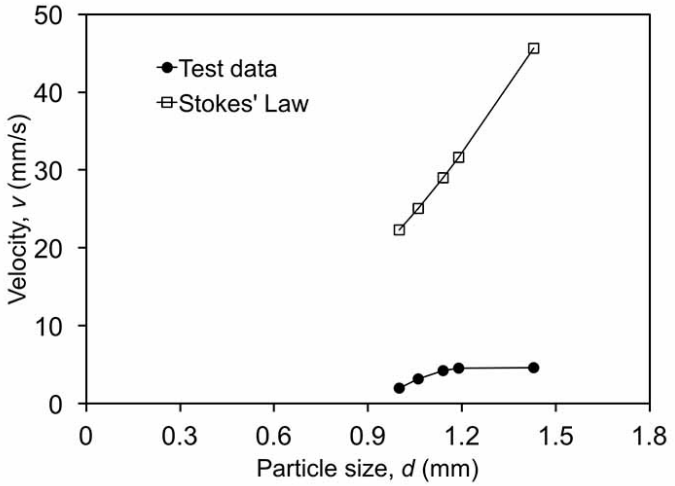

Figure 3.38. Velocities of agglomerated particles in *y* direction vs. particle size

Comparing the average settling velocity of single particle with agglomerated particles, it can be found that the average settling velocity increases with the increasing of particle size, which is shown in the plot in Figure 3.39.

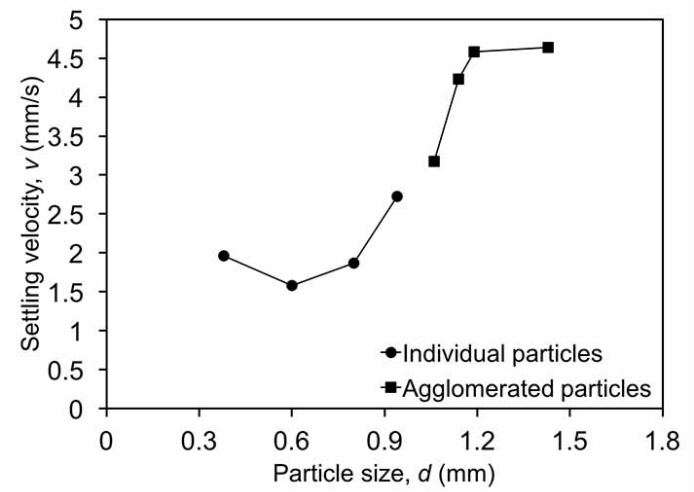

Figure 3.39 Settling velocity of individual particles and particle agglomerates in 75 % glycerol-water fluid

A comparison of settling is observed in Figure 3.41 normalized with the Stokes' law prediction for removing effect of fluid and particle density, fluid viscosity and particle size. The individual particles and agglomerated particles are from one patch as shown in Figure 3.40, thus the average velocity can be extracted. It can be found that the ratio of settling velocity with prediction made by Stokes' law for the whole patch is the same as that of particle size with around d=0.6 mm which is similar with the diameter of proppant that has been used.

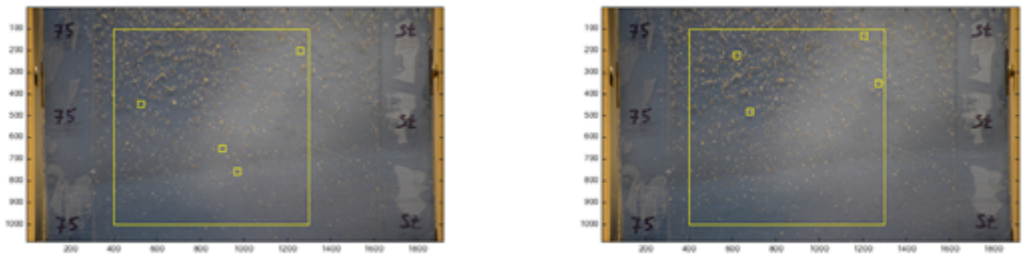

a) Chosen patches of single particles b) Chosen patches of agglomerates

Figure 3.40 Chosen patches of single and agglomerated particles

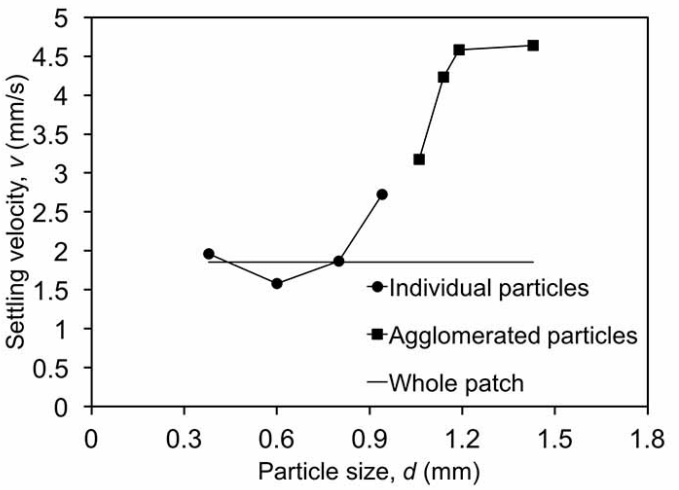

Figure 3.41 Comparison of the average experimental settling velocity of particles in the selected area of the whole patch and individual particle agglomerates of different sizes for 75 % glycerol-water solution

It can be seen that with the increasing of particle size, the settling velocity increases. It can also be found that the average velocity is consistent with velocity of single or agglomerated particle with the diameter of 0.4-0.8 mm.

3.3.3. Effects of particle volumetric concentrations on slurry settling

An area with dominant vertical motion and relatively low particle volumetric concentration of c_v=0.0312 is analyzed for investigating the influence of particle agglomerations on the average settling velocity of proppant in a narrow fracture. The size of the patch is 20 x 20 mm, which is further divided into 4 square areas. In order to investigate the difference between previous relationships with test data when the particle volumetric concentration is higher, four patches shown in Figure 3.41 with c_v=0.034, 0.024, 0.048, 0.025 are analyzed. Figures 3.42 (a) and (b) show the analyzed group of settling 20/40 mesh sand proppant in a 2 mm wide slot between two Plexiglas plates. The settling

velocities of the whole patch, square areas, individual particles and particle agglomerates are monitored during settling using the GeoPIV software.

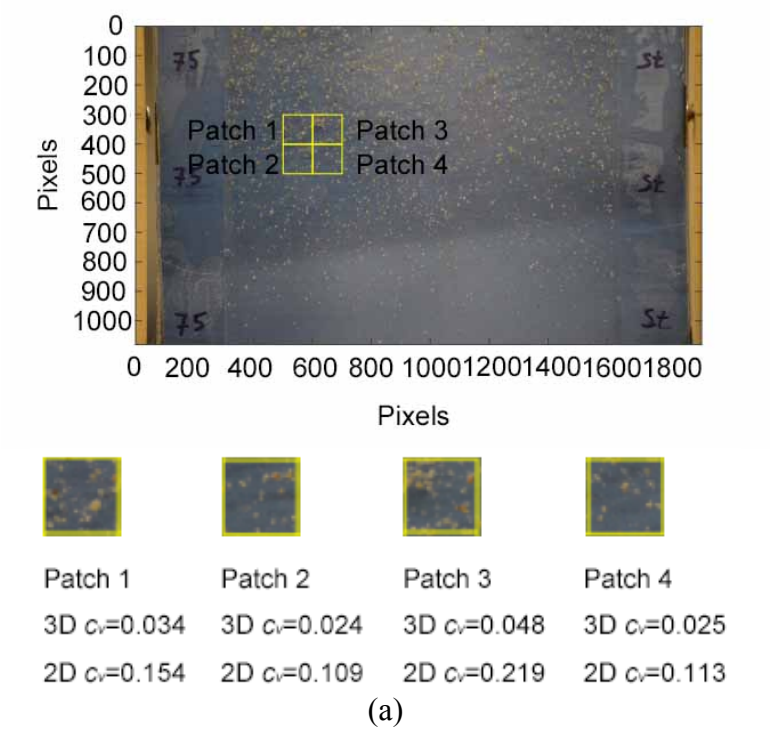

(a)

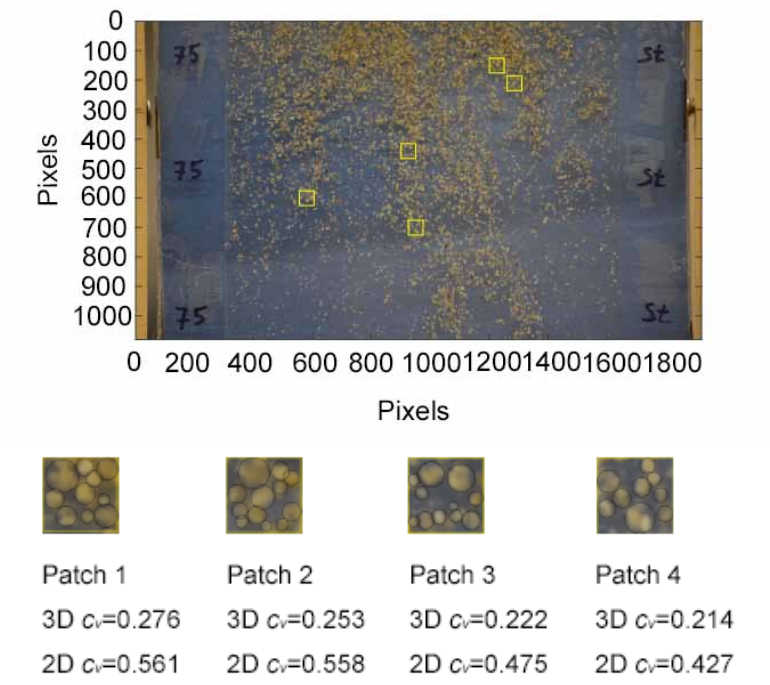

Figure 3.42. The analyzed patch of settling particles in the 75 % glycerol-water fluid, (a) low concentration, (b) medium concentration

Figure 3.43 shows results of the GeoPIV analysis for the whole patch and 4 squares shown in Figure 3.42 (a). The settling velocity profile slightly oscillates around average value. The settling velocity of two upper patches 1 and 3 is a little bit larger than the patches 2 and 4, but the average of the whole area is in the middle.

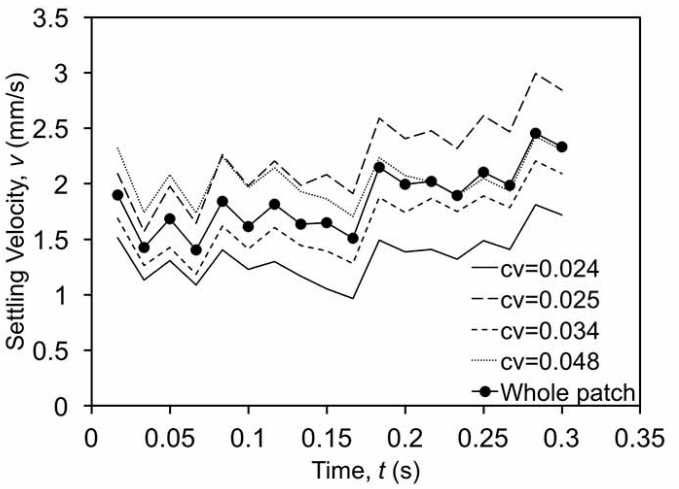

Figure 3.43. Average settling velocity of proppant in the areas of patches 1-4 and the whole analyzed area for in 75% glycerol-water fluid

The average concentration of these four patches of low concentration in Figure 3.42 (a) is c_v=0.0327, average concentration of four patches of medium concentration in Figure 3.42 (b) is c_v=0.241, for 75% glycerol-water fluid, v_0 = 9.72 mm/s when d=0.66 mm predicted by Stokes' law. The settling velocities predicted by Gadde at al. are:

$$v_s = 9.72\times(2.37\times0.0327^2 - 3.08\times0.0327 + 1) = 8.77 \text{ mm/s},$$
$$v_s = 9.72\times(2.37\times0.241^2 - 3.08\times0.241 + 1) = 3.85 \text{ mm/s}.$$

The experimental results are shown in Figure 3.44 (a) and (b) and compared with the prediction by Gadde et al. It can be seen that for low particle volumetric concentrations Gadde et al. over predicts the settling velocity of the slurry, while the slurry settles faster at higher concentrations.

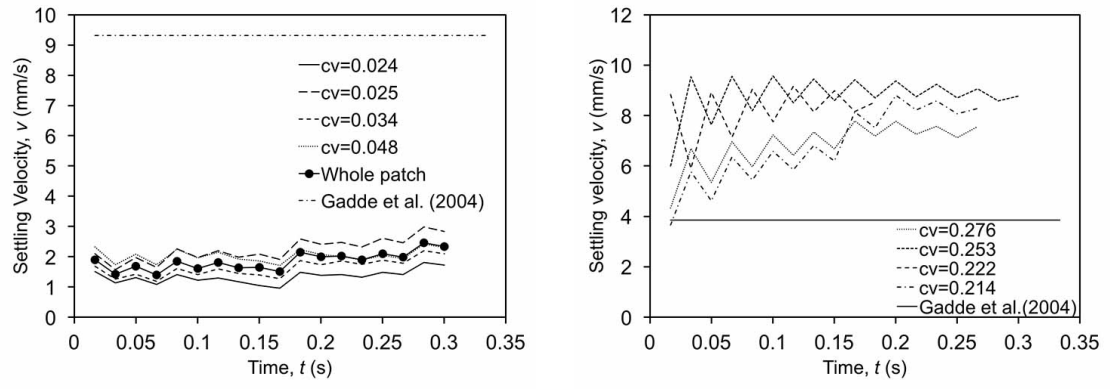

(a) (b)

Figure 3.44 Settling of particles at low concentrations in narrow slot with promoted agglomeration, compared to the relationship given by Gadde et al. (2004) in 75 % glycerol-water fluid at (a) low concentration, (b) medium concentration

Daneshy (1978) prediction for 75% glycerol-water fluid for the c_v=0.0327 and c_v=0.241 is:

$$v_s = v_0\left[\frac{1-c_v}{10^{1.82c_v}}\right] = 9.72\times\frac{1-0.0137}{10^{1.82\times0.0137}} = 9.05 \text{ mm/s},$$
$$v_s = v_0\left[\frac{1-c_v}{10^{1.82c_v}}\right] = 9.72\times\frac{1-0.241}{10^{1.82\times0.241}} = 2.71 \text{ mm/s}.$$

Figure 3.45 shows settling velocity of slurry compared with the predictions by Daneshy (1978).

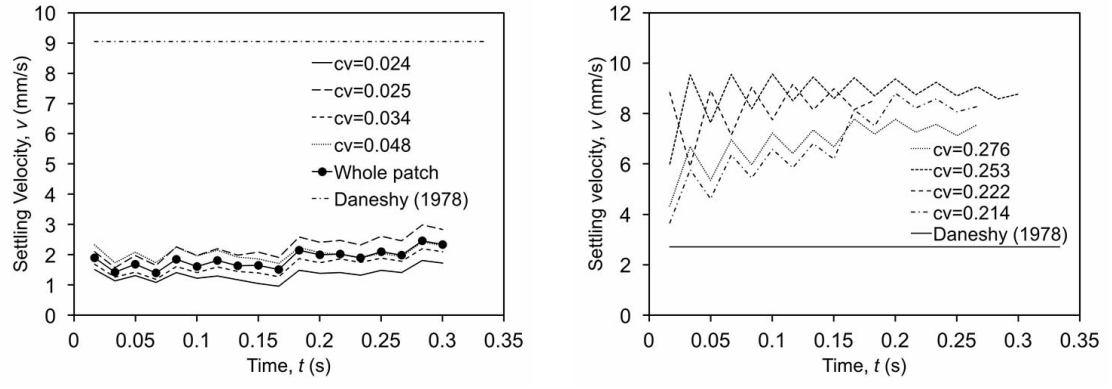

(a) (b)

Figure 3.45 Comparison of the average experimental settling velocities with the relationship proposed by Daneshy (1978) for a narrow slot in 75 % glycerol-water fluid at (a) low concentration, (b) medium concentration

At low concentrations the settling velocity according to Daneshy (1978) are higher than recorded from experimental data, as shown in Figure 3.43 (a). However, as shown in Figure 3.44 (b), at higher concentration Daneshy (1978) under predicts the experimentally obtained slurry settling velocities.

Clark et al. (1981) give the following predictions:

$$v_s = \frac{1}{1+6.88c_v} v_0 = \frac{1}{1+6.88\times 0.0137} \times 9.72 = 8.88 \text{ mm/s}.$$
$$v_s = \frac{1}{1+6.88c_v} v_0 = \frac{1}{1+6.88\times 0.241} \times 9.72 = 3.70 \text{ mm/s}.$$

Figure 3.45 shows the comparison between average settling velocity of analyzed patched with predicted velocity according to Clark et al. (1981). The prediction made by Clark et al. (1981) is still much higher than the test data as predictions made by Gadde et al. (2004) and Daneshy (1978) as shown in Figure 3.45 (a). When the concentration is low, the settling velocity will not be influenced a lot compared with Stokes' law according to these three relationships. Similar with relationships proposed by Gadde et al. (2004) and Daneshy (1978), the prediction made by Clark et al. (1981) is also affecting Stokes' law prediction a lot while the concentration is higher.

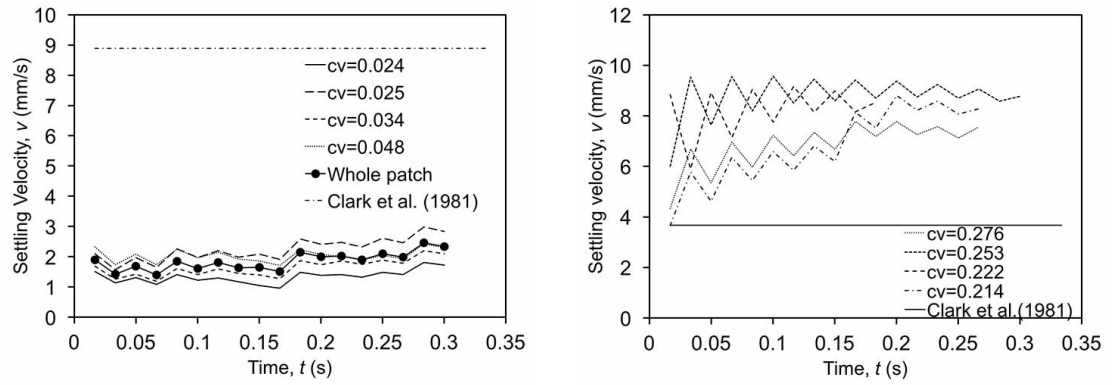

(a) (b)

Figure 3.46 Comparison of the average experimental settling velocities with the relationship proposed by Clark et al. (1981) for a narrow slot in 75 % glycerol-water fluid at (a) low concentration, (b) medium concentration

Figure 3.47 shows the settling velocities of particles with different concentrations in 75 % glycerol-water fluid, the relationships proposed by Gadde et al. (2004), Clark et al. (1981) and Daneshy (1978) are also plotted. The trends of these three relationships are decreasing while increasing concentration. However, the settling velocity from previous relationships are larger than test data got from narrow slot while the concentration is really low and less than 0.1. For higher concentrations as shown in Figure 3.47 (b), the experimental results have higher velocities than predictions made by these three relationships. Figure 3.48 shows the comparison between settling velocity in 75 % glycerol-water fluid of different concentration with relationships proposed by Gadde et al. (2004), Clark et al. (1981) and Daneshy (1978) by using superficial concentrations.

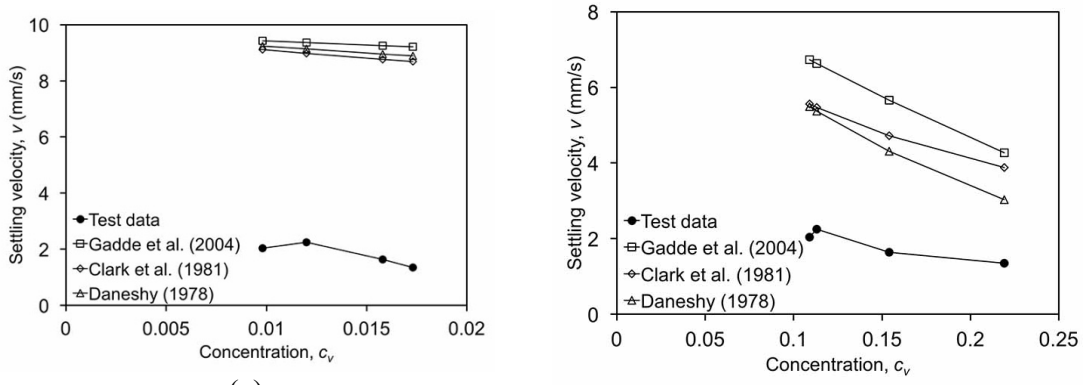

Figure 3.47 Comparison of the average experimental settling velocities with previous relationships for a narrow slot in 75 % glycerol-water fluid at (a) low concentration, (b) medium concentration

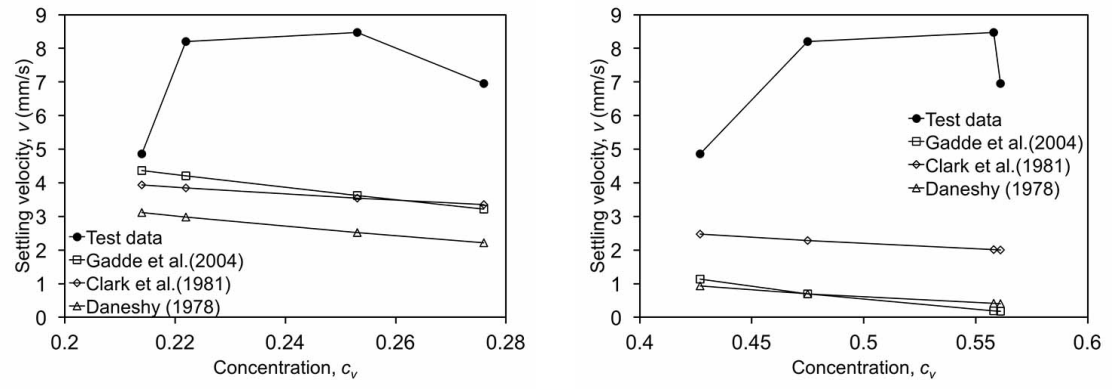

Figure 3.48 Comparison of the average experimental settling velocities with previous relationships for a narrow slot in 75 % glycerol-water fluid for two dimensional estimate of particle concentrations at (a) low concentration, (b) medium concentration

Comparing Figure 3.48 with Figure 3.47 it can be found that the relationships can better predict the settling by using volumetric concentrations. The particles in narrow slot could not be predicted by using superficial concentration regarding to previous relationships when the concentration is higher than 0.1. However, the predictions according to previous relationships by using volumetric concentrations are smaller than experimental results. The proppant agglomeration is not taking account in these three relationships, however, the agglomeration can increase slurry settling velocity with respect to previous chapters. Thus, these three relationships are not well predicted proppant settling.

3.3.4. Effects of narrow slot on slurry settling

The effect of narrow walls is not taken into account in Gadde et al. (2004). Therefore, another comparison is made with the relationship proposed by Liu and Sharma (2005):

$$f(\mu) = 0.16\mu^{0.28} = 0.16\times 0.0355^{0.28} = 0.063 \left(\frac{d}{B} = 0.33 < 0.9\right)$$

$$\frac{v_{\mathrm{w}}}{v_0} = 1 - f(\mu)\frac{d}{B} = 1 - 0.063\times\frac{0.66}{2} = 0.960,$$

$$v_w = 0.960 \times 9.72 = 9.33\text{mm/s}.$$

Figure 3.49 shows that settling velocities are higher than predicted by Liu and Sharma (2005), which takes into account the effect of particle and wall dimensions' ratio. It is significant that observed settling in a narrow slot is smaller than predicted, even at low particle concentrations in 75 % glycerol-water fluid.

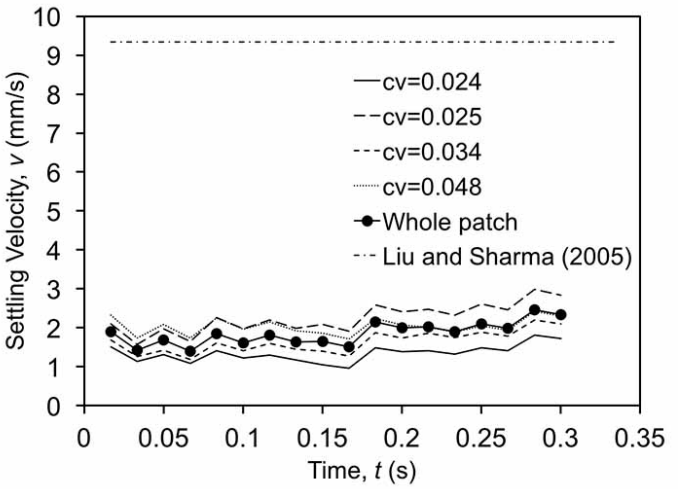

Figure 3.49. Comparison of the average experimental settling velocities with the relationship proposed by Liu and Sharma (2005) for a narrow slot and low particle concentration in 75 % glycerol-water fluid

In 75 % glycerol-water fluid, there are some agglomerates occurring. The narrow slot which is using in the lab is 2 mm width, so when particle agglomerates together, predicted velocities from Liu and Sharma (2005) can no longer use d=0.66 mm. Table 3.5 shows the predicted velocities according to Liu and Sharma (2005).

Table 3.5. Prediction of slurry settling between parallel walls for agglomerated particles

Agglomerate diameter, d (mm)	Liu and Sharma, v_w (mm/s)
1.00	9.14
1.06	9.10
1.14	9.06
1.19	9.03
1.42	8.89

Figure 3.50 shows the comparison between relationship proposed by Liu and Sharma (2005) with experimental results. It is obviously that the prediction is still larger than test data. However, while the increasing of particle size, the difference between prediction with experimental results becomes smaller. Thus, with larger particle size, the wall effect becomes a more important parameter during settling.

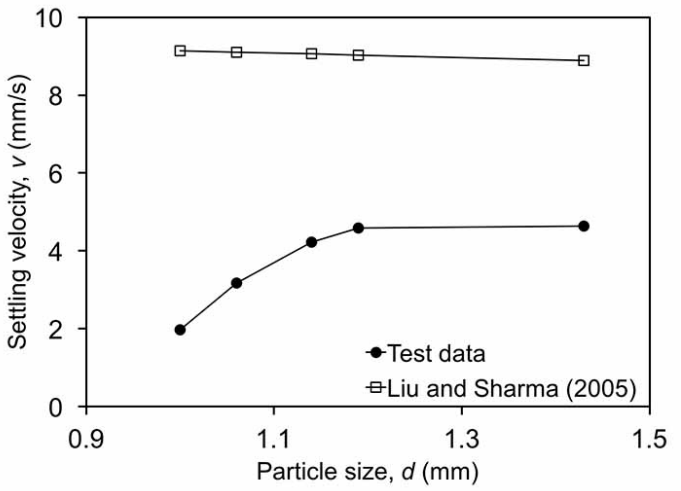

Figure 3.50. Comparison of the average experimental settling velocities with relationship proposed by Liu and Sharma (2005) for a narrow slot of different particle size in 75 % glycerol-water

3.4. Proppant settling in 85 % glycerol-water solution

3.4.1. General slurry behavior

In order to analyze the slurry behavior in 2 mm narrow slot at 85 % glycerol-water fluid, several patches are chosen to be investigated at early settling times. Figure 3.51 shows the beginning of the slurry settling.

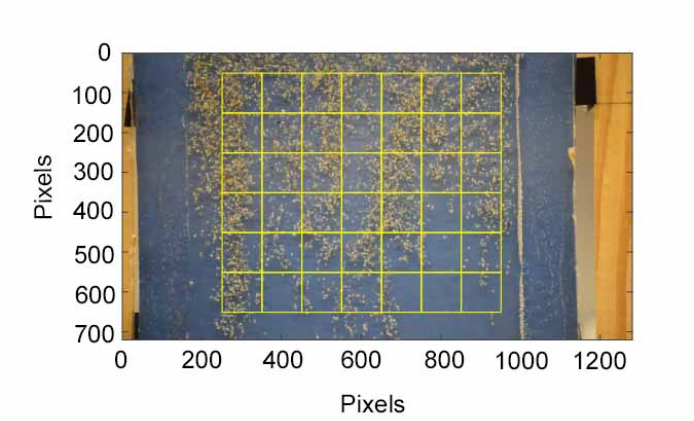

Figure 3.51 Selected patches in 85% glycerol-water fluid

Figure 3.52 shows the displacement vector of selected patches in Figure 3.51.

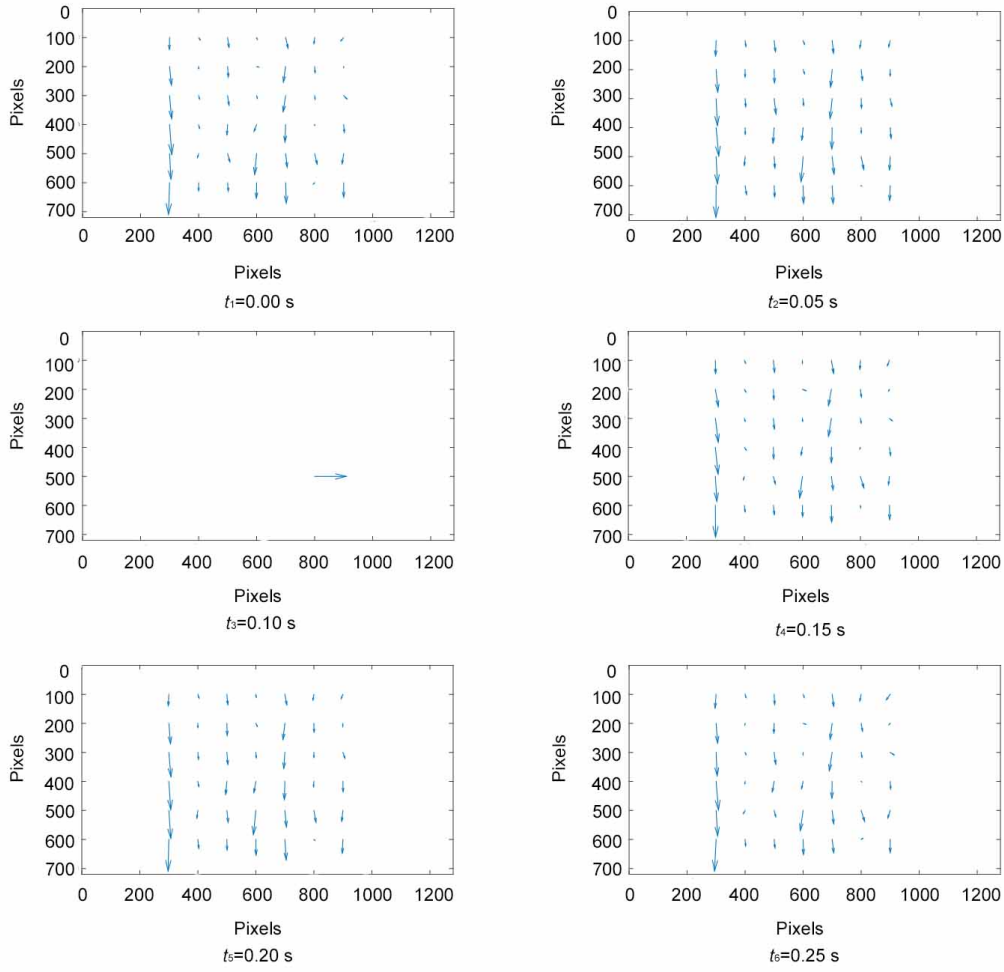

Figure 3.52 Displacement vectors of selected patches

It can be found that not as that in 75 % glycerol-water fluid, here in 85 % glycerol-water fluid, the displacements are not always vertical. There are many channels during settling as seen in Figure 3.51. The channels of particle movements are more likely to be settling while the others are sometimes have very small movements. Besides, when t=0.15 s, it can be found that the movement of particles are horizontal for one patch while the others are stable.

3.4.2. Analysis of individual particle and agglomerate settling rates

Settling of individual particles is analyzed using the GeoPIV method, where individual particles of several different sizes are identified and their motion is analyzed in settling regime. The chosen particle sizes are shown in Figure 3.53.

Figure 3.53 Diameters of one single particle in 85 % glycerol-water mixture

By using the Stokes' law, the settling velocity of an ideal spherical particle with respect of particle sizes was presented in Table 3.6.

Table 3.6 Prediction by Stokes' law for single particle

Particle diameter, d (mm)	Stokes' terminal velocity, v_s (mm/s)
0.66	3.11
0.70	3.50
0.75	4.01
0.80	4.57
0.90	5.78

Figure 3.54 shows the comparison between test data with prediction made by Stokes' law. It can be seen that when the particle size increases, the difference between

prediction made by Stokes' law with test data also increases. The measured settling velocities of single particles of different sizes are similar, with a very small increase as the particle size increases. A good correlation with the Stokes' law is not found analyzing the given particle sizes. Even for the smallest diameter, the Stokes law over predicts the settling rate.

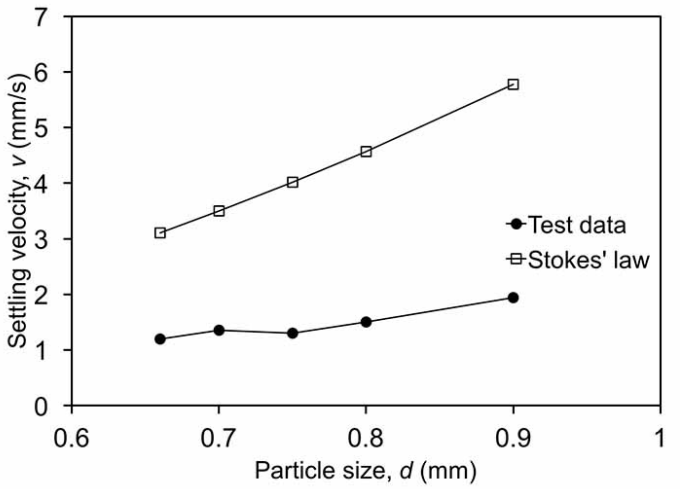

Figure 3.54 Velocities of one single particle in *y* direction vs. particle size

The single particles are agglomerated with each other and form different sizes of group particles. Figure 3.55 shows the estimated agglomerated particle size in 85 % glycerol-water mixture fluid.

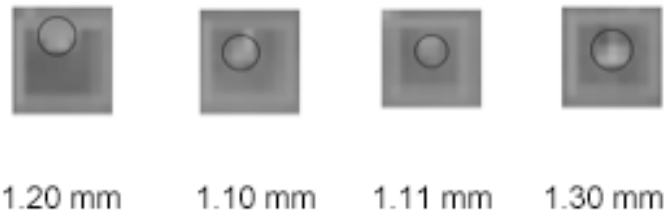

Figure 3.55 Different sizes of one single particle in 85 % glycerol-water mixture

As shown in Figure 3.56, different sizes of agglomerated particles have different average settling velocities. While the agglomerated particle has larger diameter, the settling velocity becomes higher.

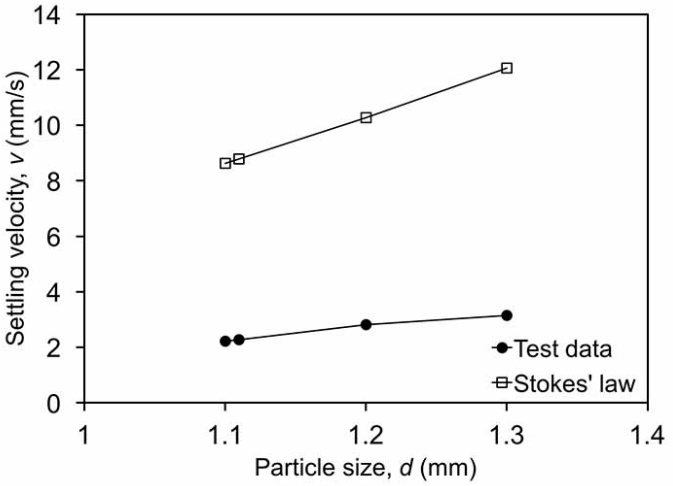

Figure 3.56 Velocities of agglomerated particles in *y* direction vs. particle size

Comparing the average settling velocity of single particle with agglomerated particles, it can be found that the average settling velocity increases with the increasing of particle size.

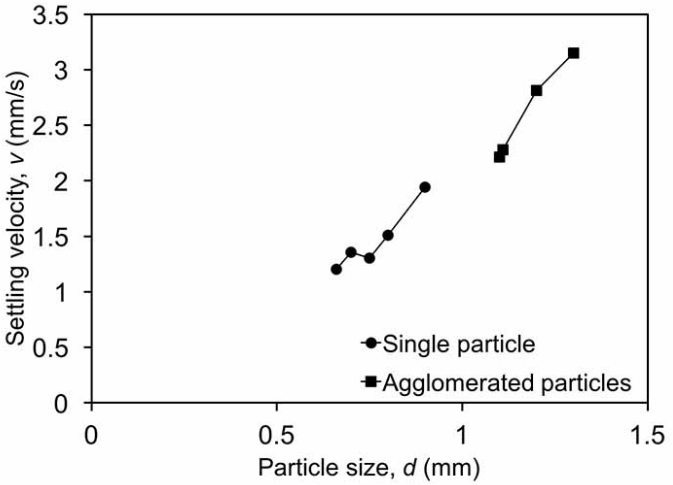

Figure 3.57 Settling velocity of individual particles and particle agglomerates in 85 % glycerol-water fluid

Comparing the settling velocity of individual particles and agglomerated particles with the average settling velocity as shown in Figure 3.58, it can be found that the average velocity is similar with particle size around 0.8. The average settling size is more likely the same as the velocity where the agglomerated diameter is formed of several sand particles.

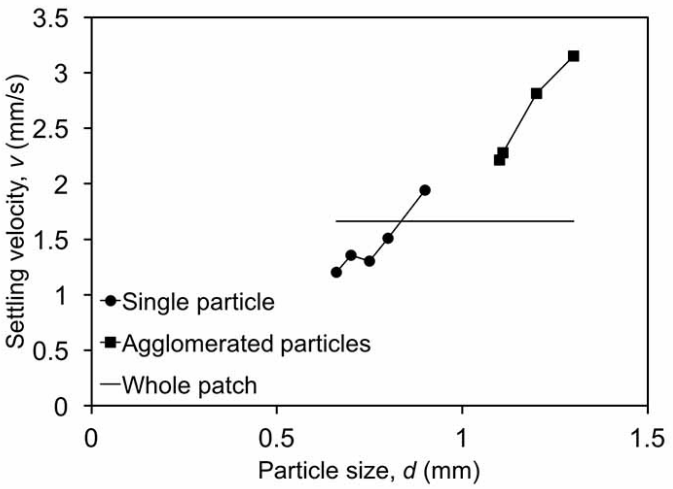

Figure 3.58 Settling velocity of individual particles and particle agglomerates with average settling velocity in 85 % glycerol-water fluid

3.4.3. Effects of particle volumetric concentrations on slurry settling

During settling, different selected patches usually have different concentrations. Figure 3.59 shows patches with different concentrations at the same time stage. In Figure 3.59 (a), the concentrations are a little bit lower than those in Figure 3.59 (b).

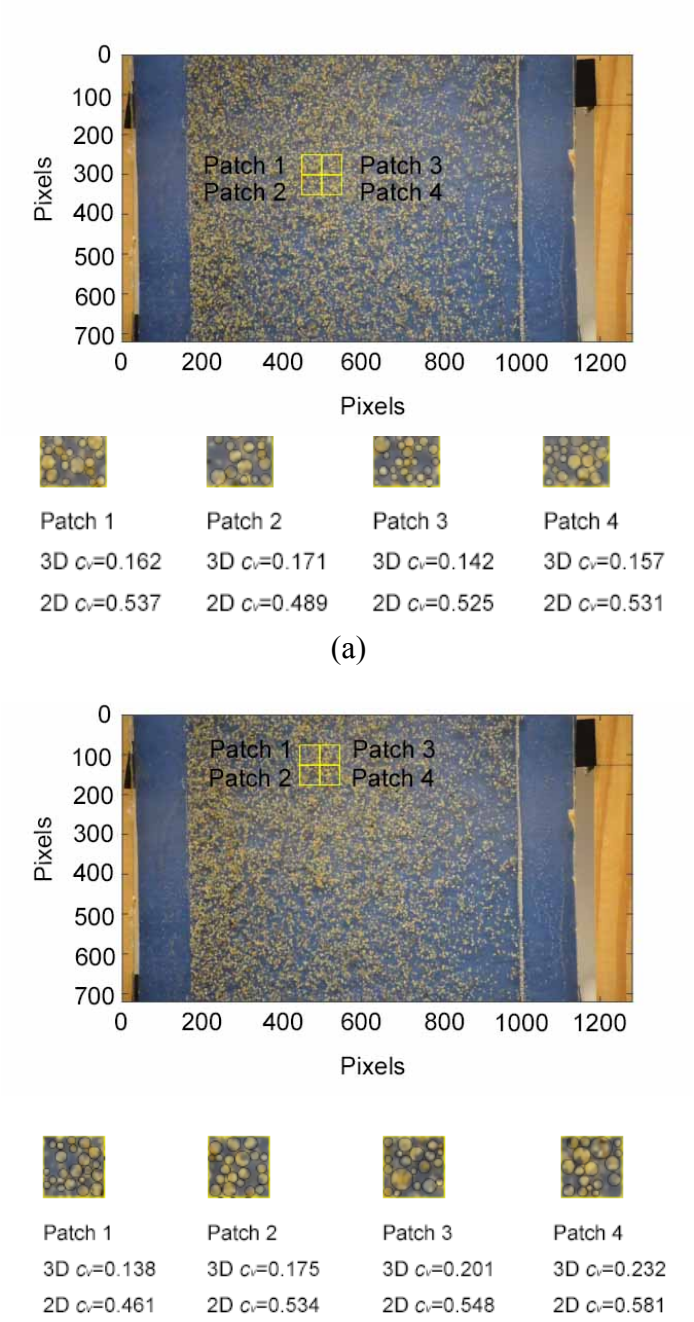

Figure 3.59 The analyzed patch of settling particles in the 85 % glycerol-water fluid at (a) low concentration c_v=0.158, (b) medium concentration c_v=0.187

Figure 3.60 shows results of the GeoPIV analysis for the whole patch and 4 squares shown in Figure 3.59. Both Figures 3.60 (a) and (b) show that the settling velocity profile slightly oscillates around average value. It is obvious that he settling velocity of two

patches with higher concentration in Figure 3.59 (b) is a little bit larger than the patches of lower concentration as shown in Figure 3.59 (b), but the average of the whole area is in the middle.

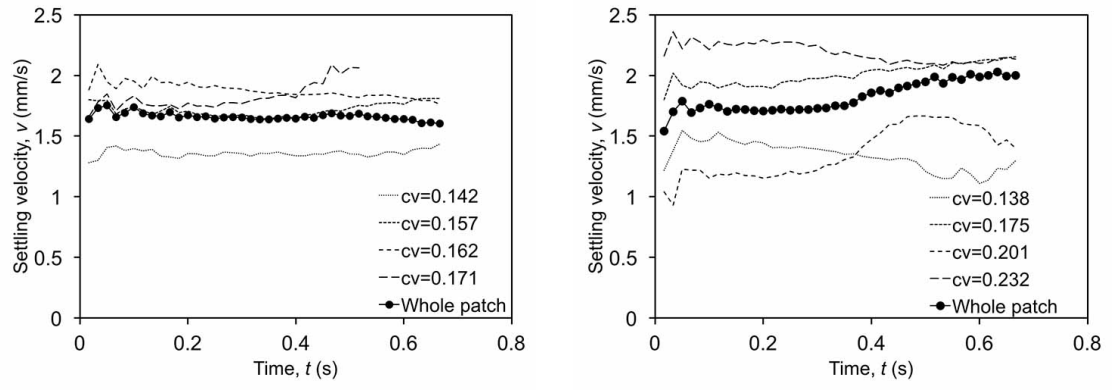

(a) (b)

Figure 3.60 Average settling velocity of proppant in the areas of patches 1-4 and the whole analyzed area in 85 % glycerol-water fluid at (a) low concentration, (b) medium concentration

Gadde et al. (2004) predicts for c_v=0.158 and c_v=0.187, for 85 % glycerol-water fluid, where v_0 = 3.11 mm/s when d=0.66 mm predicted by Stokes' law:

$$v_s = 3.11\times(2.37\times0.158^2 - 3.08\times0.158 + 1 = 1.78 \text{ mm/s},$$
$$v_s = 3.11\times(2.37\times0.187^2 - 3.08\times0.187 + 1 = 1.59 \text{ mm/s}.$$

As shown in Figure 3.61, the prediction made by Gadde et al. (2004) is around the center of different test data of four patches. Comparing Figure 3.61 with Figure 3.61, it can be found that the prediction made by Gadde et al. (2004) is closer to the average velocity. However, it can also be found that the relationship proposed by Gadde et al. (2004) is slower than test data. Thus, when the fluid viscosity is higher and the volumetric concentration is larger than 0.1, the prediction made by Gadde et al. (2004) is reliable but a little bit slower.

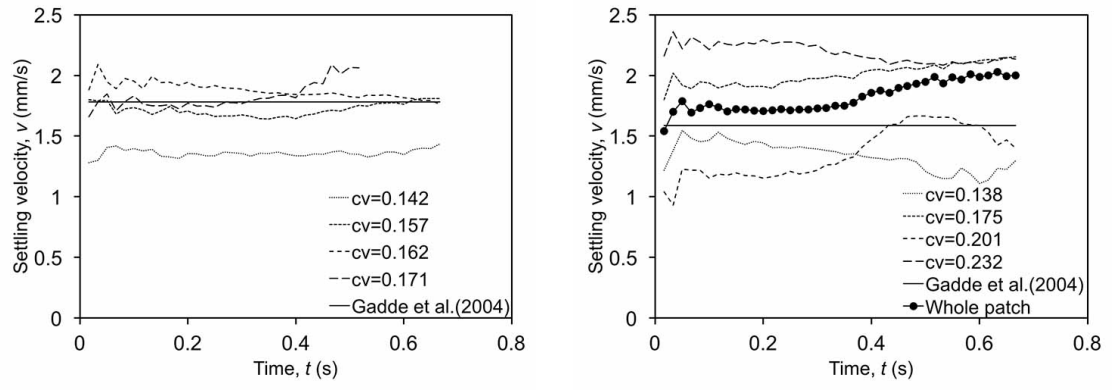

(a) (b)

Figure 3.61 Settling of particles at low concentrations in narrow slot with promoted agglomeration, compared to the relationship given by Gadde et al. (2004) in 85 % glycerol-water fluid at (a) low concentration, (b) medium concentration

Clark et al. (1981) prediction is:

$$v_s = \frac{1}{1+6.88c_v} v_0 = \frac{1}{1+6.88\times0.158} \times 3.11 = 1.49 \text{ mm/s}.$$
$$v_s = \frac{1}{1+6.88c_v} v_0 = \frac{1}{1+6.88\times0.187} \times 3.11 = 1.38 \text{ mm/s}.$$

Figure 3.62 shows the comparison between average settling velocity of analyzed patched with predicted velocity according to Clark et al. (1981) in narrow slot. The prediction made by Clark et al. (1981) is slower than the test data of selected patches of higher concentrations but still higher than patches with lower concentrations.

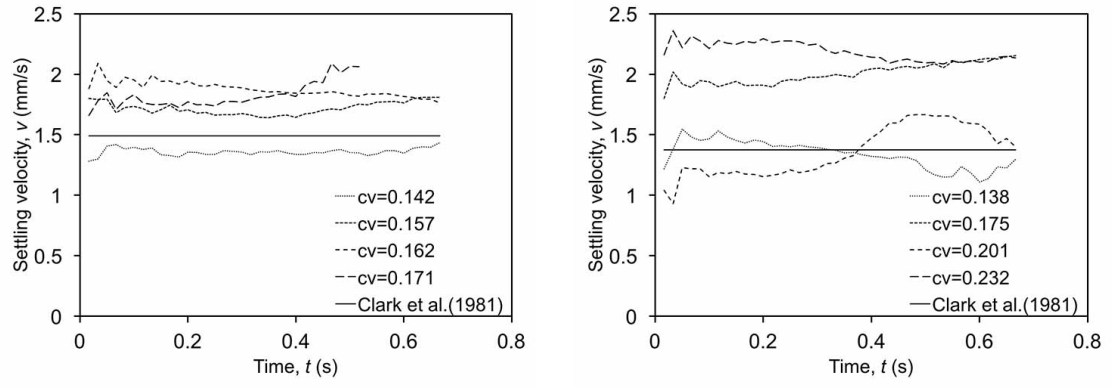

(a) (b)

Figure 3.62 Comparison of the average experimental settling velocities with the relationship proposed by Clark et al. (1981) for a narrow slot in 85 % glycerol-water fluid at (a) low concentration, (b) medium concentration

Figure 3.63 shows settling velocity of particles at low concentrations in a narrow slot, where the concentration dependent prediction is also plotted. It can be seen that the prediction made by Daneshy (1978) is different from Stokes' law prediction. The settling velocity according to Daneshy (1978) is smaller than experimental result as shown in Figure 3.63.

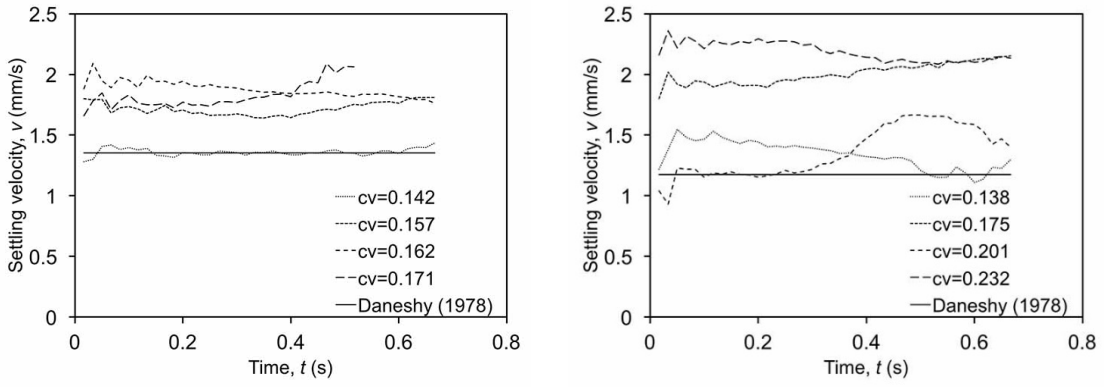

(a) (b)

Figure 3.63 Comparison of the average experimental settling velocities with the relationship proposed by Daneshy (1978) for a narrow slot in 85 % glycerol-water fluid at (a) low concentration, (b) medium concentration

Figures 3.64 and 3.65 show the settling velocities of particles with different concentrations in 85 % glycerol-water fluid, where the relationships proposed by Gadde et al. (2004), Clark et al. (1981) and Daneshy (1978) are plotted together. Figure 3.64 (a) and (b) show the predictions made by three relationships by using volumetric concentration and superficial concentrations in calculation and comparison with experimental data. Comparing Figure 3.64 (a) and (b) it can be found that when the concentration is higher than 0.14, the predictions are similar with experimental results. However, the settling velocity is much higher than prediction made by previous relationships (Gadde et al., 2004; Clark et al., 1981 and Daneshy, 1978). Thus in order to estimate average settling with

different proppant concentration, using volumetric concentration would be more convincing.

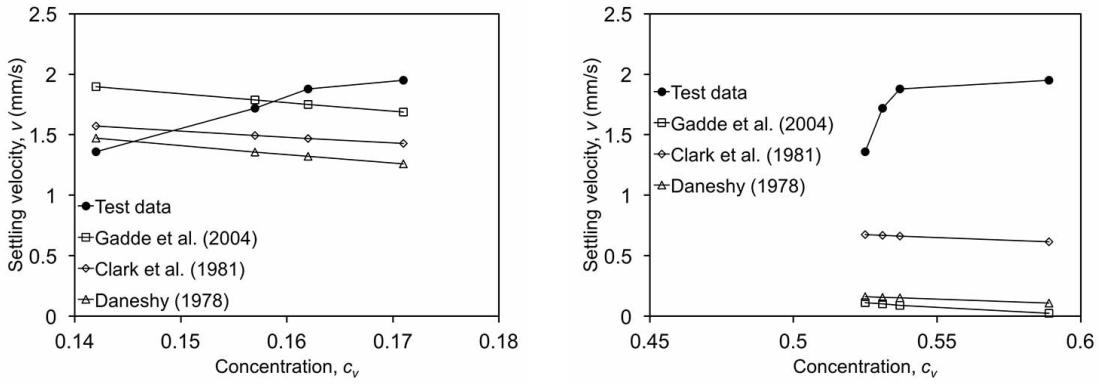

Figure 3.64 Comparison of the average experimental settling velocities with previous relationships for a narrow slot in 85 % glycerol-water fluid at low concentration by using (a) volumetric concentration, (b) superficial concentration

Similar results are obtained from the analysis of experimental data from patches with proppant at medium particle concentrations shown in Figure 3.65.

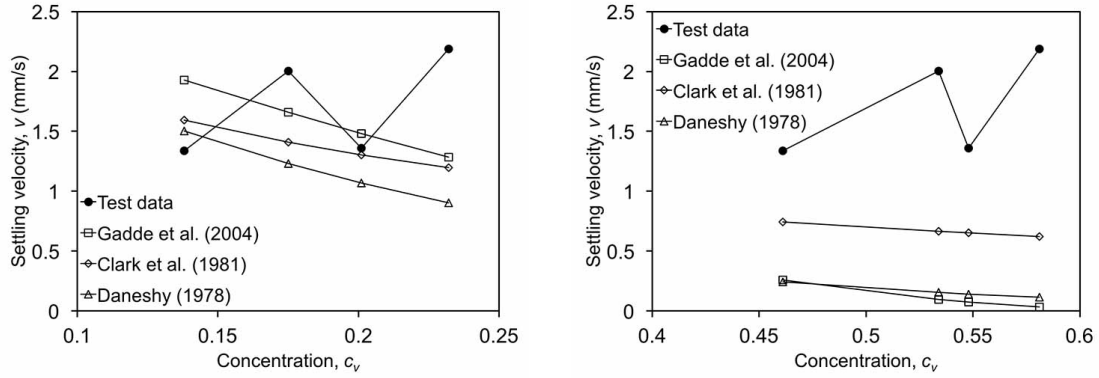

Figure 3.65 Comparison of the average experimental settling velocities with previous relationships for a narrow slot in 85 % glycerol-water fluid at medium concentration by using (a) volumetric concentration, (b) superficial concentration

3.4.4. Effects of narrow slot on slurry settling

Another comparison is made with the relationship proposed by Liu and Sharma (2005):

$$f(\mu) = 0.16\mu^{0.28} = 0.16\times 0.109^{0.28} = 0.086\left(\frac{d}{B} = 0.33 < 0.9\right),$$
$$\frac{v_{\mathrm{w}}}{v_0} = 1 - f(\mu)\frac{d}{B} = 1 - 0.086\times\frac{0.66}{2} = 0.972$$
$$v_w = 0.972\times 3.11 = 3.02\mathrm{mm/s}.$$

Figure 3.66 shows that settling velocities are slower than predicted by Liu and Sharma (2005), which takes into account the effect of particle and wall dimensions' ratio. It is significant that observed settling in a narrow slot is smaller than predicted.

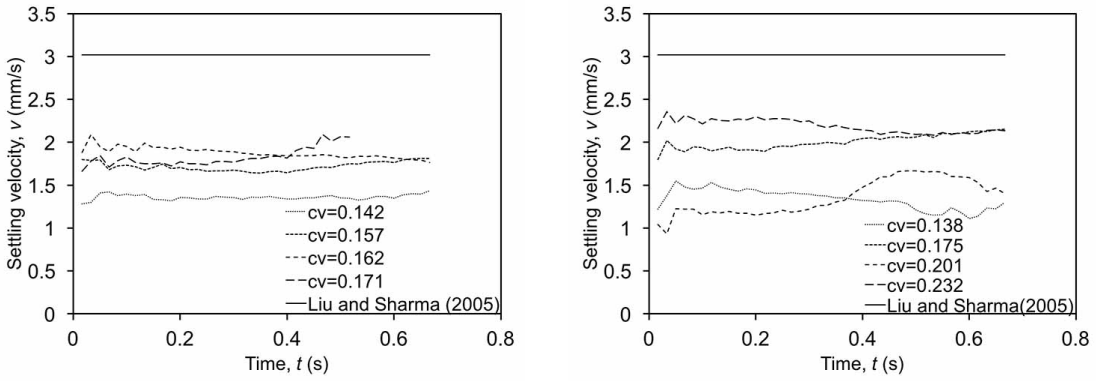

(a) (b)

Figure 3.66 Comparison of the average experimental settling velocities with the relationship proposed by Liu and Sharma (2005) for a narrow slot in 85 % glycerol-water fluid

In 85 % glycerol-water fluid, as shown in previous results it can be seen that there are some agglomerates occurring. The narrow slot which is using in the lab is 2 mm width, so when particle agglomerates together, predicted velocities from Liu and Sharma (2005) can no longer use 0.66 mm. Table 3.7 shows the predicted velocities of different particle sizes according to Liu and Sharma (2005).

Table 3.7. Prediction of slurry settling between parallel walls for agglomerated particles

Agglomerate diameter, d (mm)	Liu and Sharma, v_w (mm/s)
1.10	2.960
1.11	2.959
1.20	2.947
1.30	2.934

Figure 3.67 shows the comparison between relationship proposed by Liu and Sharma (2005) with experimental results. It is obviously that the prediction is closer to test data than that in 75 % and 50 % glycerol-water fluid. Moreover, while the increasing of particle size, the prediction made by Liu and Sharma (2005) is the same as test data with particle size around 1.25.

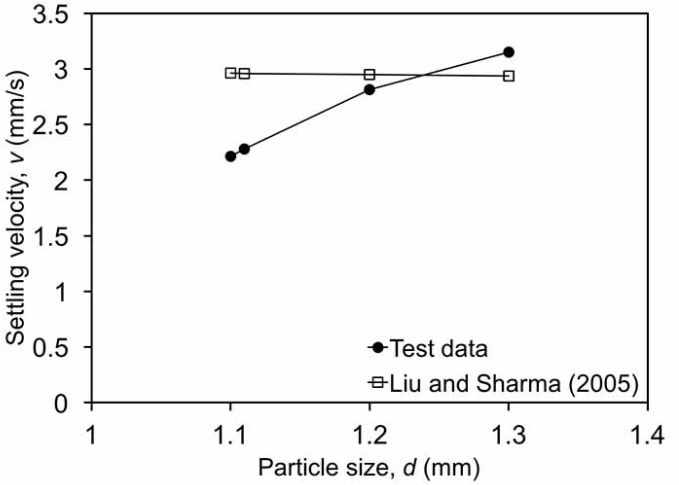

Figure 3.67 Comparison of the average experimental settling velocities with relationship proposed by Liu and Sharma (2005) for a narrow slot of different particle size in 85 % glycerol-water

3.5 Fluid viscosity effects on slurry settling in a narrow slot

This chapter summarizes experimental findings and comparisons of slurry settling with previously published relationships for 50 %, 75 % and 85 % glycerol-water solutions. The effects of particle concentrations in fluid and ratio of particle and wall diameter are assessed for a narrow slot. The agglomeration of proppant in different fluids is also be analyzed in this chapter.

3.5.1 Concentration effect on slurry settling in narrow slot

The average settling velocity obtained from experimental results for 50 % glycerol-water fluid is around 10 mm/s, for 75 % glycerol-water fluid is around 7 mm/s and around

1.8 mm/s for 85 % glycerol-water fluid as shown in Figure 3.68. The average settling velocity of a single particle is different because of varying fluid dynamic viscosity, which is represented with the Stokes' law. It can be seen that the particles have the highest settling velocity in 50 % glycerol-water fluid and the lowest average settling velocity in 85 % glycerol-water fluid. Moreover, the average settling velocities in the same fluid can also be different because of different concentrations. Figure 3.68 shows both the experimental results of average settling velocity and the predicted settling velocities according to relationships proposed by Gadde et al. (2004), Clark et al. (1981) and Daneshy (1978).

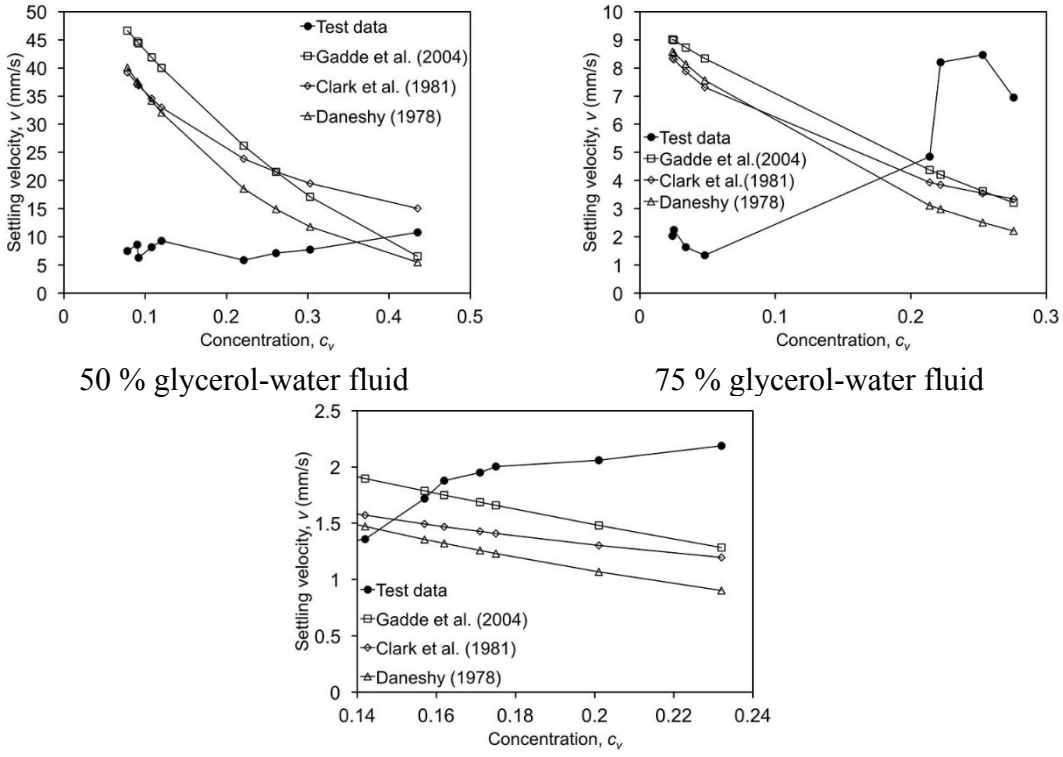

Figure 3.68 Comparison of the average settling velocities with the previous relationships

It can be seen in the Fig. 3.67 that previous relationships derived in larger slots by Gadde et al. (2004), Clark et al. (1981) and Daneshy (1978) predict a decrease of proppant setting velocity as the proppant concentration increases. The observed trend in experiments

conducted for slurry settling in three different dynamic viscosity fluids consistently shows an opposite trend, and increases with the concentration increase in all the observed fluids. It is also significant to observe that for the lower fluid viscosity of 50 %, the experimental proppant settling velocity is smaller than predictions until the volumetric particle concentration reaches c_v=0.4, while in 75 % glycerol-water fluid c_v=0.2 and in 85 % glycerol-water fluid c_v=0.16. Thus, it is observed that increasing of fluid viscosity promotes proppant settling. As shown in the Chapter 3, the agglomerates settle faster compared to a single particle in the same environment. The occurrence of agglomeration of particles in fluid is observed in all experiments, where the agglomeration is promoted with fluid viscosity increase. Faster settling of agglomerates directly influences the overall settling rate of the slurry.

3.5.2 Wall effect on slurry settling in narrow slot

The wall effect on proppant settling in different fluids is shown here, with the comparison with previously published relationships. Figure 3.69 shows the comparison between settling velocity of experimental results with prediction made by Liu and Sharma (2005) which takes particle size into account.

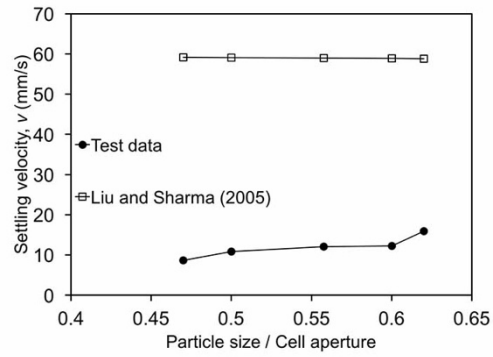

(a) 50 % glycerol-water
6 × difference

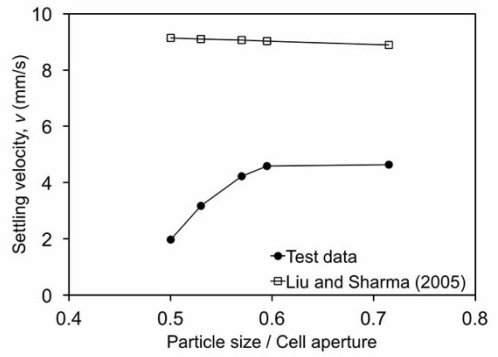

(b) 75 % glycerol-water
2.5 × difference

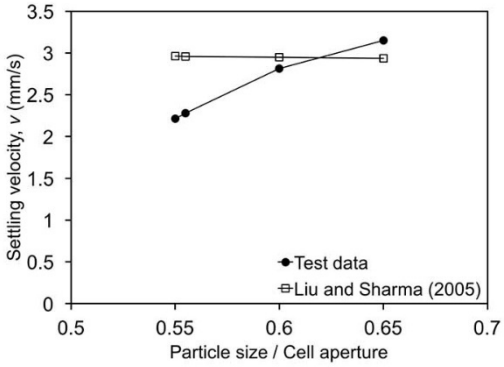

(c) 85 % glycerol-water

Figure 3.69 Comparison between average settling velocity with relationship proposed by Liu and Sharma (2005)

The predicted settling velocities according to Liu and Sharma (2005) by using agglomerated particle diameter are compared with experimental results. The experimental and theoretical slurry settling rates ratio versus particle size to cell aperture is shown as in Figure 3.68. The prediction made by Liu and Sharma (2005) is almost six times larger than experimental result for 50 % glycerol-water fluid. For 75 % glycerol-water, the prediction of Liu and Sharma (2005) is 2.5 times larger than the experimental results. While proppant is settling in 85 % glycerol-water fluid, the prediction is similar with average settling velocity obtained in laboratory. When the ratio of particle diameter to cell aperture is smaller than 0.9, Liu and Sharma (2005) predict that the settling velocities for proppant do not deviate significantly from the Stake's law. Observing the experimental results for

narrow slots, the wall effect would reduce settling velocity a lot for fluid with lower viscosity even the ratio of particle diameter to cell aperture is smaller than 0.9. As shown in Figure 3.68 it can be found that the experimental results for 50 % glycerol-water fluid and 75 % glycerol-water fluid would be significant influenced even when ratio of particle diameter to cell aperture is smaller than 0.8. However, for fluid with higher viscosity as 85 % glycerol-water fluid, the ratio of particle diameter to cell aperture is not the main parameter which would influence proppant settling.

3.6 Proppant settling with different agglomeration in different fluids

In order to investigate effect of agglomerations in fluids with different viscosity on proppant settling, the similar proppant concentrations in different fluids are selected. Figure 3.70 shows the chosen patches in different fluids with the similar volumetric concentration c_v=0.27 with various agglomerates and particle sizes. The distributions of particle size in different fluids are not the same. By grouping particles into particle size which is less than 1 mm, bigger than 1 mm but smaller than 1.5, and bigger than 1.5, the distribution is listed in Table 3.8.

(a) 50 % glycerol-water fluid
3D c_v=0.272
2D c_v=0.561

(b) 75 % glycerol-water fluid
3D c_v=0.272
2D c_v=0.592

(c) 85 % glycerol-water fluid
3D c_v=0.274
2D c_v=0.574

Figure 3.70 Selected patches in different viscosity fluids with similar concentration

Table 3.8 Particle size distribution in different fluids

Particle size, *d* (mm)	Numbers of particles		
	50 % glycerol-water fluid	75 % glycerol-water fluid	85 % glycerol-water fluid
≤1	5	3	1
1 – 1.5	2	2	5
1.6 – 2.0	2	3	2

Larger number of bigger size agglomerates is observed in higher viscosity fluids for example 75 % and 85 %glycerol-water solution, while in 50 % glycerol-water solution dominate single particles and smaller agglomerates. In order to investigate the influence of agglomerates on the slurry settling, the average settling velocities are shown in Figure 3.71. The velocities vary from different fluids, depending on fluid viscosity.

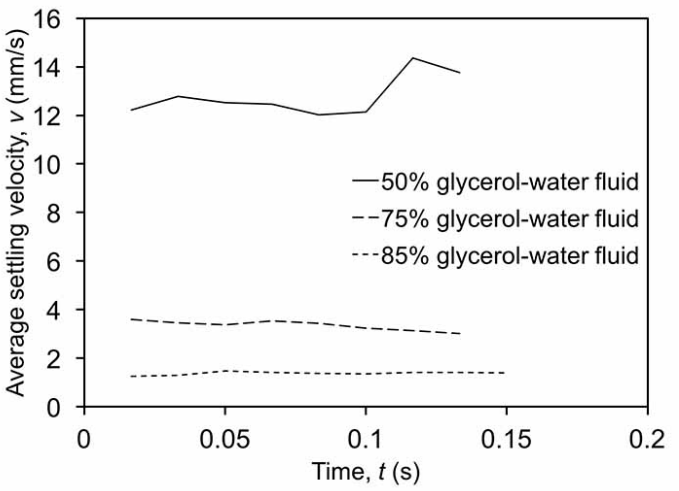

Figure 3.71 Average velocity in different fluids in patches with same concentration

In order to eliminate the effect of different viscosities of fluids, the settling velocity is normalized with prediction made by Stokes' law, taking into account the average original particle diameter of the sand that was used, d=0.66 mm. Figure 3.72 shows the normalized settling velocity in different fluids with same concentration. It can be found that the 85 % glycerol-water fluid has fastest relative settling while 50 % glycerol-water fluid has slowest relative settling compared to the Stokes' law. When normalized the settling velocity with

Stokes' law, the viscosity effects can be eliminated and the only parameter here is the distribution of single particles and agglomerated particles. If the agglomerates did not exist, and all the particles settled individually, the normalization would yield same slurry settling regardless of the fluid. Therefore, it can be argued that fluid viscosity, single sand particle size and concentration of particles in the slurry are not the only parameters which govern slurry settling. The presence of agglomerates increases the overall settling velocity, and it is observed here that higher fluid viscosity promotes particle agglomeration.

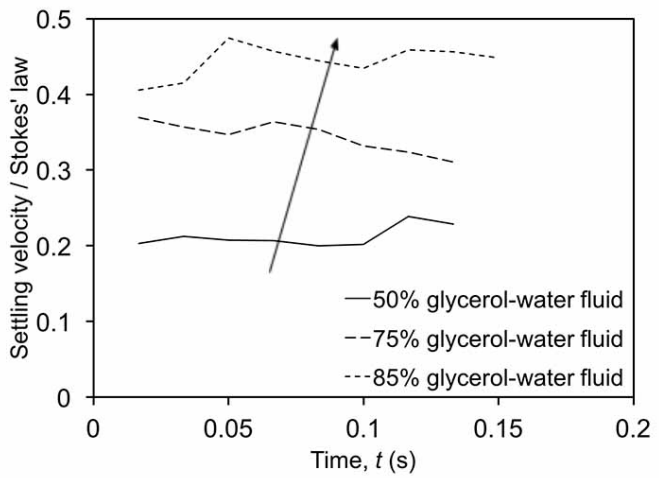

Figure 3.72 Ratio of settling velocity to Stokes' law in different fluids with same concentration

In order to get the relationship between number of agglomerates with normalized settling velocity, the particles with size larger than 1 mm are treated as agglomerated particles and particles with size smaller than 1 mm are regarded as single particle. Figure 3.73 and Figure 3.74 shows the relationships between normalized average settling velocity of different fluids with particle distribution. Figures 3.73 and 3.74 show that normalized average slurry settling velocity decreases with single particle number increase, and increases with increase of number of agglomerates. Figures 3.73 and 3.74 also show that the number of single particles vs. agglomerates governs slurry settling velocity.

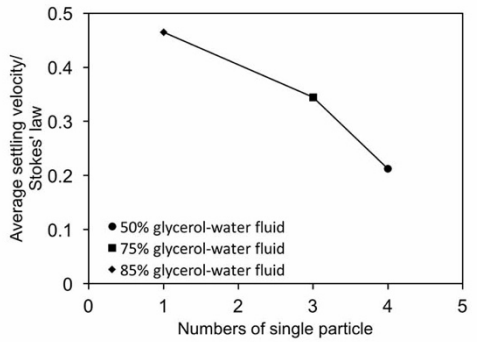

Figure 3.73 Ratio of patch average velocity with Stokes' law of different fluids with effect of numbers of single particle

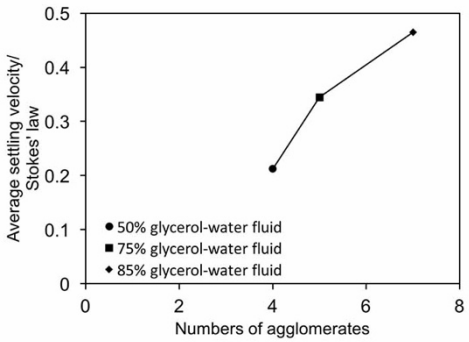

Figure 3.74 Ratio of patch average velocity with Stokes' law of different fluids with effect of numbers of agglomerated particles

CHAPTER 4: PROPPANTS SETTLING IN SLOT WITH ROUGH SURFACE

4.1 Overview

In order to analyze the particles settling in rock fracture and get a better understanding about particle-particle and particle-walls interaction on proppant settling in fracture, the analysis in a narrow slot with rough surface is conducted in this chapter. To get rough surface which can be conducted in the lab, a three-dimensional scan of induced fracture surfaces was obtained. By using the data from scanner, a .STL file was established to get ready for 3D printing (Figure 4.1). STL is a file format created by 3D system. This file format is widely used for rapid prototyping, 3D printing and computer-aided manufacturing. Figure 4.2 shows the rock surface printed by 3D printer by using data from laboratory hydraulic fracturing test in rock (Brenne, 2014).

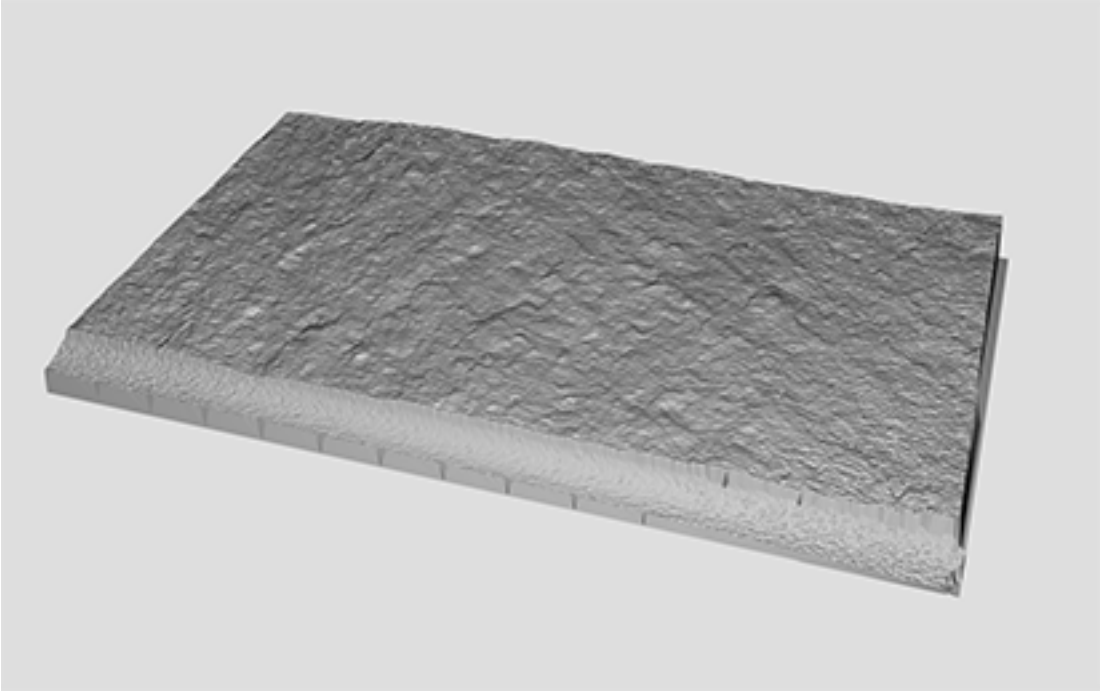

Figure 4.1 STL file of scanned rock surface

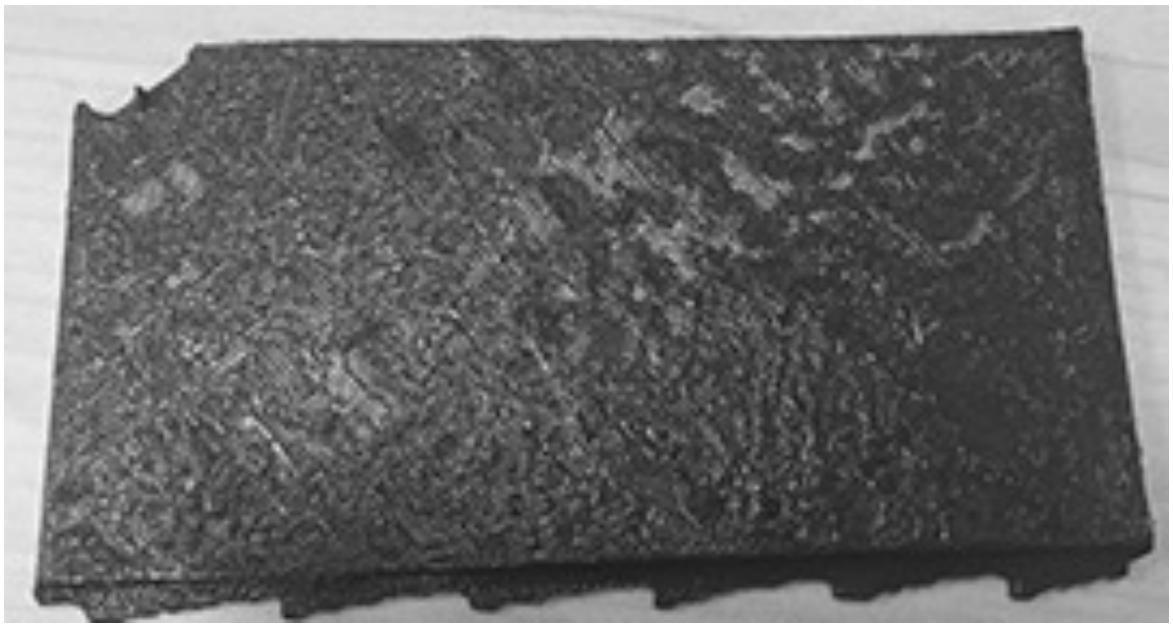

Figure 4.2 3D printed rock surface

Mean fracture average height values with standard deviations are shown in Figure 4.3 (Brenne, 2014). From Figure 4.3 it can be seen that the surfaces of stylolite fracture reached the highest heights of around 5.5 mm.

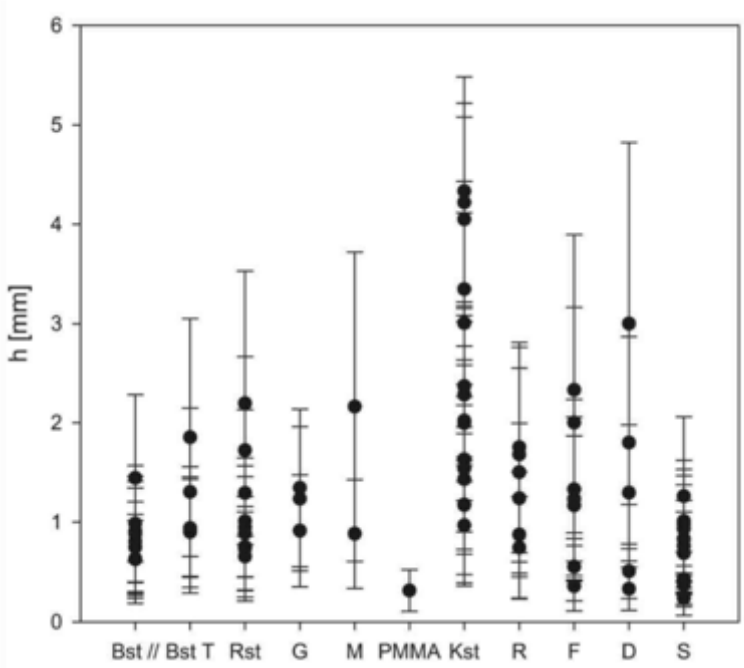

Figure 4.3 Average height values (Brenne, 2014)

The details of the experiment preparation and setup are given in the previous chapter. The settling experiments of proppant slurry with 50 %, 75 % and 85 % glycerol-water solution are repeated in the newly build cell with one rough surface.

4.2 Proppant settling in 50 % glycerol-water solution

For 50% glycerol-water fluid, series of patches are chosen to get the general behavior of particles in narrow slot with rough surface. Figure 4.4 shows the selected patches at the beginning period of movements. In order to get the general displacement vector of analyzing zone, couples of patches which can cover the whole area are selected as shown in Figure 4.5.

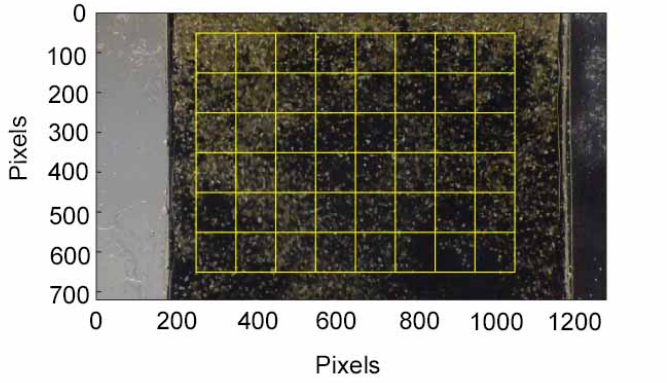

Figure 4.4 Selected meshes of patches at the beginning period of movements

Figure 4.5 shows the displacement vectors of chosen patches in Figure 4.4. It is obvious that the movements are not settling but swirling. The movement of *x* direction cannot be ignored, and at the beginning of the test, movements of particles cannot be treated as settling. Thus, in 50 % glycerol-water fluid, particles move downwards, but in erratic paths dominated by swirling and rotational motion instead of settling motion.

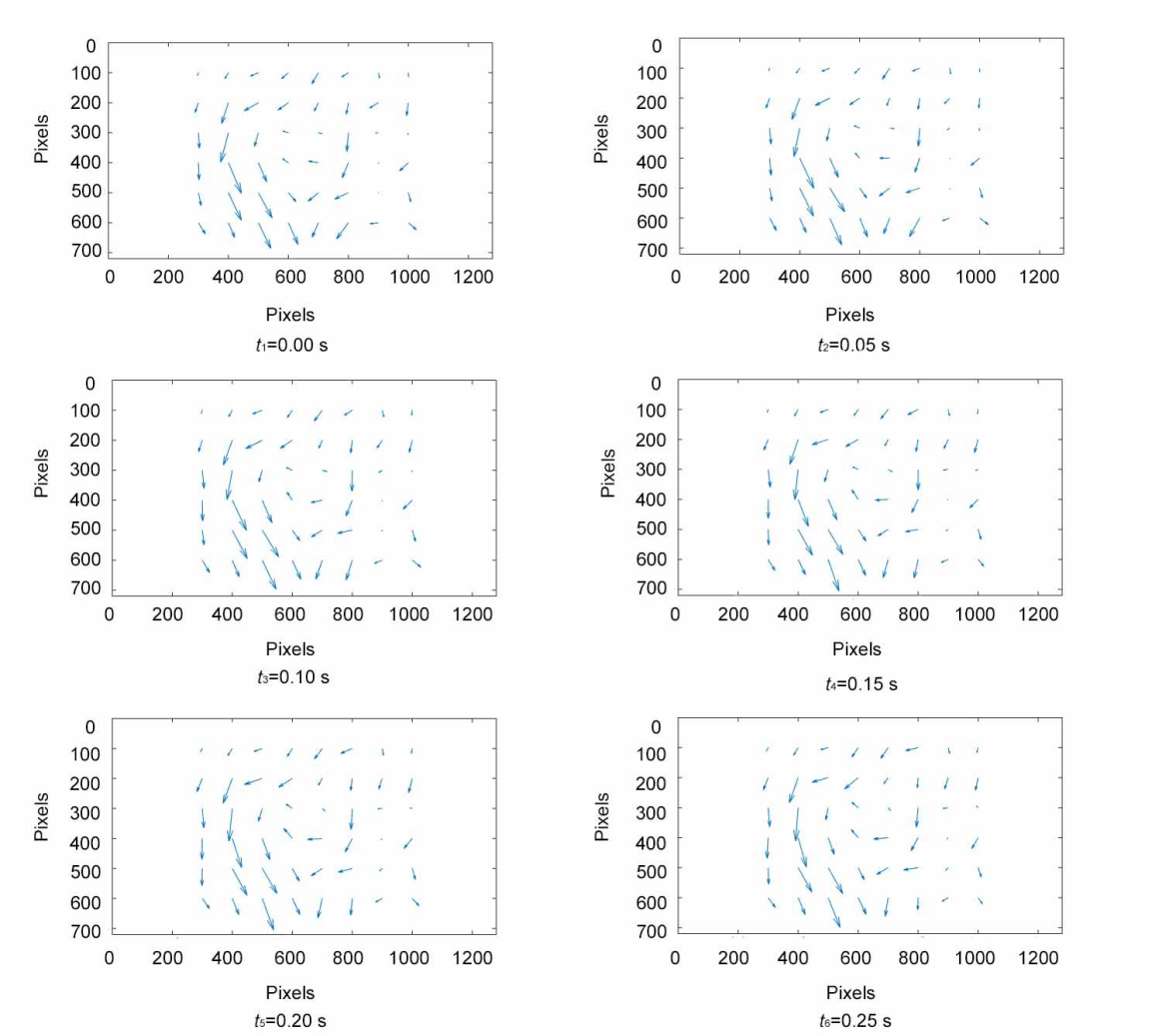

Figure 4.5 Displacement vector of selected patches

In order to see if the movements are always swirling, another figure which is at t=5 s is chosen to be analyzed. Similar with Figure 4.4, brands of patches are chosen to cover the whole area as shown in Figure 4.6.

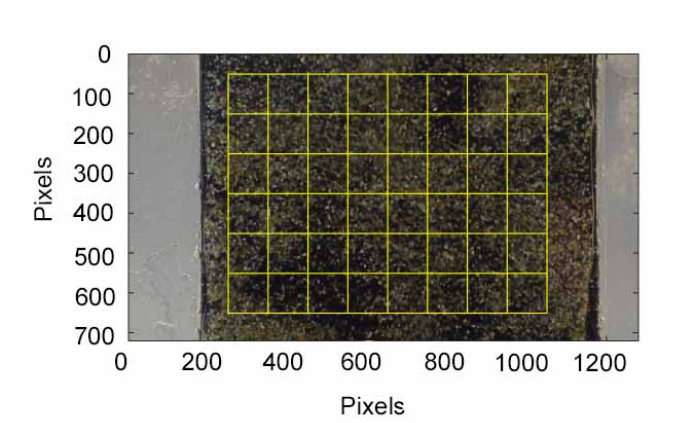

Figure 4.6 Selected meshes of patches at later period of movements

Figure 4.7 shows the displacement vectors of selected patches in Figure 4.6.

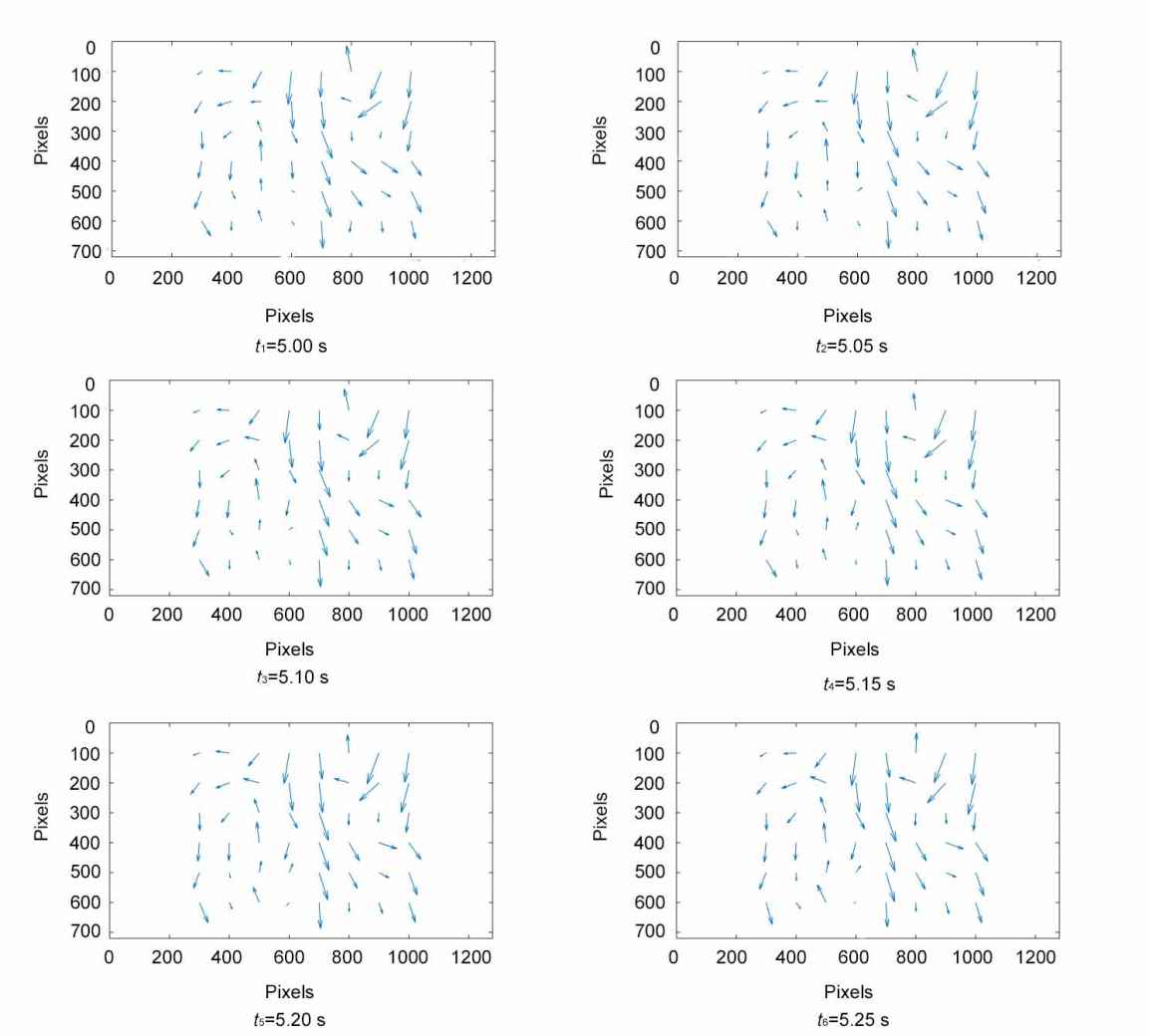

Figure 4.7 Displacement vector of selected patches

The movements are irregular and still not settling. Thus, when the particles are moving in the narrow slot with rough surface, a stable settling motion could not be established in the experiment. Compared to the slurry motion observed between two smooth Plexiglas plates, it can be concluded from qualitative experimental observation that fracture surface roughness promotes particle-wall interaction and erratic proppant behavior.

4.3 Proppant settling in 75 % glycerol-water solution

The observed slurry settling in rough surface has less erratic nature than in the 50 % glycerol-water solution resulting with settling motion after some time. An area with dominant vertical motion and relatively low particle volumetric concentration of c_v=0.118 is analyzed. The 20 x 20 mm patch is further divided into 4 square areas, as shown in Figures 4.8. The settling velocities of the whole patch, square areas are monitored during settling using the GeoPIV software.

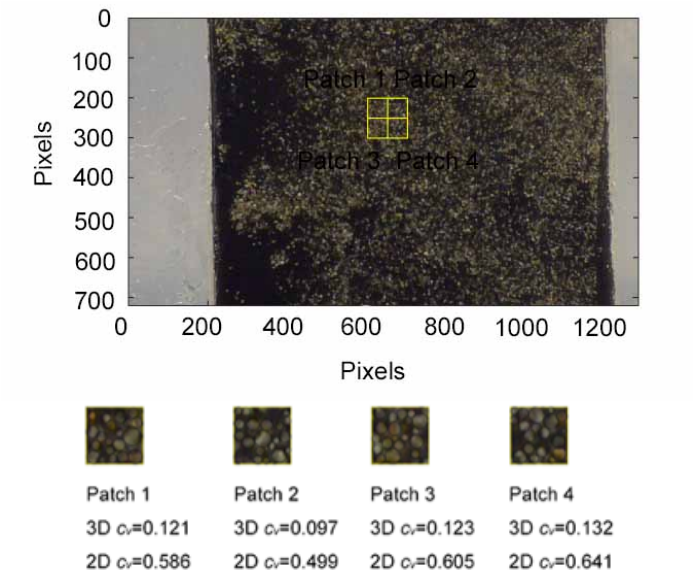

Figure 4.8 The analyzed patch of settling particles in the 75 % glycerol-water fluid with c_v=0.118

Figure 4.9 shows the results of average settling velocities by using GeoPIV method. Comparing with Figure 3.43 (b) which shows the average settling velocity of 75% glycerol-water fluid in narrow slot with smooth surface with concentration of 0.241, the settling velocities are similar. However, the volumetric concentration is 0.118 as shown in Figure 4.7 while the concentration in smooth fracture is 0.241.

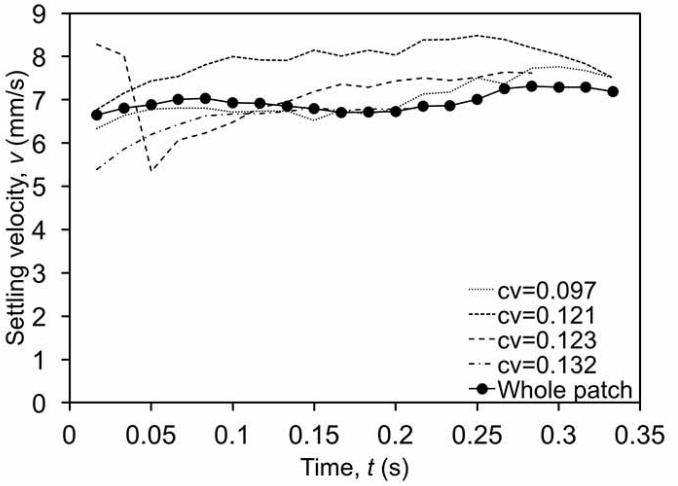

Figure 4.9 Average settling velocity of proppant in the areas of patches 1-4 and the whole analyzed area for in 75 % glycerol-water fluid

When the volumetric concentration is 0.118, by using relationship proposed by Gadde et al. (2004), the predicted average settling velocity for the whole patch is 6.51 mm/s. Figure 4.10 shows the average settling velocity of particles in a narrow slot with rough surface, where the prediction made by Gadde et al. (2004) is also plotted.

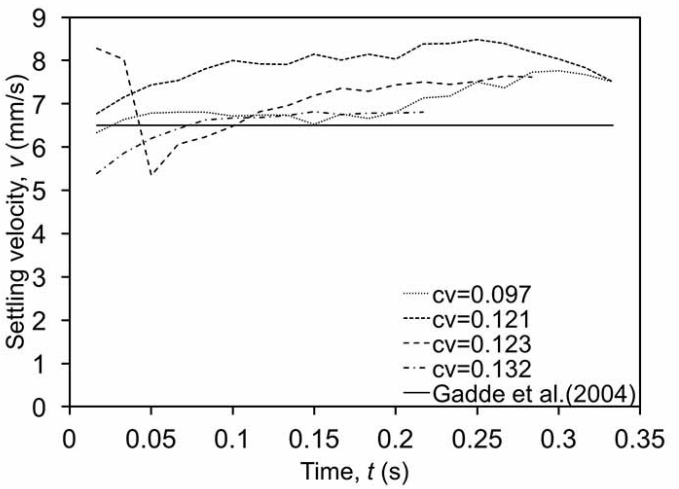

Figure 4.10 Settling of particles at low concentrations in narrow slot with promoted agglomeration, compared to the relationship given by Gadde et al. (2004) in 75 % glycerol-water fluid

The prediction made by Clark et al. (1981) can also be calculated, the predicted settling velocity for the whole patch is 5.27 mm/s. Comparing Figure 4.11 with Figure 3.45 (b), similar with the prediction made by Gadde et al. (2004), the relationship can better predict particle settling in narrow slot with rough surface than with smooth surface.

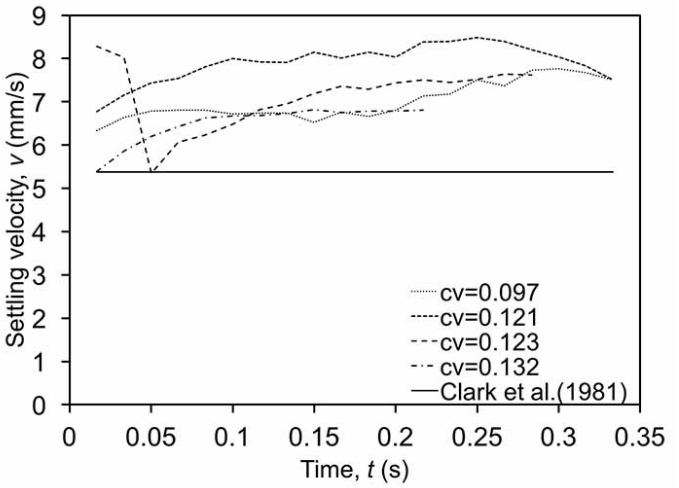

Figure 4.11 Comparison of the average experimental settling velocities with the relationship proposed by Clark et al. (1981) for a narrow slot in 75 % glycerol-water fluid

Besides, the prediction made by Daneshy (1978) for c_v=0.118 in 75 % glycerol-water fluid is 5.23 mm/s. Comparing Figure 4.12 with Figure 3.44 (b), it's similar with relationships proposed by Gadde et al. (2004) and Clark et al. (1981).

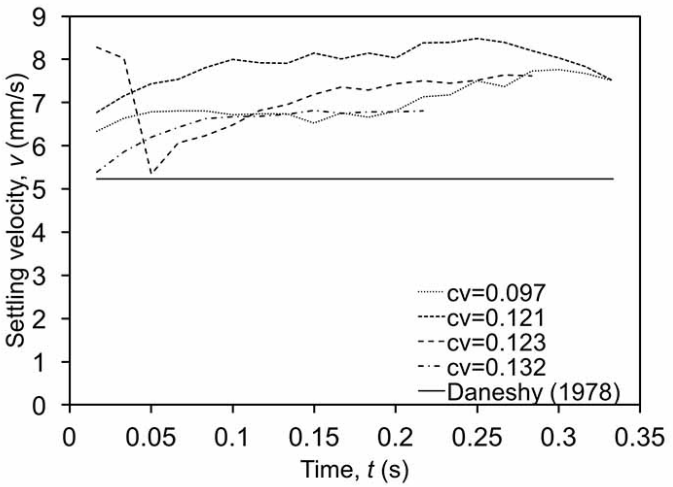

Figure 4.12 Comparison of the average experimental settling velocities with the relationship proposed by Daneshy (1978) for a narrow slot in 75 % glycerol-water fluid

Figure 4.13 shows the settling velocities of particles with volumetric concentrations in 75 % glycerol-water fluid, the relationships proposed by Gadde et al. (2004), Clark et al. (1981) and Daneshy (1978) are also plotted.

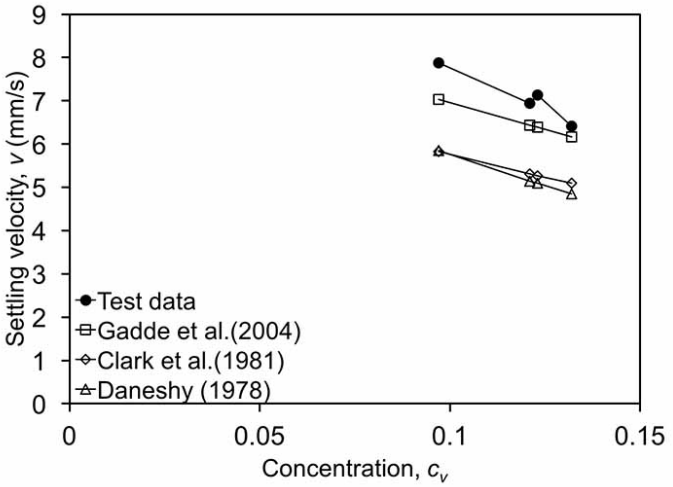

Figure 4.13 Comparison of the average experimental settling velocities with previous relationships for a narrow slot in 75 % glycerol-water fluid

The trends of these three relationships are decreasing while increasing concentration, as well as, in experimental results. However, the average settling velocity of experimental results are larger than predictions made the three relationships.

Figure 4.14 shows the settling velocities of particles with superficial concentrations in 75 % glycerol-water fluid, the relationships proposed by Gadde et al. (2004), Clark et al. (1981) and Daneshy (1978) are also plotted.

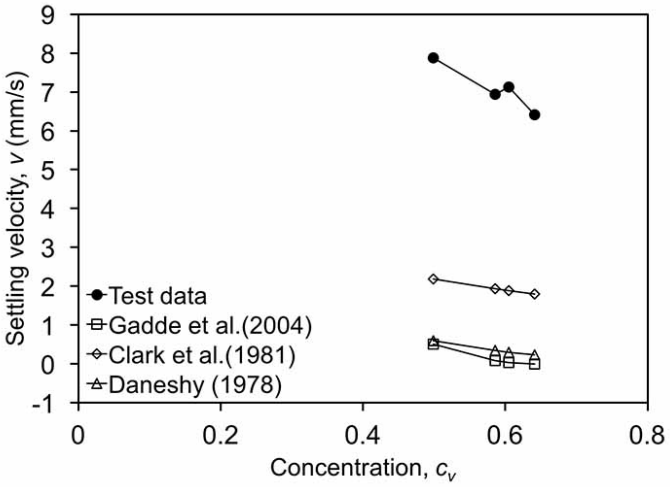

Figure 4.14 Comparison of the average experimental settling velocities with previous relationships for a narrow slot in 75 % glycerol-water fluid taking into calculation the superficial proppant concentration

The effect of narrow walls is not taken into account in Gadde et al. (2004), Clark et al. (1981) and Daneshy (1978). Therefore, another comparison is made with the relationship proposed by Liu and Sharma (2005). By using average particle diameter d=0.66 mm, the prediction made by Liu and Sharma (2005) for 75 % glycerol-water fluid is 9.33 mm/s. Figure 4.15 shows the comparison between test data with relationship proposed by Liu and Sharma (2005). It can be found that the experiments show slower settling velocities than prediction made by Liu and Sharma (2005) as shown in Figure 4.15.

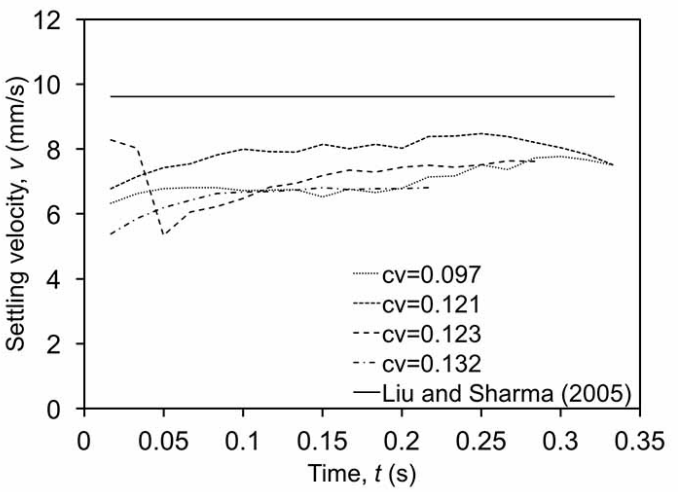

Figure 4.15 Comparison of the average experimental settling velocities with the relationship proposed by Liu and Sharma (2005) for a narrow slot with rough surface

4.4 Proppant settling in 85 % glycerol-water solution

During particles settling in 85% glycerol-water fluid, selected patches of average concentration c_v=0.111 are analyzed as shown in Figure 4.16.

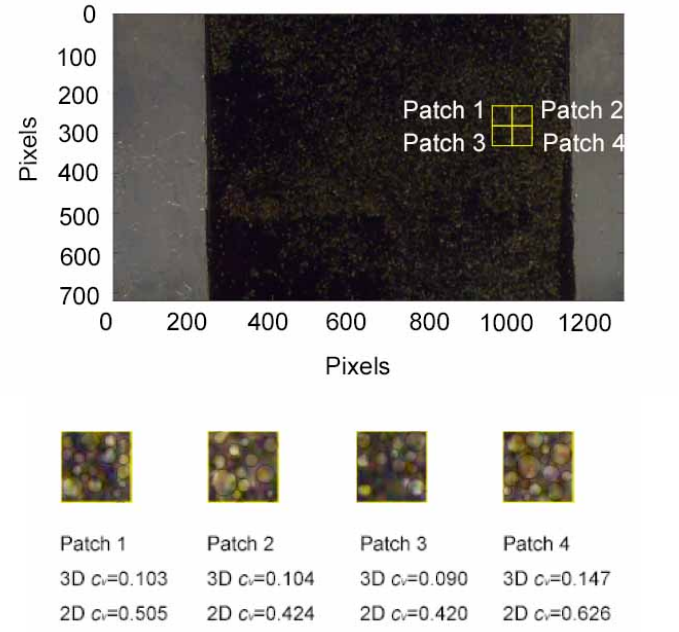

Figure 4.16 The analyzed patch of settling particles in the 85 % glycerol-water fluid with c_v=0.111

Figure 4.17 shows results of the GeoPIV analysis for the whole patch and 4 squares as shown in Figure 4.16. Comparing Figure 4.17 with Figure 3.56 (a) for the average settling velocity with smooth surface, it can found that the average settling velocity of experimental results are very similar.

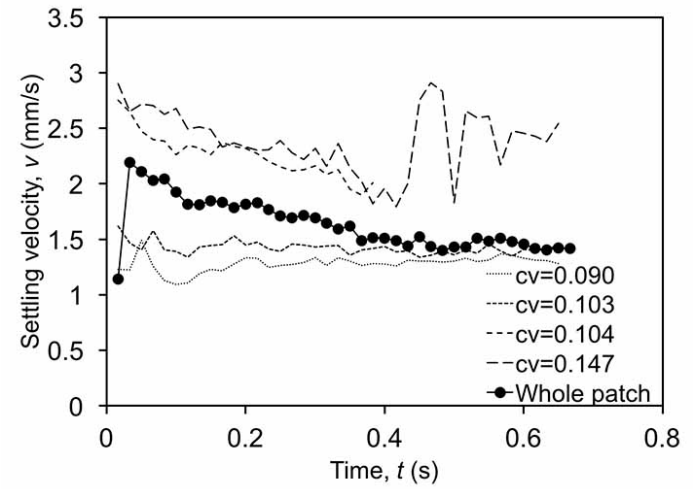

Figure 4.17 Average settling velocity of proppant in the areas of patches 1 - 4 and the whole analyzed area in 85 % glycerol-water fluid

The prediction made by Gadde et al. (2004) of c_v=0.111 is 2.14 mm/s. Figure 4.18 shows the comparison between test data with relationship proposed by Gadde et al. (2004).

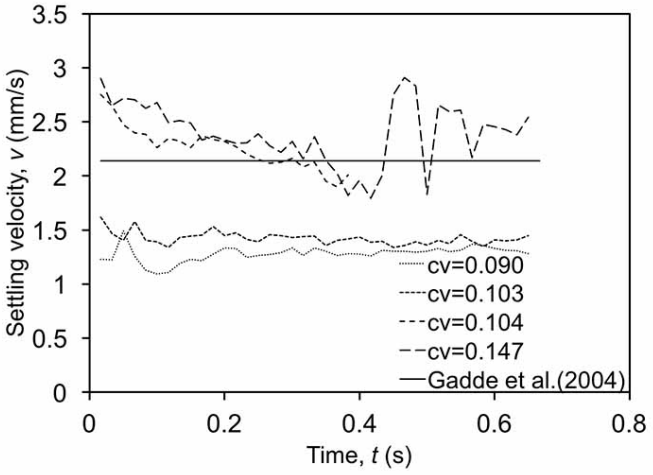

Figure 4.18 Settling of particles at low concentrations in narrow slot with promoted agglomeration, compared to the relationship given by Gadde et al. (2004) in 85 % glycerol-water fluid

The relationship proposed by Gadde et al. (2004) can predict well when concentration is around 0.15.

When the volumetric concentration is 0.11, the predicted settling velocity made by Clark et al. (1981) is 1.77 mm/s. Figure 4.19 shows the comparison between average settling velocity of analyzed patched with predicted velocity according to Clark et al. (1981) in narrow slot with rough surface. The prediction made by Clark et al. (1981) is slower than the test data of selected patches of higher concentrations but still higher than patches with lower concentrations.

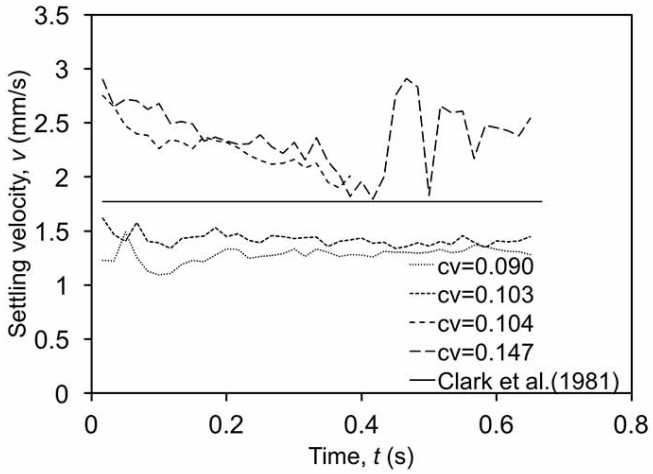

Figure 4.19 Comparison of the average experimental settling velocities with the relationship proposed by Clark et al. (1981) for a narrow slot in 85 % glycerol-water fluid

Figure 4.20 shows settling velocity of particles at low concentrations in a narrow slot, where the concentration dependent prediction is also plotted. The predicted settling velocity according to Daneshy (1978) when c_v=0.11 is 1.75 mm/s. It can be seen that according to Daneshy (1978), the settling velocity is different from Stokes' law prediction while concentrations are higher than 0.1.

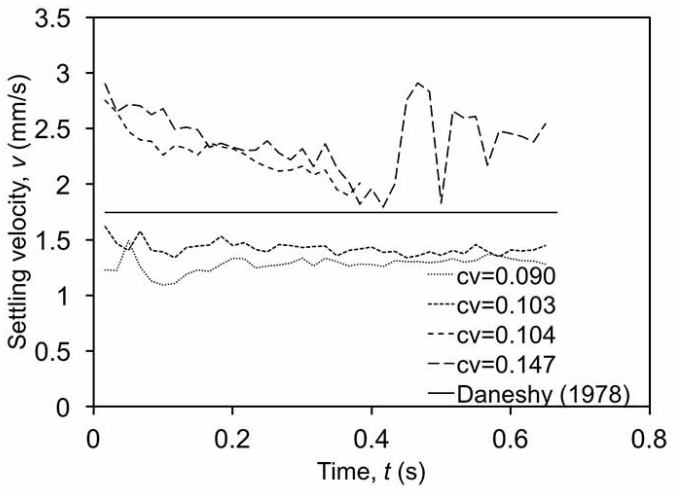

Figure 4.20 Comparison of the average experimental settling velocities with the relationship proposed by Daneshy (1978) for a narrow slot in 85 % glycerol-water fluid

Figure 4.21 and Figure 4.22 show the settling velocities of particles with different concentrations in 85 % glycerol-water fluid, the relationships proposed by Gadde et al. (2004), Clark et al. (1981) and Daneshy (1978) are also plotted. Figure 4.21 shows the predictions made by three relationships by using volumetric concentration. It can be found that the difference between test data with predictions is smaller when the concentration is higher than 0.1. However, the settling velocity from previous relationships by using superficial concentrations are much smaller than test data got from narrow slot as shown in Figure 4.22. Since it is assumed that the real concentration lies somewhere between the volumetric and superficial estimate, it can be concluded that the previous relationship underestimates the proppant settling velocity.

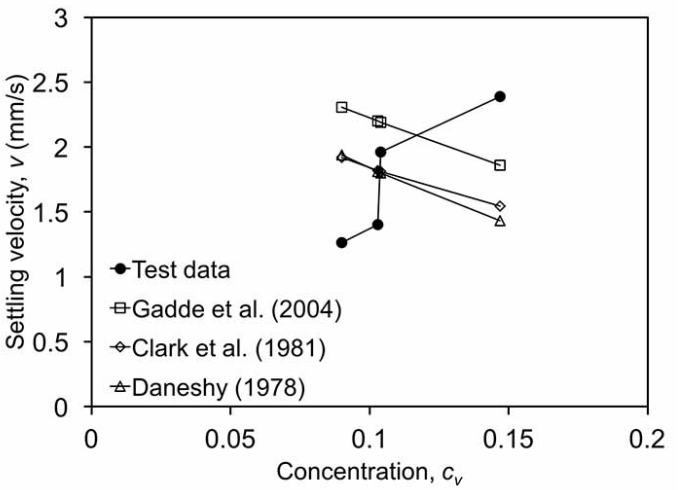

Figure 4.21 Comparison of the average experimental settling velocities with previous relationships for a narrow slot in 85 % glycerol-water fluid at low concentration by using volumetric concentration

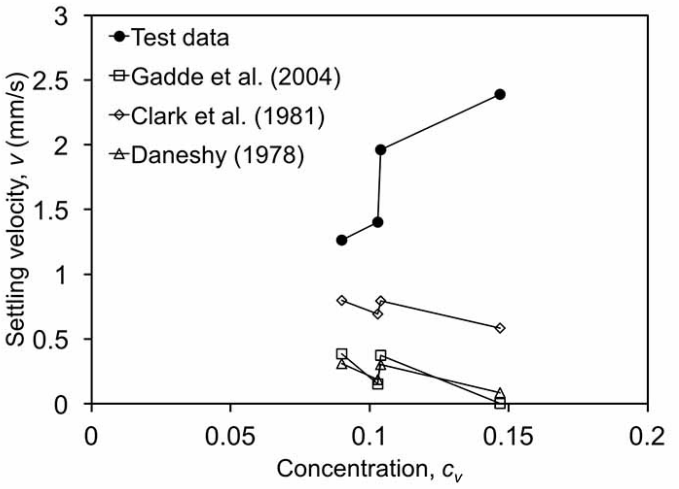

Figure 4.22 Comparison of the average experimental settling velocities with previous relationships for a narrow slot in 85 % glycerol-water fluid at low concentration by using superficial concentration

Considering the effect of narrow walls, the prediction made by Liu and Sharma (2005) comes up with the average settling velocity of 3.02 mm/s. Figure 4.23 shows that settling velocities are slower than predicted by Liu and Sharma (2005), which takes into account the effect of particle and wall dimensions' ratio. Comparing with the prediction using for narrow slot with smooth surface as shown in Figure 3.62, it is significant that

observed settling in a narrow slot with rough surface can be better predicted than that in a narrow slot with smooth surface.

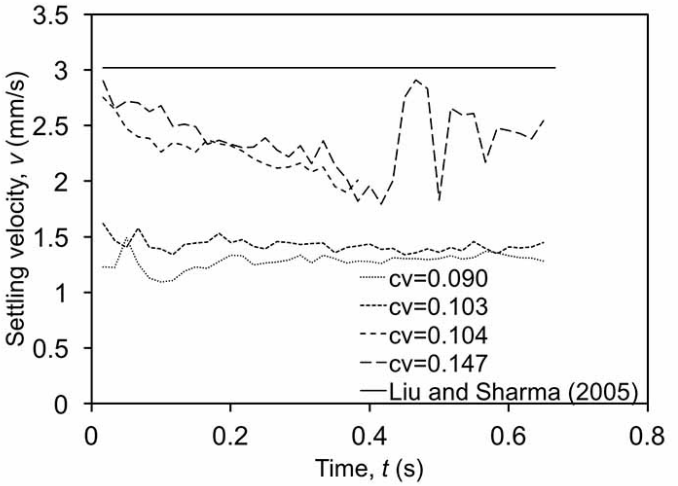

Figure 4.23 Comparison of the average experimental settling velocities with the relationship proposed by Liu and Sharma (2005) for a narrow slot in 85 % glycerol-water fluid

CHAPTER 5: COMPARISON OF SLURRY SETTLING IN NARROW SLOT BETWEEN SMOOTH SURFACE AND ROUGH SURFACE

Proppant settling in narrow slot with both smooth surface and rough surface is being analyzed in previous chapters. The results are synthetized for better understanding effects of realistic rough surface on the slurry settling, compared to the idealized smooth wall. Idealized smooth walls are used in previous experiments which yielded governing equations for proppant settling, as well as, flow and transport in hydraulic fractures. The apparent fracture aperture can be used for numerical interpretation of wavy slot surface for fluid flow. However, the slurry consists of proppant solids and fluid, and in a narrow fracture the previous approach needs to be further evaluated. The ratio between the average settling velocity and the prediction made by Gadde et al. (2004) is analyzed for particles settling in narrow slot with both smooth surface and rough surface. Figure 5.1 shows the ratio of average settling with the prediction made by Gadde et al. (2004) in 75 % glycerol-water fluid.

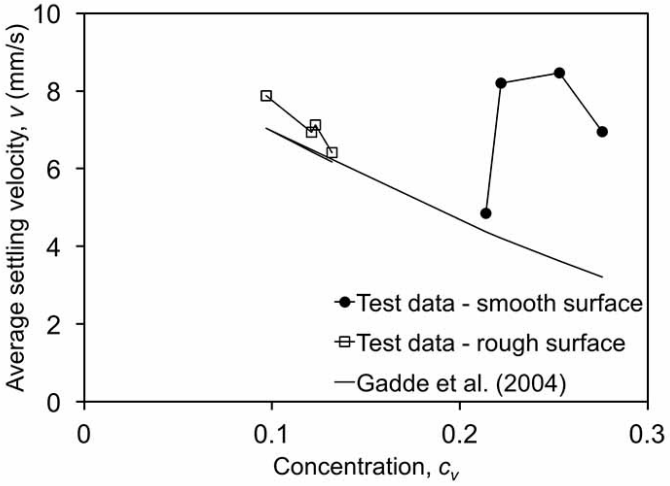

Figure 5.1 Comparison between average settling velocity in 75 % glycerol-water fluid in smooth surface and rough surface with prediction made by Gadde et al. (2004)

The settling velocity in narrow slot with both smooth surface and rough surface is higher than prediction made by Gadde et al. (2004) when proppant concentration is larger than 0.1. Higher settling velocities indicate the effect of particle agglomeration. The settling velocity of proppants in rough surface with concentration of 0.1 is similar to the concentration of 0.25 in smooth surface. The rough surface settling velocity is closer to the Gadde's et al. (2004) prediction, but it can be argued that the particle volumetric concentration is very low, and the rough surface – proppant interactions are not significant enough to affect the overall result.

Figure 5.2 and Figure 5.3 show the comparison between experimental results with predicted settling velocity according to relationships proposed by Clark et al. (1981) and Daneshy (1978). Similar with the relationship of Gadde et al. (2004), the difference between experimental results with predicted settling velocity is around 30 % for slurry settling in narrow slot with rough surface at low particle concentration and 50 % for smooth surface with higher particle concentrations.

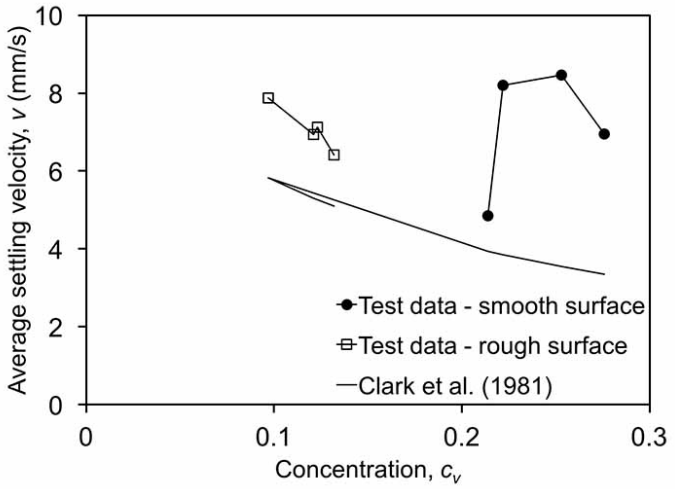

Figure 5.2 Comparison between average settling velocity in 75 % glycerol-water fluid in smooth surface and rough surface with prediction made by Clark et al. (1981)

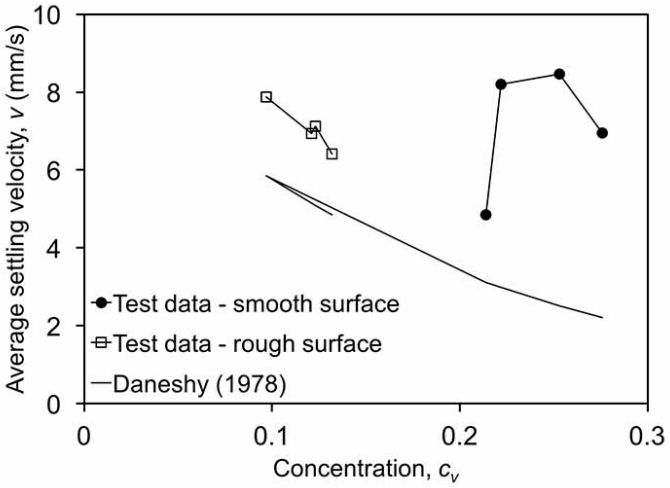

Figure 5.3 Comparison between average settling velocity in 75 % glycerol-water fluid in smooth surface and rough surface with prediction made by Daneshy (1978)

Figure 5.4 shows the comparison between slurry settling in smooth surface and rough surface with prediction made by Gadde et al. (2004) for slurry settling in 85 % glycerol-water fluid.

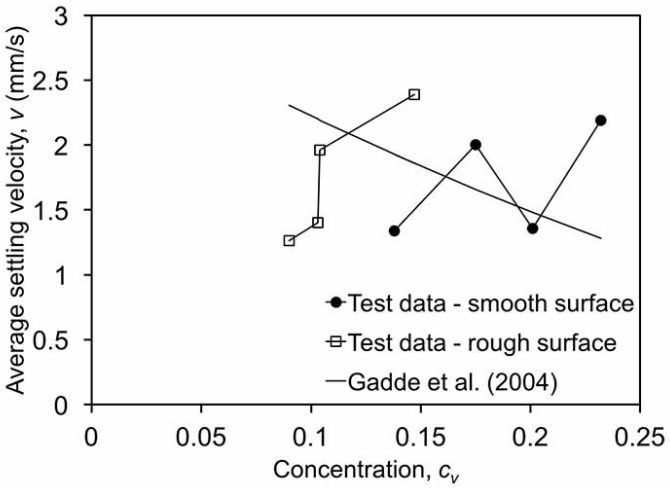

Figure 5.4 Comparison between average settling velocity in 85 % glycerol-water fluid in smooth surface and rough surface with prediction made by Gadde et al. (2004)

It can be seen that the difference between experimental results with predicted settling velocity regarding to relationship proposed by Gadde et al. (2004) are small.

However, in both smooth and rough slots the settling velocity has increasing trend as the concentration increases, which is not in according to the prediction made by Gadde et al. (2004).

Figure 5.5 and Figure 5.6 show the comparison between experimental results with relationships proposed by Clark et al. (1981) and Daneshy (1978).

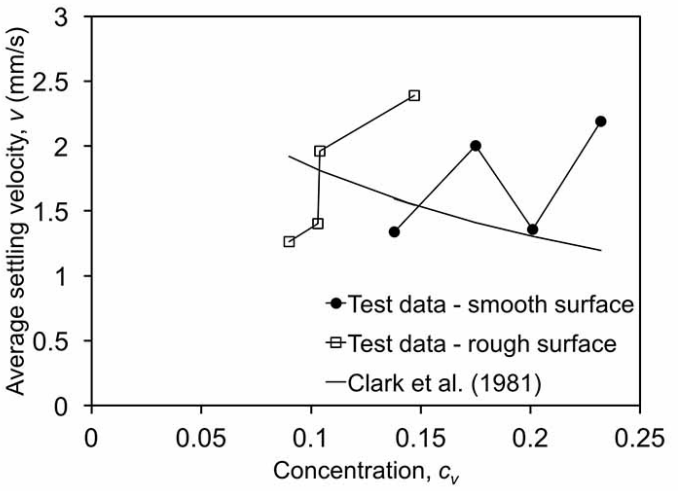

Figure 5.5 Comparison between average settling velocity in 85 % glycerol-water fluid in smooth surface and rough surface with prediction made by Clark et al. (1981)

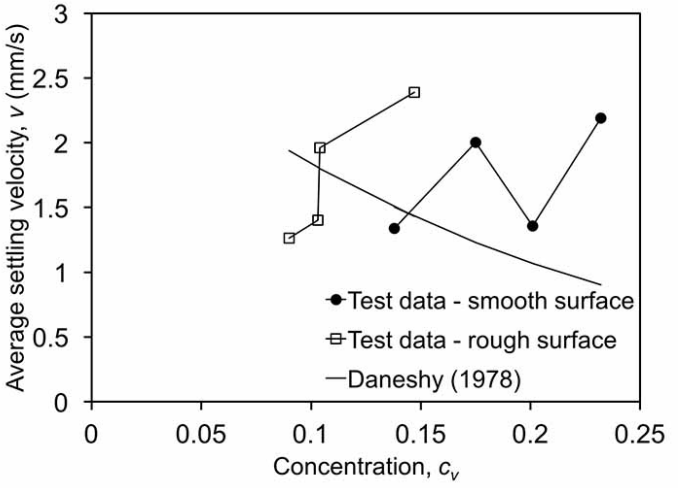

Figure 5.6 Comparison between average settling velocity in 85 % glycerol-water fluid in smooth surface and rough surface with prediction made by Daneshy (1978)

Figure 5.5 and Figure 5.6 have similar trend and magnitude. The experimental results are higher than predictions according to Clark et al. (1981) and Daneshy (1978) when proppant concentration is higher than 0.1. As shown in previous chapters, the proppant agglomeration can increase proppant settling to some extent.

CHAPTER 6: CONCLUSIONS

The research presented in this thesis involves developing a simple experimental laboratory setup to perform experiments of proppant gravitational settling in a narrow smooth and rough wall fracture. The settling of proppants was recorded with camera using 60 frames per second recording rate. Afterwards, the frames were extracted into digital data for analysis using the GeoPIV software. By using the GeoPIV method, the proppants were tracked to get movements of every time interval. Couples of patches which represent fixed areas of the face of the see through Plexiglas slot wall are chosen from recorded frames to analyze the velocity of slurry settling. Conclusions and observations from experimental results of slurry settling in fluids with different viscosities are shown here. For slurry settling in 2 mm narrow slot with smooth surface, 50 % glycerol-water fluid, 75 % glycerol-water fluid and 85 % glycerol-water fluids were analyzed. The slot size represents a narrow fracture of 2 mm in diameter. The walls of the first set of tests were chosen to be smooth representing idealized fracture, very often used in numerical, theoretical and experimental analysis. Similar set of tests was also performed in another slot cell with the back side representing realistic rough rock surface. The rock surface was replicated using 3D printing from the scan of the hydraulic fracture obtained in the laboratory by fracturing the rock at the University of Bochum, Germany. The analysis of proppant settling was focused on better understanding the effects of particle size, proppant concentration and rate of particle agglomerations, effect of wall roughness and fluid dynamic viscosities.

The conclusions resulting from this work are:

1. The average settling velocity from experimental result is compared with prediction

made by Stokes' law which is derived for sphere particles settling in unbounded fluid. It can be found that the Stokes' law can be applied for slurry settling even in narrow lot when the ratio of particle diameter to slot aperture is as small as 0.15. When the particles are agglomerated with each other and the diameter becomes the larger, the Stokes' law cannot predict the velocity of agglomerated particle settling in a narrow slot.

2. The proppant concentration was found to primarily affect the rate of proppant settling. It can be found that higher proppant concentrations resulting in quicker proppant settling. Comparing the experimental results while the concentration is low with previous relationships proposed by Gadde et al. (2004), Clark et al. (1981) and Daneshy (1978), the average settling velocities are much smaller than predication. With increasing concentration, the difference between predicted velocity with experimental result can be reduced. When the concentrations are higher 0.2, experimental results are higher than prediction made by previous relationships. These three relationships only consider the effect of concentration but not the effect of agglomerates. In fact, the rate of agglomerates is high especially when the concentration reaches high.
3. Wall effect is also an important parameter during settling. Comparing experimental results with predicted velocities according to Liu and Sharma (2005), it can be found that the experimental results appear much slower than prediction. Liu and Sharma (2005) proposed that the wall effects will influence settling velocity with large ratio of particle diameter to fracture aperture (d/B>0.9). However, in this study, the experimental results indicate that wall effects at lower particle diameter

to wall distance (d/B=0.33) already significantly slow down the slurry settling rates.

4. When concentrations of three different fluids are the same, the agglomerates are different. The increased number of agglomerates in higher viscosity fluids is observed and it is concluded that agglomerates aid in settling velocity increase after normalizing settling velocity with Stokes' law.

Based on this study, the proppants settling in narrow slot can be expected to be dependent on agglomerates distribution, concentration and ratio of particle diameter to slot aperture.

Adding the rough surface can better simulate slurry movements in rock fracture. The rough surface is getting from the scanned data of rock surface. The tests are conducted by adding rough surface in narrow slot.

1. The slurry settling in narrow slot with rough surface is influenced by concentration of proppants. It can be found that the proppant concentrations would slow down slurry settling. Comparing the experimental results with predictions made by Gadde et al. (2004), Clark et al. (1981) and Daneshy (1978), the experimental results are approximately 10 % higher than prediction.
2. The agglomeration of proppants occurs during settling. However, the roughness of rock surface decreases the rate of agglomerates. When the agglomerated proppants formed a larger scale, some of the proppants would get stack in the surface. Thus, the agglomerated proppant falls apart.
3. The wall effect is another dominating factor in rough surface. Comparing average settling velocity with prediction made by Liu and Sharma (2005), it can be found that the experimental results are approximately 20 % smaller than predicted results.

The relationship proposed by Liu and Sharma (2005) consider the effect of ratio of particle diameter to fracture aperture. However, when settling in rough surface, the wall effect would be significant increased because of surface roughness.

The differences between settling in rough surface with smooth surface are significant. Comparing slurry settling in narrow slot of smooth surface with rough surface can better evaluate proppants movement.

1. Channels of proppants occur more significantly in rough surface than smooth surface. When settling in smooth surface, the proppants mostly move with similar velocity in stable period. However, the proppants move in different velocities when form different channels in rough surface.
2. The settling velocities are normalized with Gadde et al. (2004), Clark et al. (1981) and Daneshy (1978) to eliminate the effect of different concentration and viscosity. The experimental solution for rough surface ends up with approximately 10 % reduction of average settling velocity comparing to smooth surface. The roughness of printed rock surface can eventually retard the slurry settling in narrow slot.
3. In this study, the slurry settling in rough surface indicates less rate of agglomeration than in smooth surface. Moreover, when average settling velocity in rough surface are the same as smooth surface, as the concentration is smaller in rough surface. According to the previously published relationships, the proppant concentration decreases the slurry settling velocity, which indicates that the settling in smooth surface with higher concentration should be faster. However, the experimental results on narrow slot show contrasting solution. It was observed in this study experimentally that the agglomerates occur in slurry and their presence aids in

increasing the overall settling velocity. Thus, the agglomerates and wall effects due to ratio of particle dimeter to slot aperture in smooth surface influence the settling velocity. On the contrary, the agglomerates in rough surface occurred at a smaller scale.

The results of this laboratory experimental work has provided some insights to understand the detailed proppant transport behavior in narrow facture. Additional studies are recommended to further expand this understanding. With all the knowledge acquired during this research, a larger scale of experiment with horizontal flow, inclined flow, flow with come leak off and flow with different pressure can also be conducted.

REFERENCES

Adrian, R.J. 1991. Particle-imaging techniques for experimental fluid mechanics. *Annual Reviews of Fluid Mechanics.* 23: 261—304

Barnocky, G. and R.H Davis. 1988. Elastohydrodynamic collision and rebound of spheres: experimental verification, Physics of Fluids, 31: 1324.

Brule, B. and G. Gheissary. 1993. Effects of fluid elasticity on the static and dynamic settling of a spherical particle. *Journal of Non-Newtonian Fluid Mechanics*. 49:123-132.

Clark, P.E., M.W. Harki, H. A. Hahl and J. A. Sievert. 1977. Design of a large vertical prop transport model. *SPE Annual Fall Technical Conference and Exhibition.*

Clark P.E., F. Manning, J. Quadir, N. Guler. 1981. Proppant transport in vertical fractures. *56th annual fall technical conference and exhibition of the society of petroleum engineers of AIME.*

Daneshy, A.A. 1981. Numerical solution of sand transport in hydraulic fracturing. *Journal of Petroleum Technology*. 30(1): 132-140.

Davis, R.H., J.M. Serayssol, and E. Hinch. 1986. The elastohydrodynamic collision of two spheres. Journal of Fluid Mechanics. 163(1):479-497.

Deng, S. H. Li, G. Ma, H. Huang, X. Li. 2014. Simulation of shale–proppant interaction in hydraulic fracturing by the discrete element method. *International Journal of Rock Mechanics & Mining Sciences*. 70: 219–228.

Dontsov, E. V. and A. P. Peirce. 2014. Slurry flow, gravitational settling and a proppant transport model for hydraulic fractures. *Journal of Fluid Mechanic.* 760: 567–590.

Dontsov, E. V. and A. P. Peirce 2015. Proppant transport in hydraulic fracturing: Crack tip screen-out in KGD and P3D models. *International Journal of Solids and Structures.* 63: 206–218.

Eskin, D. and M.J. Miller. 2008. A model of non-Newtonian slurry flow in a fracture. *Powder Technology.* 182: 313–322.

Feng, J. et al. 1994. Direct simulation of initial value problems for the motion of solid bodies in a Newtonian fluid. Part 1: sedimentation. *Journal of Fluid Mechanics*. 261:95–134

Gadde, P.B., Y. Liu, J. Norman, R. Bonnecaze and M.M. Sharma. 2004. Modeling proppant settling in water-fracs. *SPE annual technical conference and exhibition*.

Goel, N. and S. Shah. 2001. A rheological criterion for fracturing fluids to transport proppant during a stimulation treatment. *SPE Annual Technical Conference and Exhibition*.

Goel, N., S.N. Shah, B.P. Grady. 2002. Correlating viscoelastic measurements of fracturing fluid to particles suspension and solids transport. *Journal of Petroleum Science and Engineering*. 35:59–81.

Hammond, P.S. 1995. Settling and slumping in a Newtonian slurry, and implications for proppant placement during hydraulic fracturing of gas wells. *Chemical Engineering Science.* 50: 3247–3260.

Joseph, D.D. 1994. Aggregation and dispersion of spheres falling in viscoelastic liquids. *Journal of Non-Newtonian Fluid Mech*. 54: 45–86.

Liu, Y. and M. Sharma. 2005. Effect of fracture width and fluid rheology on proppant settling and retardation: an experimental study. *SPE annual technical conference and exhibition.*

King, G.E. 2010. Thirty Years of Gas Shale Fracturing: What Have We Learned?. *SPE Annual Technical Conference and Exhibition.*

Malhotra, S. and M.M. Sharma. 2012. Settling of spherical in unbounded and confined surfactant-based shear thinning viscoelastic fluids: An experimental study. *Chemical Engineering Science.* 84: 645–655.

McClure, M.W., S. Shiozawa and J. Huang. 2015. Fully Coupled Hydromechanical Simulation of Hydraulic Fracturing in Three-Dimensional Discrete Fracture Networks. *SPE Hydraulic Fracturing Technology Conference.*

Palisch, T.T., Vincent, M.C., and Handren, P.J., 2008, Slickwater Fracturing – Food for Thought. *2008 SPE Annual Technical Conference and exhibition*.

Patankar, N.A, D.D. Joseph, J. Wang, R.D. Barree, M. Conway, M. Asadi. 2002. Power law correlations for sediment transport in pressure driven channel flows. *International Journal of Multiphase Flow.* 28: 1269–1292.

Roy, P., L. Wyatt and D. Stuart. 2015. Proppant transport at the fracture scale: simulation and experiment. *American Rock Mechanics Association Conference.*

Sahai R., J.L. Miskimins and K. E. Olson. 2014. Laboratory results of proppant transport in complex fracture systems. *SPE Hydraulic Fracturing Technology Conference.*

Shiozawa S. and M. McClure. 2015. Simulation of proppant transport in 2D discrete fracture network. *Fortieth Workshop on Geothermal Reservoir Engineering.*

Shiozawa S. and M. McClure. 2016. Comparison of pseudo-3D and fully-3D simulations of proppant transport in hydraulic fractures, including gravitational settling, formation of proppant banks, tip-screen out, and fracture closure. *SPE Hydraulic Fracturing Technology Conference.*

Shokir1 E.M. and A.A. 2009. Quraishi. Experimental and Numerical Investigation of Proppant Placement in Hydraulic Fractures. *Petroleum Science and Technology*. 27:1690–1703.

Sievert J.A. and H.A. Wahl, P.E. Clark and M.W. Harkin. Proppant transport in a large vertical model. *SPE/DOE Low Permeability Symposium.*

Stevenson, P., R.B. Thorpe, J.E. Kennedy and C. McDermott. 2001. The transport of particles at low loading in near-horizontal pipes by intermittent flow. *Chemical Engineering Science.* 56: 2149–2159.

Tomac, I. and M. Gutierrez. 2013. Discrete element modeling of non-linear submerged particle collisions. *Granular Matter*. 15: 759–769.

Tomac, I. and M. Gutierrez. 2014. Fluid lubrication effects on particle flow and transport in a channel. *International Journal of Multiphase Flow*. 65:143–156.

Tomac, I. and M. Gutierrez. 2015. Micromechanics of proppant agglomeration during settling in hydraulic fractures. *Journal of Petroleum Exploration and Production Technology*. 1–18.

Trykozko, A., M. Peszynska and M. Dohnalik. 2016. Modeling non-Darcy flows in realistic pore-scale proppant geometries. *Computers and Geotechnics*. 71:352–360.

Wan G. 2004. Can ceramics withstand the pressure from frac sands.

Willert, C.E. and M. Gharib. 1991. Digital particle image velocimetry. *Experimental Fluids*. 10: 181—193

White, D.J. et al. 2002. A deformation measurement system for geotechnical testing based on digital imaging, close-range photogrammetry, and PIV image analysis. *15th International Conference on Soil Mechanics and Geotechnical Engineering*

White, D.J. et al. 2003. Soil deformation measurement using particle image velocimetry (PIV) and photogrammetry. *Géotechnique*. 53: 619—631.

Zhao, Z., B. Cui, Y. Yue, L. Wang and Y. Wu. 2008. Numerical simulation of horizontal migration of proppant. *Journal of Hydrodynamics*. 20: 74–80.